



Marina da Silva Teixeira

Bachelor degree in Biochemistry

Development of new hybrid gene delivery carriers

Dissertation to obtain the Master degree in
Biochemistry

Advisor: Professor Lídia Maria Diogo Gonçalves, PhD,
Faculty of Pharmacy, University of Lisbon

Co-advisor: Professor António José Leitão das Neves
Almeida, PhD, Faculty of Pharmacy, University of Lisbon

Examination Committee:

Chairperson: Prof. Dr. Carlos Alberto Gomes Salgueiro

Rapporteurs: Prof. Dr. Ana Francisca de Campos Simão Bettencourt

Prof. Dr. Lídia Maria Diogo Gonçalves



FACULDADE DE
CIÊNCIAS E TECNOLOGIA
UNIVERSIDADE NOVA DE LISBOA

September 2017



Marina da Silva Teixeira

Bachelor degree in Biochemistry

Development of new hybrid gene delivery carriers

Dissertation to obtain the Master degree in
Biochemistry

Advisor: Professor Lúcia Maria Diogo Gonçalves, PhD,
Faculty of Pharmacy, University of Lisbon

Co-advisor: Professor António José Leitão das Neves
Almeida, PhD, Faculty of Pharmacy, University of Lisbon

Examination Committee:

Chairperson: Prof. Dr. Carlos Alberto Gomes Salgueiro

Rapporteurs: Prof. Dr. Ana Francisca de Campos Simão Bettencourt

Prof. Dr. Lúcia Maria Diogo Gonçalves



FACULDADE DE
CIÊNCIAS E TECNOLOGIA
UNIVERSIDADE NOVA DE LISBOA

September 2017

Copyright

“Development of new hybrid gene delivery carriers”

Copyright © Marina da Silva Teixeira, Faculty of Science and Technology, NOVA University of Lisbon

The Faculty of Science and Technology and the NOVA University of Lisbon have the right, forever and without geographical limits, to file and publish this dissertation through printed copies reproduced in paper or by digital means, or by any other mean known or that may be invented, and to disclose it through scientific repositories and to allow its copyright and distribution for non-commercial educational or research purposes, provided that the author and editor are credited.

A Faculdade de Ciências e Tecnologia e a Universidade Nova de Lisboa têm o direito, perpétuo e sem limites geográficos, de arquivar e publicar esta dissertação através de exemplares impressos reproduzidos em papel ou de forma digital, ou por qualquer outro meio conhecido ou que venha a ser inventado, e de a divulgar através de repositórios científicos e de admitir a sua cópia e distribuição com objetivos educacionais ou de investigação, não comerciais, desde que seja dado crédito ao autor e editor.

*“Nothing in life is to be feared, it is only to be understood.
Now is the time to understand more, so that we may fear less.”*

Marie Curie

Acknowledgments

On a first note I would like to give a special thank you to my adviser, Professor Lídia Gonçalves, for all the attention, time and support provided to teach and supervise me during this project. I would also like to thank Professor António Almeida for accepting me in his research group and allow me to use their research facilities. To all the members of the NanoBB group and lab. 112, I would like to thank them for their huge kindness, availability, and for making me feel welcome.

I couldn't forget to express my gratitude to my lab colleague and friend, Telmo, for not only all the patience, help and support, but also the friendship and fun times.

To Dr. Joana Marto, I would kindly like to thank her good energy and the opportunity to satisfy some of my curiosity regarding the cosmetic world.

To all the friends I've made and shared this journey with, thank you! Each of you contributed in your own unique way to these fantastic years. It wouldn't have been the same without any of you, specially Barreto and Zé Rui. I feel that this acknowledgment wouldn't be complete without thanking my second family during this process, those who have seen me grow and grew with me, the girls from "Casa do Costa" (Vanessa Montês, Amorim, Raquel, Mestre, Cidália, Sofia, Iana, Mansinho and Inês). I couldn't have had it any better. A special thank you, to my eternal roommate and dearest friend, Vanessa Lopes, for all the support and amazing shared moments. I'm proud of you!

Last, but definitely not least, I would like to express my deepest thank you to my parents, for the unconditional support and affection, even when I was not the easiest person to handle; for always trusting me and pushing me further, and for all the amazing values they have taught me. None of this would be possible without you! None! To my little sister, partner in crime and friend, thank you for always being there. And finally, to the most amazing and important person I've ever met, Francisco. Thank you for always being by my side, believing and pushing me towards new goals. Thank you for the tireless support you give me. Love you all so much!

Abstract

Gene therapy has gained increased attention over the last decades due to the possibility to treat a disease at its routes. Several vehicles intended to carry and deliver a functional copy of the deficient gene have been developed. Amongst these, viral vectors are highly effective systems, capable to deliver the genetic cargo to the nucleus. However, these carriers have raised safety concerns regarding to immunogenicity and insertional mutagenesis, creating the need to develop equally efficient vehicles with higher safety profiles. Therefore, non-viral vectors have been suggested as an alternative to viral gene transfer methods, as these overcome some of the drawbacks presented by viral vectors.

The main goal of this project was to develop safe and effective non-viral gene carriers, using solid lipid nanoparticles (SLNs) with surface modulated properties.

SLNs with surface modulated properties using polyethyleneimine (PEI) combined, or not, with protamine, were produced by hot high shear homogenization. The obtained particles possessed sizes <300 nm suitable for intravenous administration, and good physical stability for 3 months, under the different storage conditions tested (4°C, room temperature and 37°C). Moreover, these particles showed good plasmid condensation levels and were able to deliver the gene into the nucleus. Additionally, no cytotoxic effects concerning membrane integrity and metabolic activity of HEK 293-T cells were observed after 24 h of exposition.

In conclusion, the developed nanoparticles presented suitable properties for gene delivery, with high capacity to condense DNA and transfect cells without cytotoxicity.

Keywords: Gene delivery; Non-viral vectors; Cationic SLNs; Hybrid nanoparticles; Cytotoxicity; Transfection.

Resumo

Nas últimas décadas, a entrega de genes para fins terapêuticos tem atraído crescente atenção por parte da comunidade científica, dada a possibilidade de tratar doenças na sua origem. De entre os vários vetores desenhados para este fim, destacam-se os vetores virais dada a sua elevada eficiência de transfecção celular. Contudo, a imunogenicidade e mutagénesis insercional observadas para estes vetores levantam algumas preocupações relativas à sua segurança, levando à necessidade de criar veículos igualmente eficientes e com perfis de segurança mais elevados. Desta forma, os vetores não virais têm sido sugeridos como alternativas aos vetores virais, visto que conseguem contornar alguns dos pontos negativos apresentados pelos seus homólogos.

Este projeto teve como objetivo o desenvolvimento de vetores não-virais seguros e eficientes, utilizando nanopartículas lipídicas sólidas (SLNs) com superfícies moduladas.

Deste modo, a superfície de SLNs produzidas por homogeneização a quente foi modulada utilizando polietilenoimina (PEI) combinado, ou não, com protamina. As partículas obtidas apresentaram tamanhos inferiores a 300 nm e boa estabilidade física nas diferentes condições testadas (4°C, temperatura ambiente e 37°C) ao longo de 3 meses. Adicionalmente, foram observadas boas capacidades de condensação plasmídea e transfecção celular. Verificou-se ainda que as nanopartículas produzidas não induziram efeitos citotóxicos a nível da integridade membranar e atividade metabólica de células HEK 293-T após 24h de exposição.

Em conclusão, as SLNs com superfícies moduladas produzidas ao longo deste projeto apresentaram propriedades adequadas à entrega de genes por via intravenosa, com elevadas capacidades de condensação de DNA transfecção celular, sem indução de citotoxicidade.

Palavras-chave: Entrega de genes; Vetores não virais; SLN catiónicas; Nanopartículas híbridas; Citotoxicidade; Transfecção.

Table of contents

Chapter 1	Introduction	1
1.1	Nanotechnology and nanomedicine	1
1.2	Gene delivery	1
1.2.1	Viral vectors	3
1.2.2	Non-viral delivery systems	4
1.2.2.1	Physical methods	4
1.2.2.1.1	Microinjection	5
1.2.2.1.2	Needle injection	5
1.2.2.1.3	Jet injection.....	5
1.2.2.1.4	Gene gun.....	5
1.2.2.1.5	Electroporation	5
1.2.2.1.6	Sonoporation	6
1.2.2.1.7	Hydrodynamic injection	6
1.2.2.2	Non-viral vectors.....	7
1.2.2.3	Polyplexes	8
1.2.2.4	Lipoplexes.....	9
1.2.2.4.1	Solid lipid nanoparticles (SLNs)	10
1.2.2.4.1.1	SLN production technology	11
1.2.2.4.1.1.1	High pressure homogenization (HPH) technique	11
1.2.2.4.1.1.2	High shear homogenization technique	12
1.2.2.4.1.1.3	Microemulsion technique	12
1.2.2.4.1.1.4	Emulsification and solvent evaporation method	13
1.2.2.4.1.1.5	Emulsification and solvent diffusion method	13
1.2.2.4.1.2	Strategies to help SLNs overcome biological barriers.....	14
1.2.2.4.1.2.1	Mononuclear phagocyte system	14
1.2.2.4.1.2.2	Cellular uptake	16
1.2.2.4.1.2.3	Endosome escape	16
1.2.2.4.1.2.4	Nuclear import	18
Chapter 2	Objective	21

Chapter 3	Materials and methods	23
3.1	Materials	23
3.2	Methods	23
3.2.1	SLN production	23
3.2.1.1	Solvent evaporation technique (SET)	23
3.2.1.2	Hot high shear homogenization technique (HSSH).....	23
3.2.2	Surface modulation	24
3.2.3	Physicochemical characterization	24
3.2.3.1	Particle size.....	24
3.2.3.2	Surface charge	25
3.2.3.3	Transmission electron microscopy	25
3.2.4	Stability assays	25
3.2.5	In vitro cell viability studies	26
3.2.6	Plasmid production and purification	26
3.2.7	pDNA-hyNP complexes	27
3.2.8	Quantitative uptake assessment.....	27
3.2.9	Fluorescence microscopy	27
3.2.10	In vitro transfection studies.....	28
3.2.11	Haemocompatibility	28
3.2.12	Statistical data analysis.....	29
Chapter 4	Results and discussion	31
4.1	Physicochemical characterization	31
4.1.1	Production technology	31
4.1.2	Surfactant choice, volume and concentration	32
4.1.3	Lipid choice and concentration	34
4.1.4	Surface modulation	36
4.1.4.1	Cationic polymer.....	36
4.1.4.1.1	Chitosan	36
4.1.4.1.2	PEI.....	38
4.1.4.2	Cationic peptide	41

4.1.5	Stability.....	43
4.1.5.1	Freeze drying.....	43
4.1.5.2	Storage stability.....	44
4.1.5.3	Storage medium.....	47
4.1.5.4	Sterilization.....	49
4.2	SLN morphology.....	51
4.3	In vitro cell viability.....	52
4.4	pDNA condensation.....	55
4.5	Cell uptake.....	58
4.6	Cell transfection.....	62
4.7	Haemocompatibility.....	62
Chapter 5	Conclusion and future work.....	65
Chapter 6	References.....	67
Chapter 7	Appendix.....	73
	Appendix A – Surfactant choice, volume and concentration.....	73
	Appendix B – Lipid choice and concentration.....	74
	Appendix C – Surface modulation: Cationic polymer.....	75
	Appendix D – Surface modulation: Cationic peptide.....	77
	Appendix E – Stability: Storage medium.....	78
	Appendix F – Stability: Sterilization.....	79
	Appendix G – Hemocompatibility.....	80

Table of figures

Figure 1.1	Representation of the various encoding regions in a plasmid.	2
Figure 1.2	Schematic representation of polyplex assembly	9
Figure 1.3	Summary representation of the main steps of the high-pressure homogenization process.....	12
Figure 1.4	Summary representation of the main steps of the microemulsion technique. ...	13
Figure 1.5	Summary representation of the main steps of the emulsification and solvent evaporation method	13
Figure 1.6	Summary representation of the main steps of the emulsification and solvent evaporation method	14
Figure 1.7	Steric hindrance provided by grafted PEG molecules	15
Figure 1.8	Chemical representation of poloxamers.....	15
Figure 1.9	Common cell transfection steps to all administration routes	17
Figure 1.10	Schematic representation of the nuclear compartments.....	19
Figure 3.1	General-purpose disintegrating head from Silverson Machines	24
Figure 3.2	Schematic electrophoretic cell representation	25
Figure 4.1	Influence of the different volumes of surfactant tested on SLN's physicochemical properties	33
Figure 4.2	Influence of the Pluronic® type and concentration on SLN's physicochemical properties.....	34
Figure 4.3	Chemical structure of Glyceryl tripalmitate, Glyceryl distearate and Glyceryl monostearate	36
Figure 4.4	Effect of surface modulation using different concentrations of PEI 25 kDa	39
Figure 4.5	Influence of pH in the production of hyNPs, using PEI 25kDa at different concentrations	40
Figure 4.6	Influence of linear and branched polyethyleneimines on SLN physicochemical characteristics, at two concentrations	41
Figure 4.7	Hybrid nanoparticles containing linear or branched PEI (0.01% w/v) and protamine (0.05% w/v) produced via HSSH	42
Figure 4.8	Influence of temperature on hyNPs containing protamine	43
Figure 4.9	The influence of refrigeration temperature (4 °C) on SLNs	45
Figure 4.10	The influence of room temperature (RT) on SLNs	46

Figure 4.11	The influence of body temperature (37 °C) on SLNs.....	47
Figure 4.12	Influence of the PBS on SLNs' physicochemical properties.....	48
Figure 4.13	Influence of SBF on SLNs' physicochemical properties after 1 and 2 h of exposure.....	49
Figure 4.14	Influence of autoclaving on SLNs' characteristics.....	51
Figure 4.15	The cell's membrane integrity by Propidium iodide uptake assay after 6h of exposure.....	54
Figure 4.16	The cell's metabolic integrity by Alamar blue assay after 6h of exposure	54
Figure 4.17	The cell's membrane integrity by Propidium iodide uptake assay after 24h of exposure.....	55
Figure 4.18	The cell's metabolic integrity by Alamar blue assay after 24h of exposure.....	55
Figure 4.19	Qualitative evaluation of pDNA condensation	56
Figure 4.20	Quantification of the efficiency of pDNA condensation regarding the mass ratios SLN/ pDNA of 104:1 and 208:1.....	57
Figure 4.21	pDNA-hyNPs physicochemical properties.....	58
Figure 4.24	Fluorescence quantification of SLN uptake	59
Figure 4.22	hyNP _x cellular uptake observed under fluorescence microscopy	60
Figure 4.23	hyNP _x P cellular uptake observed under fluorescence microscopy	61
Figure 4.25	Fluorescence quantification of the expression of pGFP	62
Figure 4.26	Evaluation of the toxic effects exerted on haemoglobin.....	63
Figure 7.1	Imwitor [®] 491 foam-like structure obtained by homogenization with Pluronic [®] F-68 (0.1% w/v).	74

List of tables

Table 1.1	Physical methods for gene delivery	7
Table 1.2	Comparison of viral and non-viral vectors for gene delivery	8
Table 4.1	Selection of the SLNs' production method	32
Table 4.2	Influence of the lipid concentration	35
Table 4.3	Influence of the lipid matrix choice	36
Table 4.4	Surface modulation using different concentrations of chitosan	37
Table 4.5	Surface modulation using chitosan by adsorption.....	38
Table 4.6	Surface modulation using PEI 25kDa	38
Table 4.7	hyNPx and hyNPxP morphology	52
Table 4.8	Haemolytic capacity of the tested SLNs.....	64
Table 7.1	Influence of the surfactants' volume	73
Table 7.2	Influence of Pluronic® type and concentration	73
Table 7.3	Surface modulation using different concentrations of PEI 25 kDa.....	75
Table 7.4	Influence of pH in the production of hyNPs	75
Table 7.5	Elucidative table respective to sample designation.....	75
Table 7.6	Influence of linear and branched polyethyleneimines.....	76
Table 7.7	Hybrid nanoparticles containing protamine and produced by HSH	77
Table 7.8	Hybrid nanoparticles containing protamine produced by adsorption.....	77
Table 7.9	Influence of PBS on SLNs' properties.....	78
Table 7.10	Influence of SBF on SLNs' properties.....	78
Table 7.11	Influence of autoclaving on SLNs' properties	79
Table 7.12	Schematic representation of the hemocompatibility assay	80

List of abbreviations

Abbreviation	Meaning
bPEI	Branched polyethyleneimine
CS	Chitosan
CTAB	Cethyl trimethylammonium
DAPI	4'-6-diamidine-2'-phenylindole dihydrochloride
DCM	Dichloromethane
DLS	Dynamic Light Scattering
DMSO	Dimethyl sulfoxide
DPPC	1,2-dipalmitoyl- <i>sn</i> -glycero-3-phosphocholine
EALA	Glutamic acid-alanine-leucine-alanine
FDA	Food and Drug Administration
GRAS	Generally Recognised As Safe
HSH	Hot high shear homogenization
HMW	High molecular weight
HPH	High pressure homogenization
hyNP	Hybrid nanoparticle
hyNP_x	Hybrid nanoparticle containing polyethyleneimine
hyNP_xP	Hybrid nanoparticle containing both polyethyleneimine and protamine
LMW	Low molecular weight
IPEI	Linear polyethyleneimine
miRNA	Micro RNA
MPS	Mononuclear phagocytic system
NLS	Nuclear localization signals
NP	Nanoparticle
NPC	Nuclear pore complex
OTC	Trasnscarbamylase
PBS	Phosphate buffer solution
pDNA	Plasmid DNA
PdI	Polydispersity index
PEG	Poly(ethylene glycol)
PEI	Polyethyleneimine
PEO	Poly(ethylene oxidel)
PF68	Pluronic® F-68
PF 127	Pluronic® F-127
pGFP	Plasmid expressing green fluorescent protein
PI	Propidium iodide
PPO	Poly(propylene oxide)
RT	Room temperature

SBF	Simulated body fluid
SD	Standard deviation
SDS	Sodium dodecyl sulphate
SET	Solvent evaporation technique
shRNA	Short hairpin RNA
siRNA	Small interfering
SLN	Solid lipid nanoparticle
TEM	Transmission Electron Microscopy
TSB	Tryptic soy broth
X-SCID	X-linked severe combined immunodeficiency
z-ave	Average size
ZP	Zeta potential
$\lambda_{\text{emission}}$	Emission wavelength
$\lambda_{\text{excitation}}$	Excitation wavelength

Chapter 1 Introduction

1.1 Nanotechnology and nanomedicine

Nanotechnology is a multidisciplinary field with a wide scope of applications in electronics, chemistry, biology and medicine, that exploits the use of nanomaterials ¹.

Although nanomaterials have been defined by the European Commission as materials containing at least one external dimension in the 1-100 nm size range ² no consensus has yet been reached inside the scientific community, since some also define these materials as those contained within the nanometric scale (1-1000 nm). This can be explained by the fact that at the 1-100 nm size range, materials often present unique properties that can be controlled and are different from those of the bulk material, due to their increased surface/volume ratios, which provides higher reactivity, different elastic, tensile and magnetic properties, as well as increased conductivity, and light reflexion and refraction ¹. However, when considering the application of these materials in biological systems, the nanomaterial definition must be a functional, i.e. "*the defining feature of the point at which a particular material can be said to be a nanomaterial is not strictly quantitative: it is the point at which a material demonstrates a novel functionality as a result of its small size*" ³. Therefore, even at a size range of 1-1000 nm, new therapeutic advances can be made, regardless of their bulk properties, since these systems are capable to overcome various hard breaking biological barriers and therefore allow the development of new therapeutics or improve those already existing.

Nanomedicine refers to the application of these materials to biological systems, for medical purposes such as diagnosis and therapeutics. The rapid advancement of this field and the development of numerous nanosystems, aiming new treatments, with a higher therapeutic index and fewer side effects, has attracted particular interest in the investigation of biosensing, bioimaging, photothermal cancer therapy and potential drug and gene delivery systems ⁴.

1.2 Gene delivery

The recognition of DNA's fundamental role in the control of cellular processes, has tuned researchers' attention to gene delivery as a result of its potential application in novel disease approaches, such as DNA vaccines and gene therapy ⁵.

DNA vaccines consist of modified bacterial plasmids, in which a region encoding for the antigen transgene and its expression, is introduced within the bacterial genetic information (Figure 1.1). Upon host cell uptake, and DNA delivery to the nucleus, the encoded antigen transgene is transcribed into mRNA, and subsequently translated into antigen protein in the cytoplasm ⁶. This protein can then be presented to the immune system, leading to its stimulation and response, in a similar way to those of a viral infection, constituting a good preventive measure against

pathogen infections ^{7,8}. These vaccines are believed to have an excellent safety profile, with minimal toxicity, presenting good tolerance in human clinical trials ^{6,7}. Furthermore, they are significantly easier, cheaper, and faster to produce than traditional vaccines, which constitutes a major advantage in the approach of new emerging diseases ⁹.

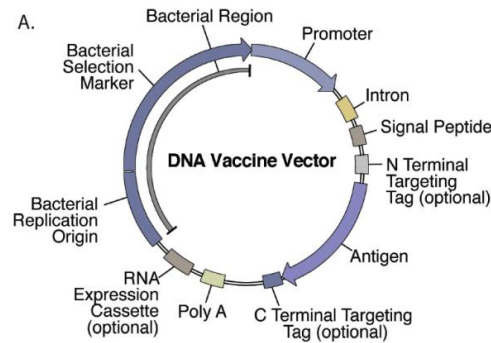


Figure 1.1 Representation of the various encoding regions in a plasmid (adapted from Williams, J. (2014) ⁶).

Nevertheless, many diseases arise from genetic mutations which compromise the normal gene function ¹⁰. The completion of the human genome project was of significant importance as it has allowed a better understanding regarding to these disease-related genes ^{5,11}.

Gene therapy aims the treatment of a genetic disease at its roots ¹². Initially, this concept referred solely to the treatment of hereditary diseases, however it was later expanded to acquired diseases as progress was being made within the field ⁵. Gene modulation for the treatment of gene-related diseases can be achieved by the insertion of functional gene copies into the host's diseased cells. These functional copies aim to replace or supplement the mutated or missing gene(s), and ultimately produce the therapeutic protein ¹³⁻¹⁵.

Moreover, as progress was being made in this field, other nucleic acids rather than DNA started to be employed. siRNA, shRNA, miRNA and antisense oligonucleotides have been used to modulate gene expression and eventually control protein expression by silencing gene expression (gene knockdown) through the prevention of mRNA translation.

Depending on the nature of the targeted cell, gene therapy can be classified as:

- (a) Germ line gene therapy, when the genetic cargo is inserted into reproductive cells, leading to heritable genetic modification of the genetic characteristics. Herein, ethical questioning has been raised, and some countries, such as France, do not allow gene therapy to be performed on these cell lines ¹³;
- (b) Somatic gene therapy, when the therapeutic genes are transferred into somatic cells, thus the genetic modifications will not be inherited ¹³.

Furthermore, gene therapy can be performed either *in vivo* or *ex vivo*. In the first case, the genetic material is inserted directly into the targeted organ or tissue via systemic injection or *in situ* administration, whereas in the latter, the genetic material is transfected into *in vitro* cultured

cells, previously isolated from the patient or donor, and subsequently (re)implanted into the patient¹¹.

Targeting the diseased cells is often a complex and difficult approach, making the insertion of naked nucleic acids seem to be a more appealing strategy. However, plasmid DNA (pDNA), siRNA, miRNA, and oligonucleotides are highly susceptible to nuclease degradation and due to their hydrophobic nature, conferred by the negatively charged phosphate groups, these molecules are often restricted from binding and passing via passive diffusion through the lipophilic cell membrane^{5,16}.

In many cases, when the disease site is not easy to access, systemic administration of the therapeutic gene is necessary. Under these circumstances, a series of systemic barriers, such as macrophage uptake, clearance and degradation of the nucleic acids, must be overcome⁵. Nevertheless, the possibility to conjugate or encapsulate nucleic acids into carriers that increase their transfection efficiency and protect them from enzymatic degradation, has arisen as an interesting and promising strategy for gene delivery¹⁶.

The success of gene therapy dramatically depends in the ability to deliver the genetic cargo without DNase degradation, which is influenced by the delivery vehicle and transfer technique employed^{11,13}. Hence, the ideal gene transfer system should¹³:

- (a) Not trigger a strong immune response;
- (b) Be capable to transport large genetic cargos;
- (c) Mask the negatively charged phosphate backbone of nucleic acids¹⁷;
- (d) Lead to sustained and regular gene expression;
- (e) Only transfect targeted cells;
- (f) Transfect dividing and non-dividing cells;
- (g) Be easy to prepare, inexpensive, and available at high concentrations commercially;
- (h) Not integrate the genome randomly;
- (i) Protect the genetic cargo from enzymatic degradation¹⁷.

1.2.1 Viral vectors

Viral and non-viral vectors have been used to deliver genetic material into cells, each presenting distinct advantages and weaknesses¹¹. Amongst these vehicles, recombinant viruses, such as retrovirus, lentivirus, adenovirus and adeno-associated virus, have been widely explored as gene carriers due to their intrinsic high transfection efficiencies¹⁶. Viruses possess a highly effective machinery, that allows them to rapidly gain entrance into the host-cell, insert their genetic material into the nucleus and exploit its cellular components aiming to express their own genetic material and replicate^{5,13}.

To use viruses as vectors intended for gene delivery, their pathogenic genes are removed and replaced by the therapeutic gene, whereas their non-pathogenic structures, such as envelope

proteins and fusogenic proteins, which allow them to infect the cell are maintained¹³. Despite their favourable cellular uptake, capacity to access the intracellular machinery, and long-term gene expression¹¹, some of these virus, such as retrovirus and lentivirus, have the ability to insert their genetic cargo into the host's genome, whereby rising insertional mutagenesis concerns^{12,16}. In addition, these vectors present a limited size for the genetic cargo, large scale production difficulties¹³, immunogenicity^{12,16}, which can lead to limited administration repetitions, and transfection of untargeted cells¹⁶. In fact, the use of viral vectors intended for gene therapy trials was put in to question when a few patients developed significant reactions to the administered vector. In 2000, nine infants suffering from X-linked severe combined immunodeficiency (X-SCID) were subjected to *ex vivo* retrovirus-mediated gene transfer, and the clinical trial was credited as the first successful gene therapy. Although the treated infants were initially considered cured from the disease, four of them later developed leukaemia-like symptoms, which were subsequently determined to be the result of a random vector integration at sensitive genomic sites, that transformed nearby genes into oncogenes¹⁸. In another human trial, a subject suffering from partial ornithine transcarbamylase (OTC), a rare metabolic disease that could lead to toxic retention levels of ammonia, was treated using adenovirus vectors. Unfortunately, an acute inflammatory response was mounted against the viral coat proteins, which led to massive damage and eventually resulted in death of the patient¹⁹. Therefore, it was necessary to find an alternative to viral gene transfer methods¹².

1.2.2 Non-viral delivery systems

Non-viral delivery systems constitute an alternative approach to viral vectors and can be classified into¹³:

- (a) Physical methods: the genetic cargo is delivered without the need of a carrier. Physical forces are used to enhance cell transfection, as they weaken the cell membrane, making it more permeable to the transgene (Table 1.1);
- (b) Chemical methods: requires the use of a carrier to deliver the genetic cargo into the cell.

1.2.2.1 Physical methods

The main goal of gene delivery using physical methods is to create temporary weak points in the cell membrane. This can be attained by using mechanical, ultrasonic, or laser-based energy, to create transient defects in its structure, allowing the nucleic acids to enter the cell by diffusion¹³. However, their use is largely limited to local delivery into specific sites⁵. A brief presentation of some of the physical methods that have been employed in gene medicine is given below.

1.2.2.1.1 Microinjection

The microinjection is a simple, effective, reproducible and non-toxic technique with potential to transfer large size DNA. Herein, a needle with a diameter ranging from 0.5-5 μm , is used to penetrate the cell membrane or nuclear envelope, and directly inject the nucleic acid into a single living cell. However, as it requires individual manipulation of each cell, this technique is not suitable for gene therapy, yet it presents high potential for DNA vaccination, for which low transgene expression is sufficient to induce an immunological response ¹¹.

1.2.2.1.2 Needle injection

Needle injection constitutes an attractive technique for clinic application due to its simplicity and safety. Herein, the genetic cargo is directly injected into the targeted organ, tissue or blood stream. However, as the inserted DNA is unprotected, it is rapidly degraded and poor gene expression is obtained. Hence this procedure is a useful tool for DNA vaccination ¹¹.

1.2.2.1.3 Jet injection

The jet injection technique represents a needle-free approach, used since 1947 for drug delivery. In this procedure, the DNA is driven by high pressurized gas, to form a high-speed ultrafine stream that will hit the cells. The generation of pores on the cell membrane eases DNA uptake by the cell, resulting in higher transfection efficacies than those obtained in the previous method. Additionally, the gas pressure can be adjusted according to the cells' tolerance to avoid tissue damage. Some of the side effects regarding this method include hyperemia (increased blood flow to the site of action), edema and minor bleeding ¹¹.

1.2.2.1.4 Gene gun

In the gene gun technique, elemental particles of heavy metals, such as gold, tungsten and silver, are coated with plasmid DNA. These particles are then accelerated by pressurized gas and fired at target cells or tissues, allowing them to penetrate into the tissue and release DNA into the cells. Herein, particle size, speed and dose play an important role in gene transfer efficacy. This procedure requires a lower dose of DNA to induce an immune response, comparatively to needle injection. However, its application is limited to transient gene expression, since dividing cells easily dilute the transgene expression ^{11,13}

1.2.2.1.5 Electroporation

This procedure was first applied for gene delivery *in vitro* and *in vivo* in 1982 and 1991, respectively, and can be applied to all cell types, being generally safe, efficient and with good

reproducibility. Electroporation applies high-voltage electrical currents onto the target cells, making transient nanometric pores on the cell membrane, which allow the negatively charged DNA to enter the cell and remain trapped within it ^{11,13}. The main advantages regarding this technique refer to the possibility to deliver large-sized DNA and long-term transgene expression ¹¹. However, its transfer efficacy can be influenced by various parameters, including current intensity, time interval between discharges, concentration and type of DNA, age of the recipient animal, and how well the injected gene cargo is distributed in the tissue. Furthermore, in vivo application still presents some drawbacks, such as the limited effective range between electrodes (~1cm), which restricts gene transfer for large area tissues; need of surgical procedure to place the electrodes onto internal organs; and the high-voltage applied can influence the stability of genomic DNA ^{11,13}.

1.2.2.1.6 Sonoporation

Sonoporation uses ultrasonic waves to induce cell membrane permeabilization and cellular gene entry. Air-filled microbubbles can be used to improve gene transfer efficacy. When activated by ultrasonic waves, the microbubbles rapidly oscillate, expand, shrink and thus break up, which releases local shock waves to transiently permeate the membrane of nearby cells. Sonoporation gene transfer efficacy depends on the ultrasound frequency and intensity, duration of the treatment, amount of DNA, and tissue type^{11,13}.

In contrast to electroporation, this procedure is non-invasive, as it does not require surgery, and local gene transfer can be achieved by ultrasonic treatment of a selected tissue. However, low gene transfer efficacy, comparatively to viral vectors is still a drawback ¹¹.

1.2.2.1.7 Hydrodynamic injection

Hydrodynamic injection is considered to be the most frequently employed method to transport genes in rats and mice. This technique was first described by Budker and his team in 1996. Due to the large volumes of solution required (8-9% of the body weight) in order to achieve high transfection rates, this procedure cannot be applied in humans, as an equivalent of 7.5 L of solution would be necessary to be injected in a very short period of time ¹³.

Table 1.1 Physical methods for gene delivery. Comparison of the advantages and disadvantages of the different physical methods for gene delivery (adapted from Wang, W. et al (2013) ¹¹).

Method	Advantages	Limitations
Microinjection	Simple, effective, reproducible, non-toxic, able to transfer large size DNA	Manipulation of a single cell at a time
Needle injection	Simple, safe	Low efficiency
Jet injection	Needle-free, easy to control, safe	Low efficiency, local slight tissue damage
Gene gun	Safe, effective	Tissue damage, low efficacy
Electroporation	Highly effective, reproducible, able to transfer large size DNA	Invasive, high voltage may influence gene stability, limited effective range between electrodes
Sonoporation	Safe, non-invasive	Low efficiency
Hydrodynamic gene transfer	Simple, reproducible, highly effective	Not suitable for human application

1.2.2.2 Non-viral vectors

One of the main challenges, and goals, in the design of a gene-based therapy, is the development of safe and effective delivery vectors ²⁰. Non-viral vectors make use of natural or synthetic compounds to deliver the gene of interest to the targeted cells, and have been proposed as an alternative to viral vectors, since they have the potential to address many of their limitations (Table 1.2), particularly regarding to safety ²⁰. In addition, non-viral vehicles offer protection to the genetic cargo and greater gene capacity ¹⁷; easier and lower cost of production ^{11,16}; possibility of large scale synthesis ¹⁶; low immunogenic response and potential for repeated administrations ^{5,16}, comparatively to viral carriers. Moreover, due to their structural and chemical versatility, their physicochemical properties can be manipulated ¹⁷ and targeting moieties can be added onto their surface, allowing the delivery of the genetic cargo to specific cells ^{5,11,16}.

As already mentioned before, these systems should be able to condense the negatively charged nucleic acids into a compact size, interact with the plasma membrane promoting their uptake, and protect it from enzymatic degradation, as well as minimize the off-target toxicity ¹². However, these carriers still present lower transfection efficiencies than their viral counterparts and short gene expression times ^{12,16}. Therefore, additional investigations have been being made to overcome these drawbacks and will be further discussed.

Table 1.2 Comparison of viral and non-viral vectors for gene delivery, regarding their advantages and disadvantages (adapted from Wang, T., Upponi, J. R. & Torchilin, V. P. (2012) ⁵).

Vectors	Advantage(s)	Disadvantage(s)
Viral	High transfection efficacy; Intrinsic mechanism for endosomal escape; Evolved natural mechanism for nuclear import of genes	Strong immune response, which leads to limited administration repetitions; Risk of chromosomal insertions and proto-oncogene activation; Limited size of the genetic cargo; Higher difficulty in their production.
Non-viral	Low immunogenicity; No risk of chromosomal insertion; Easier production and possibility of large scale production; Possibility to carry large-sized genetic cargo; Can be functionalized for active targeting, endosomal escape and nuclear import.	Low transfection efficiency; At high administration doses, toxicity has been observed; Lack of intrinsic mechanisms for endosomal escape and nuclear import of genes.

Several non-viral gene carriers have been investigated and developed over the last years, such as carbon nanotubes, dendriplexes, lipoplexes, polyplexes ²¹, magnetic nanoparticles and gold nanoparticles ²². Amongst these, lipoplexes and polyplexes have been widely studied ^{21,23}. Due to their cationic nature, these compounds form stable complexes with nucleic acids, and interact with the anionic plasma membrane, via electrostatic interactions ²⁴.

1.2.2.3 Polyplexes

Many efforts have been made to achieve more effective and stable gene transfection systems. The use of polymers in the manufacture of non-viral vectors can offer several advantages, due to their ease of preparation, purification, chemical modification and stability ^{5,11,17}.

Cationic polymers have been studied and used as non-viral gene carriers ^{5,11,17}, since they possess a high density of amino groups, protonatable under physiological pH, which enable DNA complexation via electrostatic interaction, forming polyplexes (Figure 1.2) ^{11,17}. Moreover, cationic polyplexes are able to interact with the anionic cell surface, enhancing DNA uptake; promote DNA escape from the endosomal compartment, and protect the payload ¹¹. However, due to their cationic net-charge, the used polymers have been correlated to high cytotoxic effects, and can present difficulty regarding to DNA release upon their arrival to the targeted site ¹⁷.

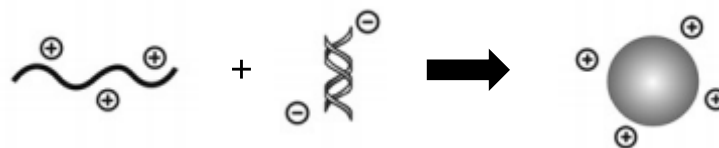


Figure 1.2 Schematic representation of polyplex assembly (adapted from Wong, S. Y., Pelet, J. M. & Putnam, D. (2007) ¹⁷).

Amongst the various used polymers, polyethyleneimine (PEI) has been considered one of the most effective polymer-based transfection agents ¹⁶. Depending on the number of repeating units of ethyleneimine, this polymer can have a branched or linear configuration ^{16,25} and a wide range of molecular weights ²⁴, with different transfection efficiencies.

Ideally, a successful transfection system should promote the necessary balance between cell transfection and toxicity ²⁶. Herein, PEI's molecular weight (MW), configuration, charge density, and polymer/DNA ratio employed have been thought to play an important role in transfection efficacy and cytotoxicity ^{16,25}. For instance, branched high molecular weight (HMW) polyethyleneimines have been found to form the smallest and most effective transfecting polyplexes ^{16,25}. However, their higher transfection efficacies have been related to increased cytotoxic effects. On the other hand, low molecular weight (LMW) PEIs' have been reported to be less toxic. Yet, their transfection efficacies were also inferior to those displayed by HMW PEIs' ²⁵. Moreover, polyplexes comprising linear polyethyleneimines have been shown to be more efficient than branched PEIs when administrated intravenously ¹⁶. Furthermore, the high density of positive charges characteristic of cationic polymers has been reported to promote colloidal instability under physiological conditions, resulting in the aggregation of these complexes ²⁴.

1.2.2.4 Lipoplexes

The use of cationic lipids capable to interact electrostatically with the negatively charged genetic cargo, forming lipoplexes ⁵, represents the most extensively studied strategy to produce non-viral gene carriers ¹⁶. These carriers, when compared to polyplexes, show increased transfection efficacies, improved cytotoxic profiles and better serum stability ²⁴. Cationic lipids share a common structure consisting of a positively charged hydrophilic head – responsible for the interaction with the negatively charged phosphate groups of nucleic acids – and a hydrophobic tail connected by a linker structure. Moreover, due to their cationic nature, lipoplexes can interact with the negatively charged cell membrane promoting cellular uptake ^{16,26}.

Liposomes are spherical structures, formed by one or several concentric lipid bilayers surrounding discrete aqueous spaces, representing one of the most studied lipoplexes. They present several advantages, such as biocompatibility, low immunogenicity, possibility for site-specific targeting, and offer the possibility to deliver several biologically active compounds and macromolecules, such as DNA, peptides, proteins and imaging agents ²⁷. However, vesicle size

is a critical parameter regarding to liposome circulation time in the bloodstream, since unmodified liposomes, typically ranging from 25 nm to 2.5 μm , are readily cleared by the mononuclear phagocytic system (MPS), thus displaying short plasma circulation times ^{26–28}.

1.2.2.4.1 Solid lipid nanoparticles (SLNs)

Solid lipid nanoparticles have emerged in the early 1990's as an effective alternative to liposomes and polymeric nanoparticles ^{29,30}. Initially these carriers were intended for the delivery of hydrophobic and hydrophilic labile drugs of various classes, yet more recently they have been studied as potential gene carriers. These dispersions constitute versatile carriers as the active substance may be located either in the particle core, shell or dispersed homogeneously within the lipid matrix. Moreover, the surface of these particles can be modified to provide site-specific targeting ³⁰. Other advantages of these colloidal systems include the possibility of large scale production, biocompatibility, and excellent physical stability ^{28,30,31}.

The SLN manufacturing does not require the use of organic solvents ³¹ and, generally, all excipients used in their formulation are FDA (Food and Drug Administration) approved or of GRAS (Generally Recognized As Safe) status ³⁰. This is particularly important for systemic administration of genes, as the risk of acute and chronic toxicity can be reduced ³¹. Furthermore, these dispersions are suitable for sterilization and present sizes in the submicron range (50-1000 nm), allowing different administration routes, including the parenteral ³⁰. Hence, solid lipid nanoparticles combine the advantages of liposomes and polymeric nanoparticles, while avoiding their limitations, such as poor physical stability or safety concerns regarding to polymer toxicity ²⁸.

These colloidal particles are composed of one or more lipids, solid at room and body temperatures, stabilized by one or more surfactants ^{28,30}. A wide variety of lipids, surfactants and co-surfactants can be employed for SLN formulation, yet SLN composition has a great impact on their characteristics ³⁰. Herein, various lipids, from glycerides to fatty acids, waxes and steroids, have been used in SLN production ^{28,30}, and higher lipid content has been related, in most cases, to an increase in particle size and broader size distributions ³⁰. Moreover, numerous surfactants, providing steric stabilization, such as phospholipids, poloxamers, and polysorbates have been used and are of considerable importance for the formulation's physical stability ³⁰. Surfactant choice depends on the administration route intended for the dispersion. Therefore, those intended for parenteral administration are more restricted ³¹, as these should not cause toxic effects. Regarding to formulation's quality, higher concentrations of emulsifier have been correlated to smaller particle sizes ³⁰. Yet, increased amounts of surfactant have also been associated to higher toxic effects ³¹.

Cationic solid lipid nanoparticles, comprising cationic lipids, surfactants ³⁰, polymers or/and peptides ²⁹, have attracted increasing research attention as gene carriers, and are further discussed in this review. These carriers can interact with the anionic nucleic acid backbone and cell membrane, promoting cellular uptake and gene transfection ³⁰.

Although these colloidal particles have been reported to have excellent physical stability, in some cases over a year, storage under refrigerated conditions has been recommended, since it has been reported that formulations kept 4 °C presented better stability profiles than those kept at room temperature. Therefore, cooled transportation systems may be required, resulting in increased storage costs. However, this may be prevented by SLN lyophilization. Moreover, the rapid recognition of SLNs by the MPS, results in low circulation half-lives³⁰ and represents another disadvantage of these systems. Nevertheless, SLN rapid clearance can be prevented and will be further discussed.

1.2.2.4.1.1 SLN production technology

Various techniques for SLN production have been described over the past years. Summarily, all involve lipid dispersion in an aqueous surfactant phase. Yet, the high pressure homogenization technique remains the most commonly used, either in laboratorial or industrial context³⁰. A brief description of these methods, along with their respective advantages and disadvantages, is presented below.

1.2.2.4.1.1.1 High pressure homogenization (HPH) technique

High pressure homogenization (Figure 1.3) is a suitable technique for the production of SLN, that can be performed using room and below temperatures (cold HPH), or high temperatures (hot HPH). In both cases, particle size is reduced by cavitation. Furthermore, this technique allows the use of lipid concentrations up to 40%, yielding generally very narrow particle size distributions (Pdl <0.200)²⁸.

Lipid melting above its melting temperature (T_m) represents an initial common step for both cold HPH and hot HPH. However, the remaining steps diverge. In the cold HPH, the molten lipid is rapidly ground under liquid nitrogen, forming solid microparticles. Subsequently, a pre-suspension is formed by high stirring of the particles in a cold aqueous surfactant solution, and SLNs are formed upon the homogenization of this pre-suspension, for generally five cycles at 500 bar. In the case of hot HPH, the molten lipid is combined with an aqueous surfactant solution, pre-heated to the same temperature as the oil phase and stirred at high speed, resulting in a pre-emulsion, that will then be processed in a temperature controlled high pressure homogenizer, generally using three cycles^{28,30}.

Although these procedures allow the possibility of scale up production, it involves the use of expensive apparatus, and mechanical stress on the resulting product³⁰.

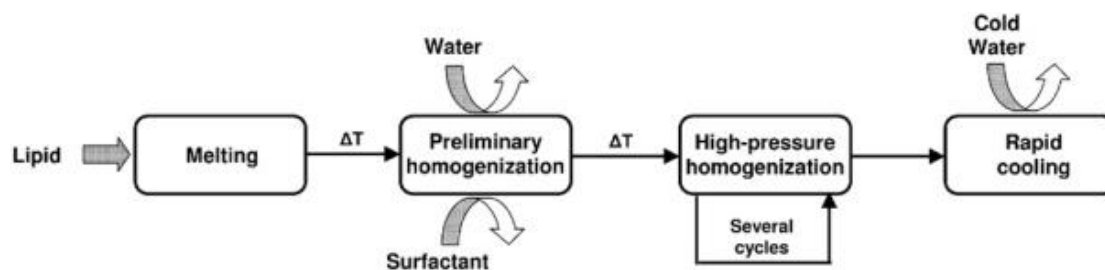


Figure 1.3 Summary representation of the main steps of the high-pressure homogenization process (adapted from Geske-Moritz, M. & Moritz, M. (2016)³⁰).

1.2.2.4.1.1.2 High shear homogenization technique

High shear homogenization represents an adaptation of the previously hot HPH described. Herein, the lipid is melted above its melting point, and subsequently combined with an aqueous surfactant solution, pre-heated to the same temperature as the oil phase. Subsequently, the dispersion is homogenized, using a high shear mixer, and cooled in a cold-water bath³².

This method allows the avoidance of organic solvents, that raise safety concerns due to their known toxicity, and enables large-scale production for commercial application. However, due to the high temperature applied, thermolabile compounds cannot be used^{32,33}.

1.2.2.4.1.1.3 Microemulsion technique

Similarly to the previously described methods, the lipid is melted above its melting point and combined with an aqueous surfactant solution (Figure 1.4), previously pre-heated to the same temperature as the oil phase³³. A warm microemulsion, containing ~10% of lipid, 15% surfactant and up to 10% co-surfactant, is prepared by stirring, and subsequently dispersed in excess cold water, to a typical 1:50 ratio, using a thermostated syringe. In order to increase particle concentration, the excess water is either removed by ultra-filtration or lyophilisation²⁸.

Although this method represents a simple technique³⁰, removal of excess water from the prepared SLN dispersion is a difficult task with regard to particle size. Also, high concentrations of surfactants and cosurfactants are necessary for formulating purposes, which is undesirable with regard to regulatory purposes and application²⁸.

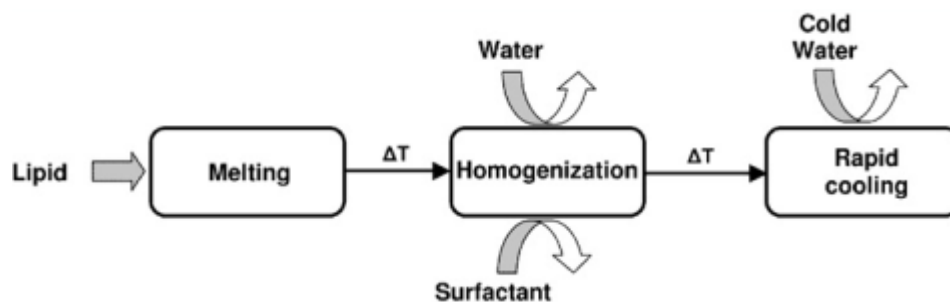


Figure 1.4 Summary representation of the main steps of the microemulsion technique (adapted from Geske-Moritz, M. & Moritz, M. (2016) ³⁰).

1.2.2.4.1.1.4 Emulsification and solvent evaporation method

The emulsification and solvent evaporation method is a simple technique, that allows to avoid the use of high temperatures for formulation purposes ³⁰. Herein, the lipid is dissolved in a water-immiscible organic solvent and combined with an aqueous phase, resulting in the formation of an emulsion (Figure 1.5). Subsequently, solvent evaporation is carried out under reduced pressure, and SLNs with an average size of 100 nm and narrow particle size distribution are formed as the lipid precipitates due to solvent evaporation ²⁸. However, the main disadvantage of this method regards to the use of water-immiscible solvents, which are harmful to humans and the environment, and may leave residues in the final dispersion ^{28,30}.

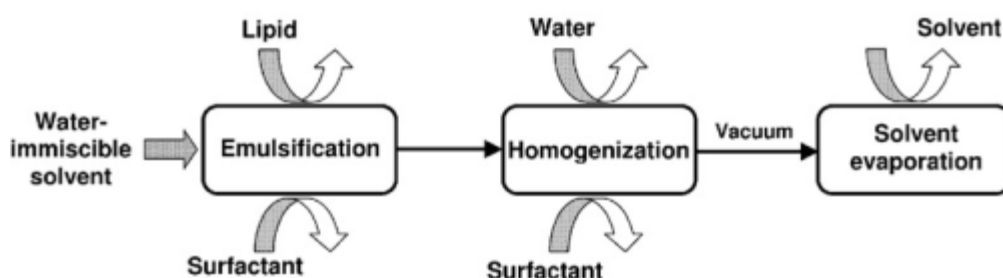


Figure 1.5 Summary representation of the main steps of the emulsification and solvent evaporation method (adapted from Geske-Moritz, M. & Moritz, M. (2016) ³⁰).

1.2.2.4.1.1.5 Emulsification and solvent diffusion method

Herein, partially water-miscible solvents are used to dissolve the lipid and combined with an aqueous surfactant solution at elevated temperatures. After the addition of excess water, SLNs form by precipitation due to the diffusion of the organic solvent from the emulsion droplet to the continuous phase (Figure 1.6). Because the dispersion is fairly dilute, concentration of the particles can be performed by ultra-filtration or lyophilisation ²⁸.

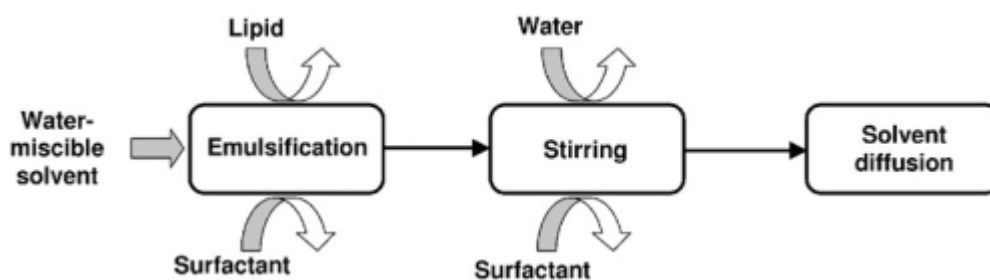


Figure 1.6 Summary representation of the main steps of the emulsification and solvent evaporation method (adapted from Geske-Moritz, M. & Moritz, M. (2016) ³⁰).

1.2.2.4.1.2 Strategies to help SLNs overcome biological barriers

The success of the gene therapy is determined by the ability of the vector to overcome the series of intra and extracellular barriers ^{12,16} which can deplete the amount of the therapeutic nucleic acid delivered to the targeted site ²⁶. The main reason for the lower transfection efficacies observed for non-viral gene delivery systems, when compared to their viral counterparts, relies in the difficulty of these systems to overcome the encountered biological hurdles ²¹, which largely depend on the intended administration route ²⁶. Therefore, the development of carriers capable to protect the genetic cargo and successfully overcome the various biological barriers, upon administration to the body, is of critical importance. For instance, the ideal gene delivery system should interact with the cell membrane, be internalized by the cell, escape the degradative endosomal compartment, and ultimately, deliver the genetic cargo to the site of action, in the case of plasmid DNA, the nucleus ²⁶. Additionally, minimal cell damage should be done during the transfection process.

1.2.2.4.1.2.1 Mononuclear phagocyte system

Upon intravenous administration of the gene delivery carriers, these are exposed to the different proteins present in the bloodstream, such as albumin, apolipoproteins and immunoglobulins ^{4,22}, that rapidly adsorb to the nanoparticle's surface, forming the protein corona ¹², which could change the physicochemical properties of the nanoparticles in circulation ⁴. This process is called opsonization and results in the carrier's sequestration by the mononuclear phagocyte system (MPS) that recognizes and attaches to these signalling proteins ²², being responsible for the clearance of these foreign particles from blood circulation ²⁶.

As mentioned before, one of the disadvantages regarding the use of SLNs refers to their rapid recognition by the MPS, which leads to their low circulation time, yet the surface of these particles can be modified to provide not only site-specific targeting ³⁰, but also prolong their half-life and enhance cell uptake and nuclear transfection.

Various grafting materials with shielding effects can be used to enhance SLNs' half-life in the bloodstream. Amongst these, poly(ethylene glycol) (PEG), a flexible, electrically neutral and

hydrophilic polymer, is one of the most commonly used materials to decrease the interaction between the nanoparticles' surface and the serum components that lead to its arrest by the MPS (Figure 1.7) ^{4,30}. This is made possible due to the tight association between ethylene glycol and water molecules that forms a hydrating layer which hinders protein adsorption and consequently avoids clearance by the MPS ²².

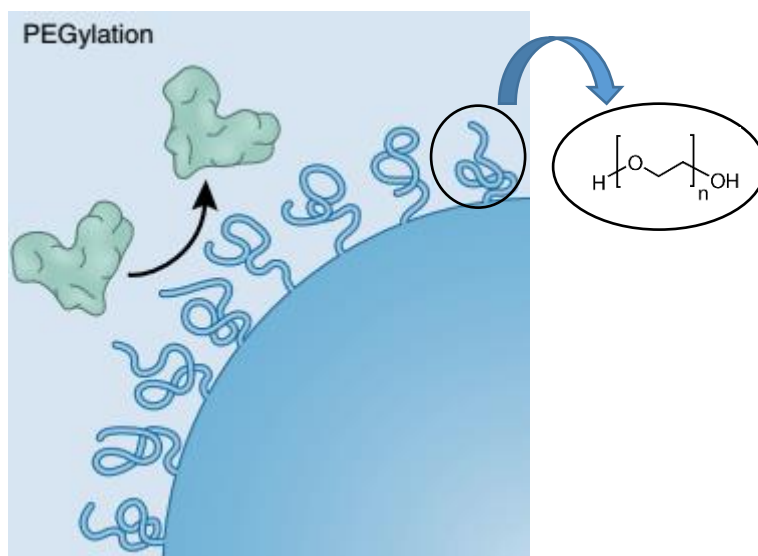


Figure 1.7 Steric hindrance provided by grafted PEG molecules onto the surface of the nanoparticle helps to prevent opsonization and MPS arrest (adapted from Blanco, E., Shen, H. & Ferrari, M. (2015) ²²).

Amongst other grafting materials, such as poly(vinyl) alcohol, polyamino acids and polysaccharides ²², triblock copolymers such as poloxamers (Pluronic[®]) (Figure 1.8) have been employed to enhance nanoparticles' circulation time ^{4,34}. These amphiphilic, non-ionic block polymers, are composed of a central hydrophobic poly(propylene oxide) (PPO), that adsorbs via electrostatic interaction onto hydrophobic surface of the SLN, flanked by two hydrophilic chains of poly(ethylene oxide) (PEO) that remain extended towards the hydrophilic interface ⁴. In a similar way to PEG, these molecules provide steric hindrance to the particle's surface, avoiding protein adsorption ³⁴.

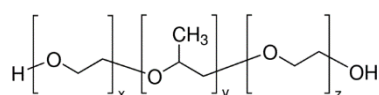


Figure 1.8 Chemical representation of poloxamers, composed by a central hydrophobic poly(propylene oxide), flanked by two hydrophilic chains of poly(ethylene oxide), that, respectively, adsorb onto the SLNs' surface and provide steric hindrance (adapted from <http://www.sigmaaldrich.com/poloxamer>)

Polysorbate 80 (Tween[®] 80) has also been reported to avoid recognition by the MPS, by providing steric hindrance. Additionally, nanoparticles coated by this non-ionic surfactant have also been reported to preferentially absorb apolipoproteins present in the bloodstream. These

proteins interact with specific receptors on the blood-brain luminal interface and are responsible for the translocation of the particles into the brain ³⁵.

1.2.2.4.1.2.2 Cellular uptake

After avoiding the MPS, the vehicles must be internalized by the cell ^{12,21}. Although direct penetration through the plasmatic membrane is possible for nanoparticles with 4 to 10 nm, in this size range particles are rapidly cleared by the kidney ¹². Therefore, interaction between the carrier and the cell membrane must occur, which can be carried out either by electrostatic interactions, in the case of non-specific cellular attachment, such as the mediated by cationic particles, or via receptor recognition, when specific targeting moieties are attached to the carrier ²¹. Next, the vector is internalized via different mechanisms that depend not only on the cell type, but also on the nanoparticle's physicochemical properties, such as size and shape of the construct, surface charge and hydrophobicity ^{12,21}, which will affect their biodistribution and clearance rate ¹².

Size has been reported to be one of the most important parameters ²¹ determining the preferential uptake mechanism, which possess its own size limitations and dynamics ¹². Endocytosis has been reported to be the main uptake mechanism for cationic nanoparticles ^{12,25}. Herein, nanocarriers in the size range of 500 nm to 10 μ m usually undergo phagocytosis and are cleared by the spleen, while particles <200 nm are preferentially internalized via clathrin-mediated endocytosis, and those comprising a size between 200-500 nm are internalized via caveolae-mediated pathway. However, prepared dispersions often contain particles of different sizes, making it likely to exist multiple uptake pathways contributing simultaneously ¹². Finally, the genetic cargo must escape the endosomal compartment and be released into the cytoplasm. Nevertheless, carriers containing plasmid DNA face an additional barrier – the nuclear envelope ^{21,22}.

1.2.2.4.1.2.3 Endosome escape

Posterior to cell internalization, the nanoparticles must be able to escape the endosomal compartment, characterized by its acidic and enzyme rich environment, capable to degrade the genetic cargo (Figure 1.9) ²².

Cationic SLNs have been suggested as an attractive approach for gene delivery, since they have the ability to interact electrostatically with both the anionic phosphate groups of the nucleic acids and the negatively charged cell membrane ³⁰.

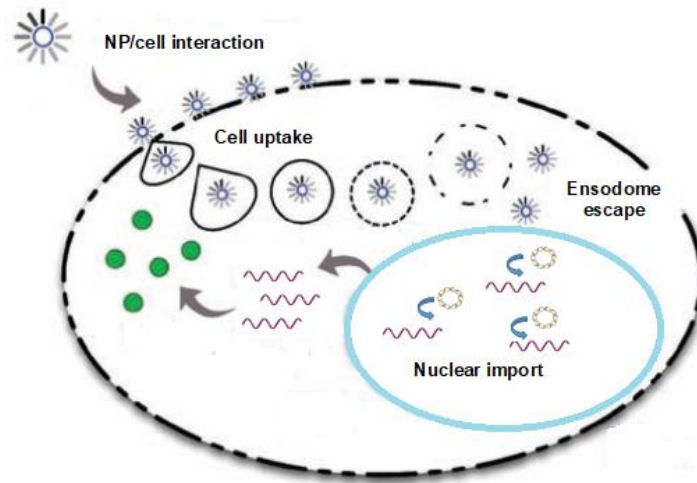


Figure 1.9 Common cell transfection steps to all administration routes. Cationic SLNs represent an attractive strategy to overcome endosome arrest and avoid nucleic acid degradation by this compartment (adapted from Hsu, C. Y. M. & Uludag, H. (2012) ¹²).

Various strategies can be used to achieve cationic SLNs. The use of cationic lipids ²¹ and surfactants ³⁰ constitutes one of the most commonly used approaches. Yet, as SLNs' surface can be modified, cationic polymers ³⁶, polysaccharides ³⁷ and peptides can also be grafted to provide a positive net-charge ^{29,38}. The present work will only focus on the latter strategy.

Polyethyleneimines (PEIs) have been mentioned before to form stable complexes with DNA, which possess improved cellular and nuclear uptake profiles ^{24,25}. Moreover, these polyplexes have been shown to protect their genetic cargo from degradation, by promoting endosomal escape ²⁴, through a still unclear mechanism.

The "proton sponge effect" is a proposed mechanism that tries to answer to how the PEI polyplexes avoid lysosomal degradation, protecting their genetic cargo. The V-ATPase proton pump is responsible for the proton influx into the endosome, conferring an acidic environment. Polyethyleneimines possess a high density of protonatable amine groups that under acidic conditions, such as those found in the endosome, act as a proton sponge and lead to the accumulation of chloride ions inside the endosomal compartment. This in turn results in increased osmotic pressure, and ultimately in the vesicles' disruption ^{12,16,21}.

Regardless of the advantages shown by PEI-based vectors for gene therapy, their use is still limited due to potential cytotoxic effects. Therefore, a combination of cationic-polymer based complexes with lipids, benefiting from the advantages of both the intervenient, has been explored to improve gene therapy ²⁴. Ewe, A. *et al* (2016) ²⁴ demonstrated that lipoplex-polyethyleneimine complexes, consisting of PEI/siRNA complexes combined with DPPC liposomes (1,2-dipalmitoyl-*sn*-glycero-3-phosphocholine), were efficient gene carriers, since these complexes showed good cellular and nuclear uptake, which resulted in the knockdown of approximately 80% of the target gene, no cytotoxic effects or erythrocyte aggregation, and improved circulation times without the need of PEG. Therefore, by extrapolation of the obtained results, the use of SLNs with surface

modulated properties using PEI provides an attractive approach for gene delivery, since SLNs possess an improved physical stability profile comparatively to liposomes.

Chitosan is a natural occurring, biocompatible and biodegradable polysaccharide, that is positively charged under acidic conditions. This compound has been investigated for gene delivery, as it is able to interact with the cell membrane due to its cationic nature, provided by the amine groups in its structure ³⁹. This polysaccharide is relatively non-toxic, with high cellular uptake ³⁰ and transfection efficacy ^{37,39}. Hence, the use of SLNs containing grafted chitosan represents an attractive approach to improve these lipid nanoparticles' transfection efficacy.

Moreover, fusogenic peptides that mimic those of the viral vectors also constitute an attractive strategy to escape the endosomal compartment. GALA is a 30-amino acid synthetic peptide, consisting of glutamic acid-alanine-leucine-alanine (EALA) sequence repetitions, that can suffer conformational transformation under low pH conditions, triggering endosomal membrane disruption ²¹.

1.2.2.4.1.2.4 Nuclear import

After gaining access to the cytoplasm, carriers intended to deliver DNA, must access the nucleus and deliver their cargo ²² Non-viral vectors, such as SLNs, are conditioned by biological barriers towards their translocation into the cell's nucleus ²⁹, as the nuclear envelope is highly selective for molecules over 40 kDa, such as plasmids ²².

Dividing cells allow the carrier to gain access to the nucleus during mitosis ²¹. However, for non-dividing cells another pathway is required to surpass the nuclear envelope. Hence, one proposed mechanism refers to the import of the genetic cargo through the nuclear pore complex (NPC) (Figure 1.10). This process requires nuclear localization signals (NLS) that promote the active nuclear transport of peptides containing arginine residues in their sequences ³⁸.

Protamine is a small cationic nuclear protein, involved in DNA packaging in sperm cells that has been used as a transfection promotor in gene therapy due to its rich content in arginine – six consecutive residues ^{29,38}. However, due to its hydrophobicity, protamine/DNA complexes present low transfection efficacies resulting from its difficulty in crossing the cellular membrane. Additionally, the strong compact complex formed between protamine and DNA results in the difficult release of the genetic cargo, compromising transfection efficacy ²⁹.

Solid lipid nanoparticles intended for plasmid DNA delivery with protamine surface modulated properties have been explored by Vighi, E. *et al* (2010) ²⁹, whom obtained small (<400 nm) and positive (+25mV) complexes, with excellent pDNA condensation properties. This group also demonstrated that a slight enhancement in cell transfection was observed for the NPs, when compared to those without transfection promoters. Moreover, they have also reported that these complexes could be located in the cytosol and nucleus after 12 h of incubation, with pGFP expression being observed after 24 h of incubation.

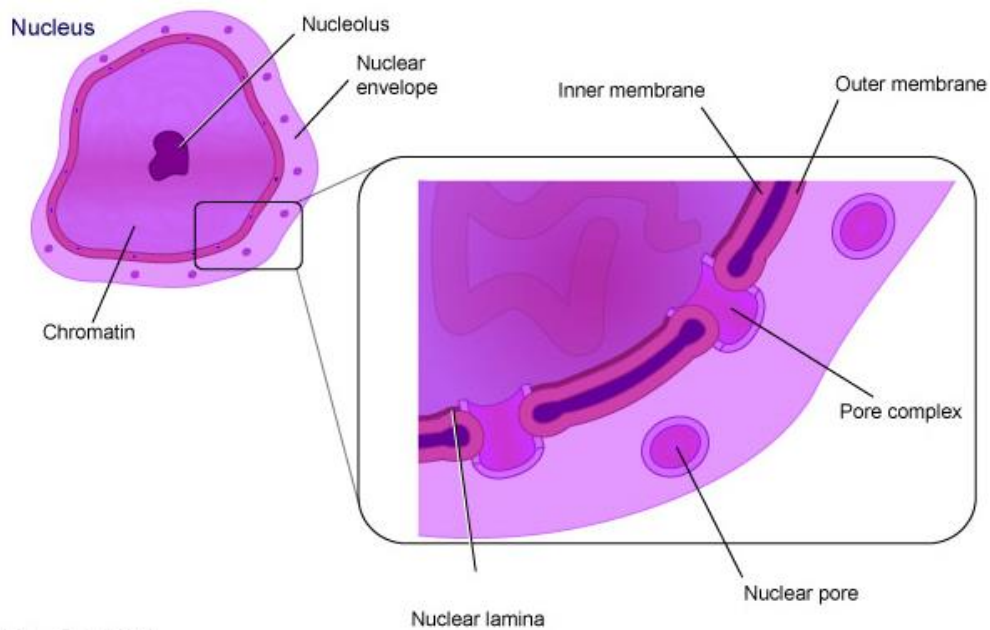


Figure 1.10 Schematic representation of the nuclear compartments. The nuclear envelope represents a major hurdle to gene delivery. However, the import of the genetic cargo through the nuclear pore complex, which requires nuclear localization signals promoting the active nuclear transport of peptides containing arginine residues, such as protamine, represents a mechanism to overcome this barrier (adapted from <http://lucykarpukhno.weebly.com/nucleus>).

Hybrid SLNs, comprising cationic polymers, peptides and stabilizers, that help them escape the endosomal environment; promote nuclear import; and avoid sequestration by the MPS, respectively, represent a new and innovative strategy for gene delivery and were therefore object of this project.

Chapter 2 Objective

The present work aimed the development of new hybrid gene delivery carriers, using cationic polymers and peptides to modulate the surface of solid lipid nanoparticles.

The key points of this project were:

1. Production of SLN varying different formulation conditions, and further surface modulation using cationic polymers and peptides;
2. Physicochemical characterization of the SLNs;
3. Physical stability evaluation under different storage conditions;
4. Evaluation of SLNs' cytotoxicity;
5. Assessment of the new SLNs' capacity to condense pDNA;
6. Evaluation of the new developed SLNs' transfection efficacy;
7. Haemocompatibility assay.

Chapter 3 Materials and methods

3.1 Materials

Precirol® ATO 5 (glyceryl palmitostearate) and Geleol™ pellets (glycerol monostearate) were kindly provided by Gattefosé (France). Tripalmitin (glyceryl tripalmitate), tristearin (glyceryl tristearate), branched polyethylenimine (MW ~25 000), branched polyethylenimine (MW 2 000), linear polyethylenimine (MW ~10 000), chitosan low molecular weight, protamine, Pluronic® F-68 (poloxamer 188) and phosphate buffer saline (PBS) were purchased from Sigma-Aldrich (USA). Pluronic® F-127 (poloxamer 407, Lutrol® F-127) was acquired from O-BASF (Germany). Imwitor® 491 powder was purchased from Oleochemicals and Tween® 80 (polysorbate 80) was bought from Merk (Germany). Purified water was obtained by inverse osmosis (Millipore, Elix 3) with a 0.45 µm pore filter. All other reagents were of analytical grade and were used without further purification. Cell viability was tested in a HEK 293T cell line (human embryonic kidney epithelial cell line, ATCC CRL-11268™). RPMI 1640 culture medium and other supplements were purchased from Thermo Fisher Scientific (UK). Plasmid extraction and purification was made using Quiagen midi kit (USA).

3.2 Methods

3.2.1 SLN production

Solid lipid nanoparticles were initially produced via the solvent evaporation method and hot high shear homogenization, for different lipids.

3.2.1.1 Solvent evaporation technique (SET)

SLNs were produced via SET, according to the procedure described by Duran-Lobato, M. *et al* (2015)⁴⁰. Briefly, the lipid was dissolved in dichloromethane (DCM) and then the aqueous phase, containing the surfactant, was added. Next, the dispersion was homogenized for 5 min using a high shear mixer, Silverson L5M and general-purpose disintegrating head (Silverson Machines, UK, Figure 3.1). The dispersion was then kept under stirring at 300 rpm for 2 h at room temperature until complete evaporation of the organic solvent. The formulations were conserved at 4 °C until further use.

3.2.1.2 Hot high shear homogenization technique (HSH)

Different lipids and emulsifying agents were tested using the HSH technique, previously described by Gaspar, D. P. *et al* (2016)³². Briefly, the lipid phase was melted at a temperature 10

°C above its melting point, and a previously prepared surfactant aqueous solution was heated to the same temperature. A pre-emulsion was formed by addition of the aqueous phase to the metered lipid. Homogenization was performed for 5 min, using the high-shear homogenizer, Silverson L5M containing the general-purpose disintegrating head (Silverson Machines, UK; Figure 3.1). The SLN dispersions were obtained by cooling the emulsion, in an ice bath, for 5 min. Samples were then stored at 4 °C until further use.

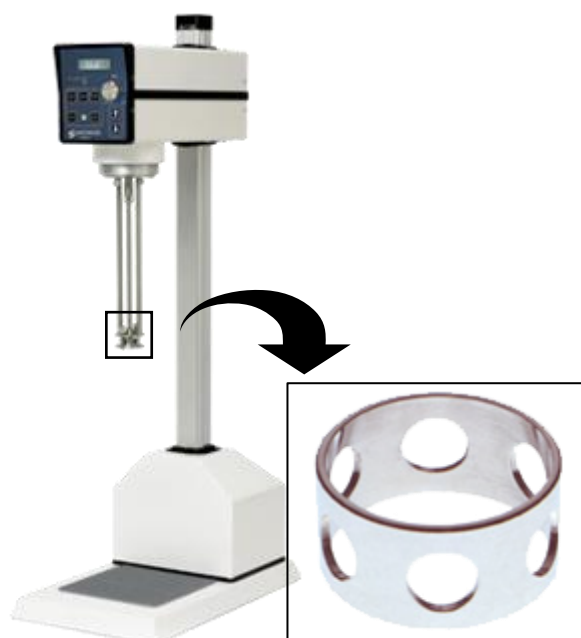


Figure 3.1 General-purpose disintegrating head from Silverson Machines used in SLN formulation (adapted from <http://www.silverson.com/us/workheads>, consulted in Aug. 15, 2017).

3.2.2 Surface modulation

SLNs containing a cationic polymer (hyNP_x) (polyethyleneimine or chitosan) and SLNs containing a combination of cationic polymer and a cationic peptide (protamine) (hyNP_xP) were produced. Hybrid nanoparticles (hyNPs) were produced via HSH and adsorption. Briefly, when produced via HSH, the polymer and peptide were dissolved in the aqueous phase, that would then be heated and added to the oil phase. When produced via adsorption, an aliquot of anionic SLNs was added to a previously prepared solution, containing the cationic polymer or peptide, under magnetic stirring.

3.2.3 Physicochemical characterization

3.2.3.1 Particle size

The mean average size was measured by Dynamic Light Scattering (DLS) using a Zetasizer Nano S (Malvern Instruments, UK), sensible to particles in the 0.6 nm to 6 µm size

range. Based on Mie's theory, DLS measures the Brownian motion and correlates it to particle size ⁴¹.

Samples were placed in a polystyrene cuvette and diluted in purified water (1:4), and for each, 3 measurements were performed. Results were expressed in terms of average size and polydispersity index (Pdl).

3.2.3.2 Surface charge

Surface charge was determined using Zetasizer Nano Z (Malvern Instruments, UK), considering the electrophoretic mobility ⁴¹.

Sample introduction into the electrophoretic cell (Figure 3.2) was carried out using a syringe containing the samples diluted 1:16 in 3 mL of purified water. For each prepared formulation, 3 measurements were performed.

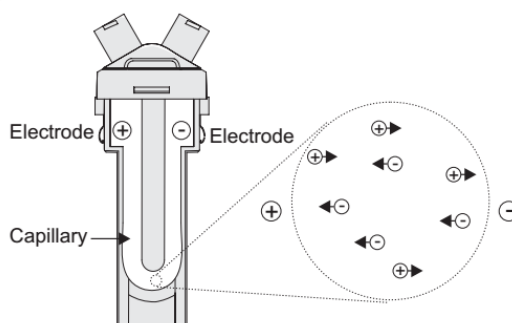


Figure 3.2 Schematic electrophoretic cell representation (adapted from Zetasizer Nano Series User Manual (2004) ⁴¹).

3.2.3.3 Transmission electron microscopy

The morphological analysis of the prepared hyNPs was conducted by Transmission Electron Microscopy (TEM). Briefly, samples were fixed on racks of copper covered by a membrane of carbon for observation. Subsequently, they were analysed with a JEOL Microscopy (JEM 2010, Japan) at 120 kV, and the images were acquired through a Gatan Orius™ camera.

3.2.4 Stability assays

Suspension stability was studied regarding temperature and dispersion medium. Samples stored at 4 °C and room temperature, were protected from the light, and their stability was followed for 3 months. Measurements regarding the mean hydrodynamic diameter and polydispersion index (Pdl) were made on the day following hyNPs' production, and once a month over the next 3 months. Zeta potential (ZP) values were only assessed on the day after hyNPs' production and on the third month. Their stability under body temperature was also determined.

Therefore, samples were placed in a 37 °C water bath for 2 h. The impact of sterilization by autoclaving (121 °C/15 min) and freeze-drying was also evaluated.

Additionally, the nanodispersions' stability in different storage mediums was studied, in 10 mM phosphate buffer solution (PBS) and simulated body fluid (SBF) ⁴². Briefly, an aliquot of each sample was diluted 1:4 in each buffer. Measurements regarding size, Pdl and ZP were performed after 1 h for samples placed in PBS, and 1 and 24 h for samples placed in SBF.

3.2.5 *In vitro* cell viability studies

The cytotoxicity of the produced hyNPs was assessed with a HEK 293T cell line (human embryonic kidney epithelial cell line, ATCC CRL-11268), using the Alamar blue reduction and propidium iodide (PI) exclusion assays ^{32,37,43}.

On the day prior to the experiment, HEK 293T cells were seeded in sterile flat-bottom 96 well tissue culture plates (Greiner, Germany), in RPMI 1640 culture medium, supplemented with 10% foetal bovine serum, 100 U/mL of penicillin G, 100 µg/mL of streptomycin sulphate and 2 mM of L-glutamine (Gibco, Thermo Fisher, UK), at a cell density of 2x10⁵ cells/mL and 100 µL per well. Cells were incubated at 37 °C and 5% CO₂

On the experiment day, the culture medium was replaced by fresh medium and hyNPs were added to a final concentration of 500 µg/mL. Each sample was tested in 8 wells per plate. Additionally, cells were also incubated with Pluronic® F-68 and culture medium (negative controls) and sodium dodecyl sulphate (SDS) (positive control). After 6 and 24 h, the exposition medium was replaced by fresh culture medium containing 0.3 µM of propidium iodide (stock solution 1.5 mM in dimethyl sulfoxide (DMSO), diluted with the culture medium 1:5000, and fluorescence was measured at λ_{excitation}=458 nm and λ_{emission}=590 nm, using the microplate reader (FLUOstar Omega, BMG LabTech, Germany). Subsequently, the medium was replaced by fresh medium containing 5 mM of resazurin (Alamar blue assay), and the cells were incubated for 3 h. New fluorescence measurements were performed at λ_{excitation} =530 nm and λ_{emission}=590 nm, using the microplate reader. The propidium iodide uptake and relative cell viability (%) were calculated according to equations 1 and 2, respectively, and compared the control cells.

$$PI\ uptake = \frac{Sample\ fluorescence}{Control\ fluorescence} \quad (1)$$

$$Cell\ viability\ (\%) = \frac{Sample\ fluorescence}{Control\ fluorescence} \times 100 \quad (2)$$

3.2.6 Plasmid production and purification

The plasmid production and purification was based on the procedure previously described by Cadete, A. *et al* (2012) ³⁷. Briefly, the plasmid expressing green fluorescent protein

(pGFP) was used to transform competent *Escherichia coli* (ATCC, USA). Cells were grown in tryptic soy broth (TSB) medium, at 37 °C with agitation, until the end of the exponential growth phase was reached. The cells were then isolated by two centrifugation cycles. The pellet obtained in the first cycle was resuspended by gentle vortex in cold MgCl₂ (0.1 M), whereas the pellet obtained in the second centrifugation cycle was resuspended in CaCl₂ (0.1 M). The obtained competent cells were stored at -80 °C, until further use.

Plasmid purification was then performed according to the Qiagen Midi Kit instructions, and the nucleic acid was quantified by UV spectroscopy at 260 nm, using the microplate reader (FLUOstar Omega, BMGLabtech, Germany) ⁴⁴.

3.2.7 pDNA-hyNP complexes

Spontaneous pDNA-hyNP complexes were formed after 15 min under mild agitation, upon addition of pDNA to an aliquot of each formulation, to the final ng SLN/ng pDNA ratios of 104:1 and 208:1. The efficacy of pDNA condensation onto the hyNPs was assessed by the gel retardation assay, using 1% agarose, and quantified by fluorescence, using propidium iodide, and compared to pDNA-PEI complexes (control group). The physicochemical properties of pDNA-hyNP complexes was also assessed, in terms of size, Pdl and surface charge.

3.2.8 Quantitative uptake assessment

Coumarin-6 loaded hyNPs were prepared via HSH, and the fluorophore was incorporated into the melted lipid, before homogenization, accordingly to the procedure described by Gaspar, D. P. *et al* (2016) ³². HEK 293T cells were grown in 96 well plates at the same density reported for the cell viability assays, and incubated in the same conditions. Subsequently, the culture medium was removed and replaced by 100 µL the different Coumarin 6 loaded hyNPs prepared, in order to obtain the final concentrations of 167 µg/mL and 83 µg/mL. Fluorescence measurements were performed at $\lambda_{\text{excitation}}=485$ nm and $\lambda_{\text{emission}}=520$ nm, immediately after hyNPs' addition and at each incubation times (37°C, 5% CO₂), after 3 washing steps with 250 µL of PBS containing 20 mM glycerine at pH 7.4 and pre-warmed at 37 °C were made. New fluorescence measurements were made after the PBS solution was removed and the cells were disrupted with 100 µL of 1% Triton X-100, in order to determine the amount of internalized hyNPs. Using particle fluorescence as a function of their concentration, it was possible to determine the amount of internalized hyNPs by the cells.

3.2.9 Fluorescence microscopy

Cell cultures were performed at same conditions as those described for the *in vitro* cell viability assays. Cells were grown on 24 multi-well plates containing sterile grass slides (Greiner, Germany). After one hour of incubation with hyNPs, cells were rinsed 3 times with 10 mM PBS

containing 20 mM glycerine at pH 7.4 before and after being fixed for 15 min at room temperature, and protected from the light, with 4% (w/v) paraformaldehyde (Sigma-Aldrich, UK). Then, cells were permeabilized with 0.1% Triton X-100 for 4 min, in order to stain the actin with rhodamine phalloidin, and rinsed 3 times with PBS. The 6.6 μ M phalloidin-TRITC solution (Life Technologies) in PBS was added to the cells for 30 min at room temperature. After the cells were newly rinsed with 10 mM PBS containing 20 mM glycerine at pH 7.4, and air-dried, the cell slides were mounted in fluorescent mounting medium ProLong[®] Gold antifade reagent with DAPI (4'-6-diamidino-2'-phenylindole dihydrochloride) (Life Technologies, UK) and their fluorescence was observed and recorded on an Axioscop 40 fluorescence microscope (Carl Zeiss, Germany), equipped with an AxioCam HRc camera (Carl Zeiss, Germany). The AxioVision Rel. 4.8.1 software (Carl Zeiss, Germany) was used to process the images.

3.2.10 *In vitro* transfection studies

Transfection assays were performed on HEK 293T cells. The latter were cultured to a cell density of 1×10^4 cells/well in RPMI media, supplemented with 10% foetal bovine serum, 100 U penicillin, and 0.1 mg of streptomycin per millilitre (Thermo Fisher Scientific, UK), at 37 °C and 5% CO₂ in a humidified atmosphere.

Cell transfection was performed in 96 well plates (Greiner, Germany) using nanoparticles containing pDNA expressing Green fluorescence protein (pGFP), at a concentration of 167 and 83 μ g/mL, to a final ratio hyNPs/pGFP (w/w) of 208:1 and 104:1, respectively, using 8 ng/well of pGFP. Additionally, a solution of PEI 1 mg/mL and culture medium were used as positive and negative controls, respectively.

The samples were prepared by mixing hyNPs with plasmid at room temperature for 30 min. Then these complexes were applied to cells and left to incubate for 14 h. After this time, the formulations were removed and 100 μ L of fresh medium was added.

The plasmid expression was observed by fluorescence at a $\lambda_{\text{excitation}} = 485$ nm and $\lambda_{\text{emission}} = 525$ nm, using a microplate reader (FLUOstar BMGLabtech, Germany), after 48 h post-transfection. Moreover, cell viability was evaluated after the assay, using the previously described Alamar blue assay, and the obtained fluorescence results were normalized to the total of viable cells.

The assay was performed in 8 wells for each formulation and repeated twice.

3.2.11 Haemocompatibility

Haemocompatibility of the produced hyNPs with red blood cells was assessed by measuring the percentage of haemolysis of the blood samples. The percentage of haemolysis was evaluated in EDTA-anticoagulated blood⁴⁰, obtained from a healthy 24-year-old male. Samples of each prepared hyNPs were placed in contact with pooled blood aliquots at a

blood/sample ratio of 100:20 (v/v), and incubated at 37°C for 2 h, under mild shaking. PBS-treated blood and (1%w/v) Triton X-100-treated blood, were used as positive and negative controls (100% lysis), respectively. Both, samples and control-treated blood, were centrifuged at 800 x g, for 15 min at 25°C. In order to estimate the extent of erythrocyte lysis, the amount of haemoglobin released into the supernatant was quantified by colorimetric detection at 545 nm and plotted in terms of percentage of haemolysis according to equation 3, where $A_{Hb (hyNP)}$ and $A_{Hb (positive control)}$ refer to the amount of haemoglobin released into the plasma when blood was exposed to the samples and Triton X-100 (1% w/v), respectively.

$$Haemolysis (\%) = \frac{A_{Hb (hyNP)}}{A_{Hb (positive control)}} \times 100 \quad (3)$$

3.2.12 Statistical data analysis

Statistical analysis of the experimental data was performed using a one-way analysis of the variance (one-way ANOVA) and the significance of the differences between groups was assessed by Turkey-Kramer multiple comparison test, assuming $p < 0.05$ as significant (GraphPad PRISM 5, USA). The data are expressed as mean and standard deviation (mean \pm SD) of separate experiments

Chapter 4 Results and discussion

4.1 Physicochemical characterization

4.1.1 Production technology

Solid lipid nanoparticles (SLN) offer several advantages as gene carriers. These include physiological well tolerated composition and relatively low cost of the excipients, various possible routes of administration, namely intravenous, easy scale-up and a wide range of technology by which they can be produced^{45,46}. Amongst the different formulation techniques, the high-pressure homogenization and microemulsion methods are the most commonly used in laboratorial context³⁰, however high-speed stirring, sonication, and emulsification and solvent evaporation techniques have also been employed⁴⁶. SLNs can be prepared using a variety of solid lipids and surfactants, which have a great impact on their physicochemical properties, as different compounds might require different preparation methods³⁰. Therefore, stepwise optimization is highly important for SLN production, especially for those intended for intravenous administration. Concerning SLN characteristics, size, polydispersity index (Pdl) and zeta potential (ZP) measurements were made in all steps, for each produced batch.

The Zetasizer Nano S is a powerful tool to characterize nanoparticles, as it covers a size range up to 6 μm ⁴¹. Therefore, data presenting values greater than the upper detection limit of the equipment, were considered unreliable and termed as “aggregation” in the presented results (Table 4.1).

In the present work, SLNs were initially produced via the solvent evaporation technique (SET) and hot high shear homogenization (HSH). Tristearin and tripalmitin were used as lipid components at a final concentration of 0.8% (w/v) when produced by SET and 1% (w/v) when produced by HSH. The selected surfactants were limited to those accepted for pharmaceutical use for parenteral administration, such as poloxamer 188 and 407 and polysorbate 20 and 80⁴⁷⁻⁴⁹. Hence, Tween® 20/Polysorbate 20 (0.5 %w/v), was originally selected as the emulsifying agent.

Table 4.1 shows the obtained mean size, Pdl and ZP values for the prepared batches. Samples prepared using SET, obtained better results than those prepared by HSH. However, this technique requires the use of DCM, an organic solvent, to dissolve the lipid. Since, the aim of the study is the development of SLNs intended for intravenous administration, the use of organic solvents should be avoided. Nevertheless, HSH was selected to be used in the subsequent steps, as the use of organic solvents could be avoided.

Table 4.1 Selection of the SLNs' production method. Nanoparticles were produced via the solvent evaporation technique (SET) and hot high shear homogenization (HSH), using tristearin and tripalmitin as the lipid matrix. Results of the first produced SLNs presented in terms of average size (Z-ave), Pdl and ZP (mean±SD, n=3).

		Z-ave (nm)	Pdl	ZP (mV)
Tristearin	SET	895±183	0.535±0.260	-25±1
	HSH	Aggregation		
Tripalmitin	SET	545±66	0.429±0.080	-26±1
	HSH	845±142	0.832±0.171	-

4.1.2 Surfactant choice, volume and concentration

Surfactants' choice and its concentration are among the variables that have great impact in SLNs' characteristics^{30,31,50}. Higher concentrations of emulsifier have been noted to decrease particle size, which is desirable for intravenous administration^{30,31}. However, higher amounts of surfactant have also been related to increased cytotoxicity³¹, and is therefore to be avoided. Thus, the lipid phase is generally dispersed in an aqueous phase of 0.5-5% (w/w)⁵¹.

Tween® 80 is a non-ionic surfactant commonly used in pharmaceutical products, such as parenteral dosage forms. In order to understand the influence of the surfactants' volume on the produced SLNs, 5, 10 and 15 mL of Tween® 80 (2% (w/v)) were added to 50 mg of tripalmitin. The resultant SLNs presented average sizes <200 nm (Table 7.1, Appendix A), and no significant differences in terms of size or ZP were found between each batch ($p > 0.05$).

Particle size distribution is a key factor for intravenous intended formulations, since the mean diameter of the fine capillaries is around 9 µm. As SLNs are not deformable, particle size should be completely in the submicron range, as capillary blockage can occur if the particle exceeds the blood vessel diameter³¹. Analysis of Table 7.1 (Appendix A) easily allows inferring that 10 and 15 mL of Tween® 80 presented the best Pdl results. In fact, these batches were significantly different in terms of Pdl values when compared to those formulated with 5 mL of Tween ($p < 0.05$), but no significant differences were found between them (Figure 4.1). Furthermore, as these formulations obtained similar results, a volume of 10 mL was selected to be used in the in the following optimization steps.

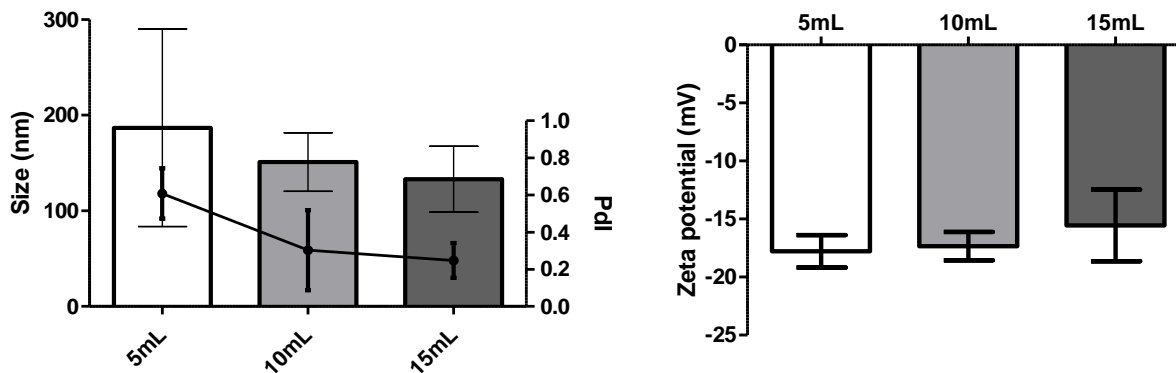


Figure 4.1 Influence of the different volumes of surfactant tested on SLN's physicochemical properties. The surfactant's volume choice was made by selecting the one that allowed to obtain the smallest particle size and the smallest particle size dispersion. Results presented in terms of: (A) Z-ave and Pdl; (B) Zeta potential. (mean±SD, n=3)

Poloxamers are amphiphilic block copolymers of poly(ethylene oxide) and poly(propylene oxide), FDA approved and suitable for intravenous administration⁴⁷. The application of these non-ionic surfactants has attracted researchers' attention for gene delivery, since they have been reported to enhance transfection efficacy⁵². Therefore, the use of Tween® 80 was abandoned, and the influence of Pluronic® F-68 (PF68) and Pluronic® F-127 (PF127) on SLNs physicochemical properties was studied. Tripalmitin was used as the lipid phase, and for both poloxamers the concentration was varied from 0.1-2% (w/v). The obtained results are presented in Table 7.2 (Appendix A).

All prepared batches obtained particles with mean sizes <500 nm. No significant differences were found in terms of average size and Pdl values between batches of different tested concentrations of PF68. However, this was not observed in terms of ZP values, where significant differences between concentrations were found for the exception of 1 and 0.5% of PF68. Interestingly, an inversion of ZP value was observed for 2% of the emulsifier. However, due to the non-ionic character of poloxamers⁵², no charge modulation should be expected, and only negative charges from the lipid should have been detected. When comparing the results obtained for batches containing PF127 as the emulsifying agent, significant differences between the tested concentrations were found in terms of size and Pdl values, but not in terms of ZP.

In order to understand the influence of the surfactant choice on SLNs quality, Pluronic® F-68 and F-127 were compared at different concentrations (Figure 4.2). No significant differences in terms of size and Pdl values were found between them, except for a concentration of 2% and 0.1% of surfactant, for size and Pdl, respectively. Zeta potential values were, however, significantly different between them. As no trend appears to be evident, the choice of the surfactant agent, for the following steps, was made by selecting the surfactant that allowed the smaller mean hydrodynamic diameter and Pdl values at the lowest concentration tested.

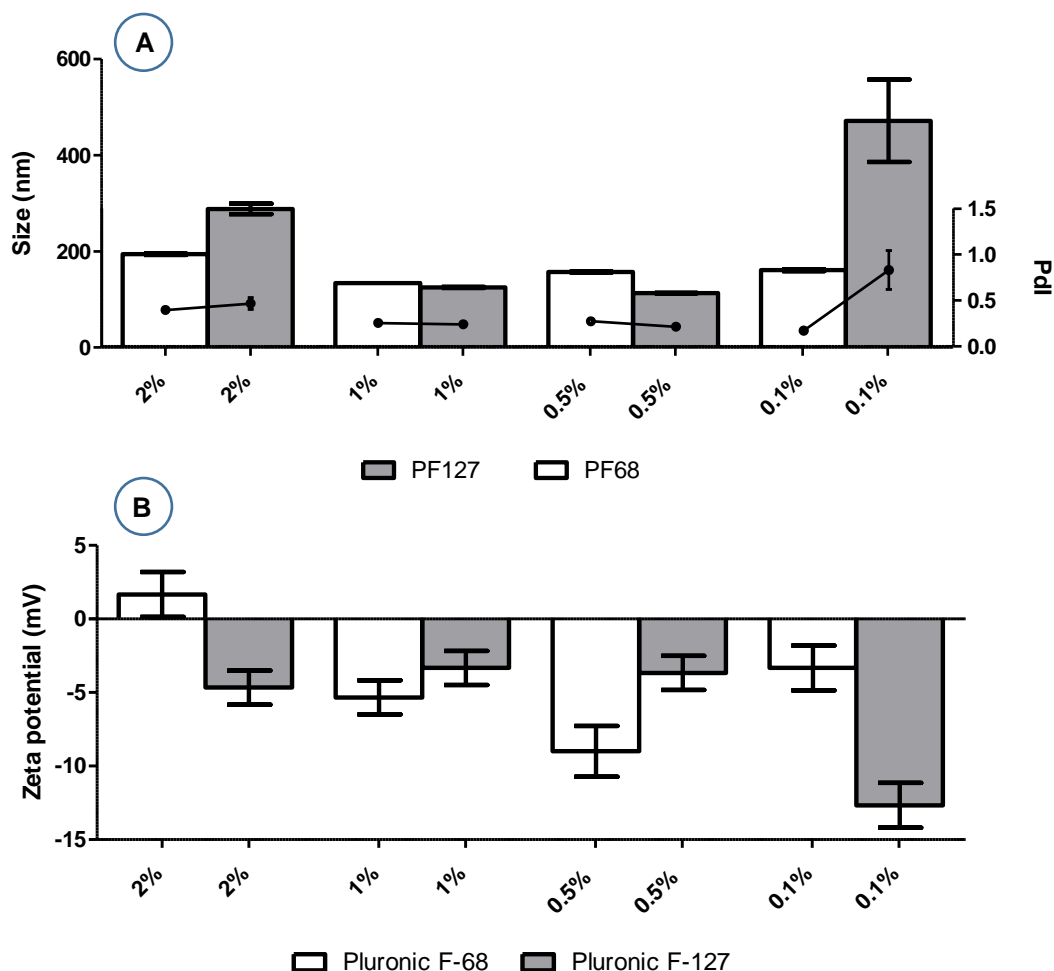


Figure 4.2 Influence of the Pluronic® type and concentration on SLN's physicochemical properties. The selected surfactant should produce the smallest particles, with the smallest particle size dispersion, at the lowest concentration. Results in terms of (A) mean hydrodynamic diameter and Pdl; (B) mean surface charge. (mean±SD, n=3)

4.1.3 Lipid choice and concentration

The amount of lipid, similarly to the surfactant, is a determinant factor in the physicochemical properties of the obtained nanoparticles. For instance, it has been found that the average particle size on SLN dispersions increases with higher melting point lipids, and that although SLNs are generally composed of 0.1-30% (w/w) of lipid⁵¹, it has been reported that an increase on the lipid content over 5-10%, in most cases, resulted in larger particles and broader size distributions³¹.

Herein, 0.5 and 1% (w/v) lipid concentration were tested, using tripalmitin. An expected increase in the negative charge density was observed for batches containing a higher amount of lipid. For both batches, particles presented, unexpectedly, sizes >1 µm and Pdl values >0.700 (Table 4.2). These results do not meet those obtained in the previous tested parameter, where for 0.5% (w/v) of tripalmitin, using the Pluronic® F-68 (0.1% w/v), the obtained particles presented a mean hydrodynamic diameter of 161±2 nm and a Pdl of 166±0.011. The mean zeta potential

was also significantly less negative than the obtained in this optimization step. Therefore, no conclusions could be drawn and the initial lipid concentration was maintained through the following steps.

Table 4.2 Influence of the lipid concentration on SLN particle size and zeta potential, using 0.5 and 1% (w/v) of lipid (mean±SD, n=3).

	%(w/v) lipid	Z-ave (nm)	Pdl	ZP (mV)
Tripalmitin	0.5%	2840±1567	0.745±0.298	-14±2
	1%	1267±434	0.793±0.132	-20±1

Acylglycerols are esters formed from glycerol and fatty acids. Depending on the degree of esterification of glycerol's hydroxyl groups, this is, the amount of fatty acids condensed to glycerol, monoglycerides, diglycerides or triglycerides can be obtained (<http://www.sigmaaldrich.com/glycerides>, consulted in Aug. 5, 2017). Fatty acids' physical properties, namely hydrophobicity and melting point, are determined by the length and degree of unsaturation of the hydrocarbon chain. Hence, the longer the hydrocarbon chain, the lower the solubility of the fatty acid in water, with only the polar carboxylic acid group accounting for the slight solubility. In fully saturated compounds, with a fully extended form, fat molecules are able to pack together tightly in nearly crystalline arrays, increasing the thermal energy required for their disorder, or in other words, their melting temperature ⁵³.

The influence of the lipid matrix of SLNs was assessed using glyceryl tripalmitate (tripalmitin, Figure 4.3 A), glyceryl distearate (Precirol[®], Figure 4.3 B) and glyceryl monostearate (Imwitor[®] 491 and Geleol[™], Figure 4.3 C) (Table 4.3). These lipids present long hydrocarbon chains, conferring a rigid and stable lipid matrix, and high melting temperatures (>40°C), essential for SLN application *in vivo*. Nanoparticles containing Precirol[®] and Geleol[™] showed the best results and were for this reason used in the following steps. SLNs containing these lipids had average sizes of 241±25 and 137±9 nm, respectively, and polydispersity indexes <0.250, indicating a narrow size distribution (Table 4.3). No significant differences between these lipids were found in terms of size or Pdl values. However, significant differences, in terms of size and population distribution, were detected between batches containing these lipids and those containing tripalmitin. The latter batches revealed a mean hydrodynamic diameter of 1895±700 nm and a broad size distribution (0.841±0.205). For this reason, the use of tripalmitin was discontinued.

No measurements were made for SLN consisting of Imwitor[®] 491, since a foam-like structure was formed when homogenizing the lipid with Pluronic[®] F68 (0.1%) (Figure 7.1, Appendix B). This could possibly be explained by energy input (temperature, light and shear force), reported to promote destabilization. Thus, as kinetic energy was increased by temperature and shear forces, generated by the homogenization process, particles collided more frequently, and without full emulsifier coverage, aggregated more easily ⁵⁴.

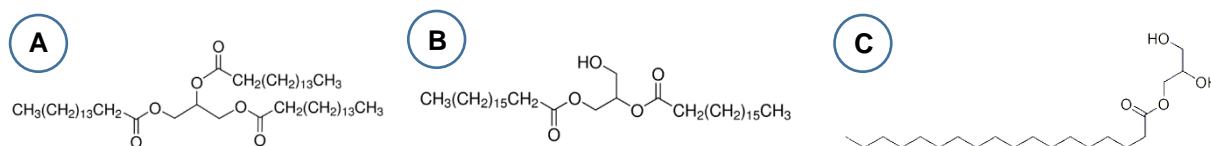


Figure 4.3 Chemical structure of A) Glyceryl tripalmitate (adapted from http://www.sigmaaldrich.com/glyceryl_tripalmitate, consulted in Aug. 20, 2017); B) Glyceryl distearate (adapted from http://www.sigmaaldrich.com/glyceryl_distearate, consulted in Aug. 20, 2017); C) Glyceryl monostearate (adapted from http://www.chemicalbook.com/glyceryl_monostearate, consulted in Aug. 20, 2017)

Table 4.3 Influence of the lipid matrix choice on SLN characteristics. Different lipids were tested and their effect on SLN quality was attained regarding size, Pdl and ZP. (mean±SD, n=3).

	Tm (°C)	Z-ave (nm)	Pdl	ZP (mV)
Tripalmitin	66-67 [*]	1895±700	0.841±0.205	-14±2
Precirol®	50-60 [**]	241±25	0.233±0.031	-15±2
Imwitor® 491	66-67 [***]	Aggregation		
Geleol™	54-64 [****]	137±9	0.248±0.066	-7±3

[*]<http://www.sigmaaldrich.com/tripalmitin> (consulted in Aug. 10, 2017);

[**]<https://www.gattefosse.com/Precirol@> (consulted in Aug. 10, 2017);

[***]<https://www.ioioleo.de/en/imwitor491> (consulted in Aug. 10, 2017);

[****]<https://www.gattefosse.com/Geleol™> (consulted in Aug. 10, 2017).

4.1.4 Surface modulation

4.1.4.1 Cationic polymer

4.1.4.1.1 Chitosan

Chitosan is a biodegradable cationic polymer, suitable for gene delivery due to its low cytotoxicity and capacity to form stable complexes with DNA⁵⁵. Surface charge modulation using chitosan was tried using two approaches: adsorption of the polymer to the surface of prepared SLNs and incorporation of chitosan into the aqueous phase used for SLN preparation. Additionally, different concentrations of chitosan were used.

The results obtained by incorporation of chitosan into the aqueous phase containing Pluronic® F-68 (0.1% w/v) are presented in Table 4.4. An interesting decrease in particle size was observed as the concentration of chitosan was lowered, for SLNs prepared using Geleol™. On the other hand, an expected decrease in ZP was also observed as the concentration of chitosan was reduced. Generally, particles showing mean ZP values lower than -30 mV and higher than +30 mV, are considered to be more stable⁴¹. Therefore, higher concentrations than 0.5 mg/mL of chitosan should be preferred.

Table 4.4 Influence of surface modulation, using different concentrations of chitosan low molecular weight (CS LMW), on SLN's physicochemical properties. CS LMW was incorporated into the aqueous phase used in SLN production by HSH. Results in terms of size, Pdl and ZP (mean±SD, n=3).

		CS LMW (mg/mL)	Z-ave (nm)	Pdl	ZP (mV)
HSH	Precirol®	1		Aggregation	
		0.5		Aggregation	
		0.25		Aggregation	
		0.1	462±72	0.305±0.046	+20±1
	Geleol™	1	779±348	0.323±0.097	+41±1
		0.5	736±41	0.251±0.023	+29±2
		0.25	501±29	0.255±0.015	+26±1
		0.1	441±48	0.259±0.019	+18±1

Results referring to chitosan adsorption onto the SLNs' surface are represented in Table 4.5. Independently of the lipid used, chitosan was not able to stabilize the SLNs and large aggregates >6 µm were observed, for all concentrations except 2.5 mg/mL of chitosan. Single ZP measurements, n=1, were made for concentrations <2.5 mg/mL, in order to understand why aggregation occurred. A mean surface charge of +28±1 mV was obtained (data not shown). As mentioned before, particles showing mean ZP values more negative than -30 mV and more positive than +30 mV, are generally considered to be more stable. At these values, the repulsive forces between equal charges are thought to be enough to prevent the aggregation process⁴¹. However, in this particular case, these charges were not enough, and higher ZP values were needed.

At a concentration of 2.5 mg/mL of chitosan, highly positive mean surface charges were obtained (+58±3 and +68±1 mV for Precirol® and Geleol™, respectively). However, during measurements, particle size was not consistent, and over time an increase in particle size within the same batch was detected, indicating that aggregation was still taking place. This process was independent of the chosen lipid. Wide Pdl values, >0.700, were also observed for both matrixes, corroborating the hypothesis of ongoing aggregation.

Taking in consideration the obtained results, the use of chitosan for surface modulation was abandoned.

Table 4.5 Influence of surface modulation, using different concentrations of chitosan low molecular weight (CS LMW), on SLN's physicochemical properties. Different concentrations of chitosan were adsorbed to previously prepared SLNs. SLNs' physicochemical properties were evaluated in terms of size, Pdl and ZP (mean±SD, n=3).

		CS LMW (mg/mL)	Z-ave (nm)	Pdl	ZP (mV)
Adsorption	Precirol®	2.5	1635±1208	0.841±0.112	+52±3
		1		Aggregation	
		0.5		Aggregation	
	Geleol™	2.5	918±308	0.745±0.223	+68±1
		1		Aggregation	
		0.5		Aggregation	

4.1.4.1.2 PEI

Polyethyleneimine (PEI) was first proposed for gene delivery by Boussif, O. *et al* (1995)⁵⁶ and is still up to date considered the “gold standard” of transfection. This polycation is able to condense the negatively charged pDNA, interact with the negatively charged membrane, and escape the harsh endosomal environment⁵⁷. The “proton sponge effect” is one of the proposed endosomal escape mechanisms, in which the presence of amine groups in PEI's structure is responsible for the influx of protons and counterions, and consequent lysis of the endosome membrane due to water influx.

Surface modulation was investigated using 1% (w/v) PEI 25 kDa. Hybrid SLNs (hyNPs) were produced using Precirol® and Geleol™ as the lipid phase, and polyethyleneimine was added to the aqueous phase containing Pluronic® F-68 (0.1% w/v). The obtained results are presented in Table 4.6. Comparison between the SLN comprising Precirol®, without (Table 4.3) and with surface modulation, revealed an increase in the mean ZP value from -15±2 mV to 22±3 mV. An increase in the mean particle size (332±14 nm) and Pdl values (0.459±0.020) was also observed for these hyNPs. Results were not so promising for SLNs comprising Geleol™ in their lipid matrix. Although these hyNPs presented increased surface charge (17±1 mV), their mean hydrodynamic diameter was 21-fold higher than those without surface modulation, presenting an average size >2.5 µm.

Table 4.6 Surface modulation using PEI 25kDa. The effect of PEI on SLNs' physicochemical properties was assessed in terms of size, Pdl and ZP measurements (mean±SD, n=3).

%PEI	Lipid	Z-ave (nm)	Pdl	ZP (mV)
1	Precirol®	332±14	0.459±0.020	22±3
	Geleol™	2884±507	0.324±0.111	17±1

Even though PEI 25kDa has been considered the “gold standard” for transfection, increased cytotoxicity has been associated to polyethyleneimines of higher molecular weights⁵⁸.

Baring this in mind, a balance between transfection efficacy and cytotoxicity must be established. Kuo, J. S. (2003)³⁴ investigated the ability of Pluronics to stabilize PEI-DNA complexes in the serum. Herein, higher PEI/DNA ratios were reported to result in higher cytotoxic effects, and that a decrease in this ratio led to lower gene expression.

The impact of two lower concentrations of PEI 25 kDa (0.5% and 0.1% w/v) on the SLN quality was investigated (Figure 4.4). As the concentration of PEI was diminished, lower ZP values were expected. However, surprisingly, the opposite was observed. As the polymers' concentration was reduced, an increase in surface charge was noticeable (Table 7.3, Appendix C). Another interesting detail was that higher ZP values were associated to higher particle sizes. As surface charge decreased, it was expected to detect bigger particles than those of higher concentrations of PEI, since less repulsive forces would be available to stabilize the hyNP, increasing particle coalescence.

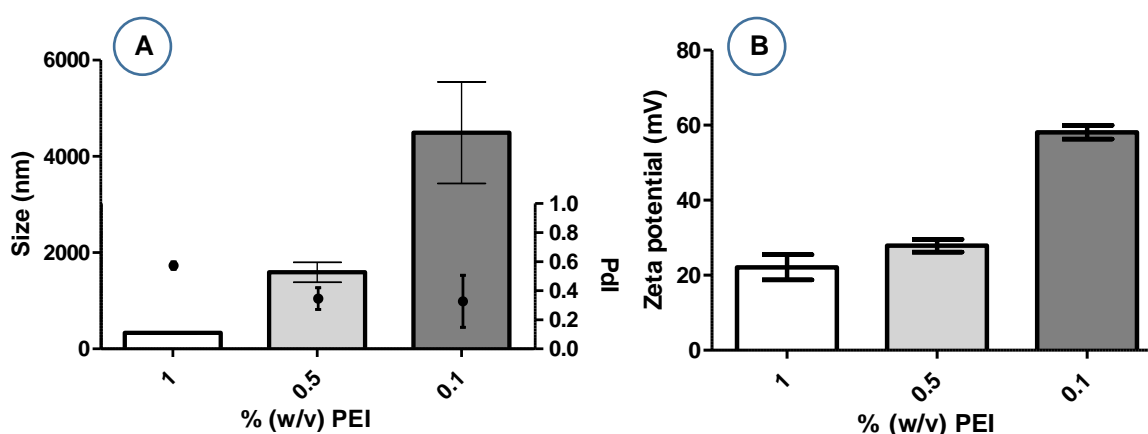


Figure 4.4 Effect of surface modulation using different concentrations of PEI 25 kDa on SLN: (A) size and size distribution (Pdl); (B) zeta potential. (mean±SD, n=3).

Cationic polymers, such as PEI, have been reported to be toxic to cells⁸. A preliminary cytotoxic assay (not presented) testing for cell membrane integrity (Propidium iodide uptake) and metabolic activity (Alamar blue) revealed that particles containing PEI 1% (w/v) led to cell death.

It has been proposed that the pH range for lipid injectable emulsions should be comprised between 6.0 and 9.0, and that it should be maintained throughout shelf-life⁵⁹. Hence, the pH of the aqueous phase containing PEI 1% (w/v) was corrected to pH 7 by addition of HCl.

Fresh nanoparticles were prepared using the corrected aqueous phase (Table 7.4, Appendix C), and compared to those previously attained without pH value adjustment (Figure 4.5). When compared to their homologous, significant difference was observed in terms of average size for hyNPs containing Geleol™ in their lipid matrix ($p < 0.05$), but not for those containing Precirol®. Significant differences were also observed in terms of size distribution and mean surface charge displayed by the fresh nanoparticles ($p < 0.05$), comparatively to those previously prepared. These two last parameters seem to walk hand-by-hand. An increase in

surface charge is expected to lead to increased stabilization and reduced coalescence, which in turn translates into a more homogenous size distribution.

Upon pH value adjustment, no significant differences were found between freshly prepared batches containing Precirol® and Geleol™, and all samples presented a mean surface charge >+50 mV. Thus, pH value seems to be a critical parameter for SLN quality.

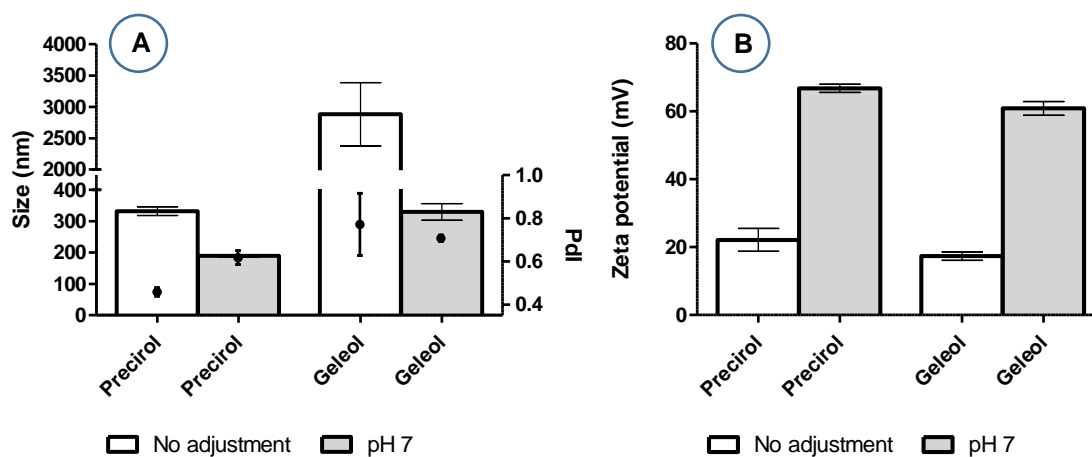


Figure 4.5 Influence of pH in the production of hyNPs, using PEI 25kDa at different concentrations. (A) size and PDI; (B) zeta potential. (mean±SD, n=3)

Polyethyleneimines can be found in a branched or linear configuration and are available in several molecular weights²⁴. Their transfection efficacy and toxicity have been correlated to their structure, charge and hydrophobicity^{8,55}. The influence of linear polyethyleneimine (IPEI 10kDa) and branched polyethyleneimines, with different molecular weights (bPEI 2 kDa and bPEI 25kDa), on cell toxicity was studied at the concentrations of 0.1 and 0.01% (w/v) under physiological pH. Samples were named according to their lipid composition and polyethyleneimine used (Table 7.5, Appendix C).

The influence of PEI's concentration on nanoparticles' quality was assessed by comparing the tested concentrations of each batch (Figure 4.6). In Table 7.6 (Appendix C) the obtained results are discriminated. Hybrid nanoparticles comprising Precirol® in their composition (hyNP₁ – hyNP₃), showed a decrease in the mean surface charge as the polymer's concentration was reduced. However, no significant size differences were found when the concentration of PEI was lowered, indicating that a concentration of 0.01% (w/v) was still able to stabilize the system. A decrease in the ZP values was also observed for batches comprising Geleol™ in their composition (hyNP₄ – hyNP₆). However, no general trend relative to the influence of PEI's concentration on particle size was evident, since for this lipid no significant size differences were registered for batches of hyNP₆, whereas a decrease in particle size was found for batches of hyNP₄ and hyNP₅. SLN composition, as already mentioned before, plays an important role in the nanoparticle's physicochemical properties. Therefore, the dispersity of results obtained for these samples could be due to the use of the combination of the different variables used.

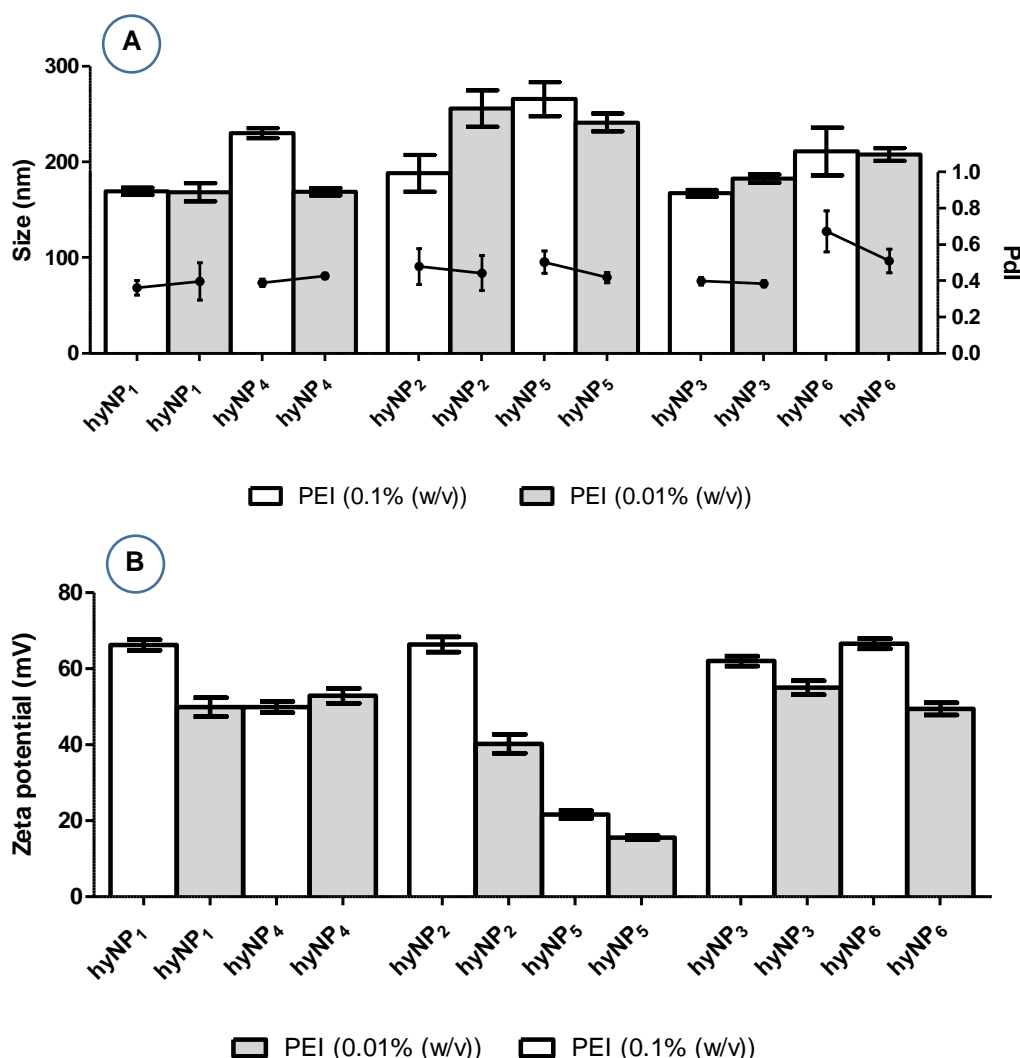


Figure 4.6 Influence of linear and branched polyethyleimines on SLN physicochemical characteristics, at two concentrations. No general trend was established between the concentration of the different PEIs used and SLNs' size. However, as for both concentrations the obtained particles presented average sizes <300 nm and ZP >+30 mV, the lowest concentration of PEI was preferred. Results in terms of (A) size and Pdl; (B) zeta potential. (mean±SD, n=3)

4.1.4.2 Cationic peptide

Upon the release of the nucleic acids into the cytoplasm, these must be delivered to the nucleus in order to access the nuclear machinery and modulate gene expression. However, this constitutes a limiting step, as the nucleus membrane is selective for molecules over 40kDa, such as plasmids. One of the hypothesised mechanisms to surpass the nuclear envelope and access its machinery, is the import through the nuclear pore complex (NPC). This process requires nuclear localization signals (NLS) that promote active nuclear transport of peptides containing arginine residues in their sequences³⁸. Protamine is a small cationic protein, FDA approved for parenteral administration and reported to enhance cell transfection, due to its rich content in arginine – six consecutive residues^{29,38}.

Hybrid SLNs containing (0.01% w/v) of PEI and (0.05% w/v) of protamine (hyNP_xP) were produced via HSH (Figure 4.7, Table 7.7 (Appendix D)). Batches were named in the same way as hyNP_x. Significant differences between particles comprising Precirol® (hyNP₁P-hyNP₃P) or Geleol™ (hyNP₄P-hyNP₆P) were observed, regarding to size and ZP values ($p < 0.05$). Particles containing Geleol™ presented a mean surface charge $< +20$ mV, which could explain the higher average sizes (> 400 nm) obtained. Therefore, the use of Geleol™ was discontinued.

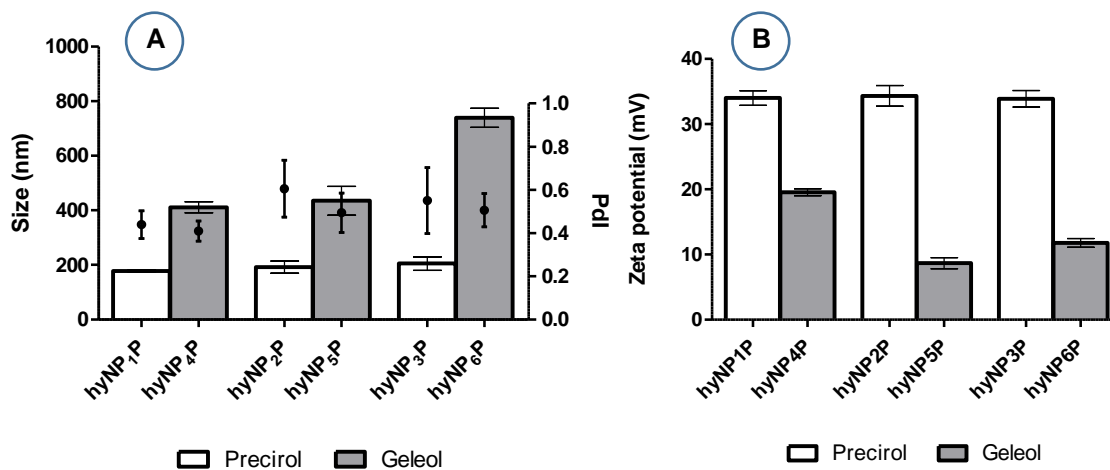


Figure 4.7 Hybrid nanoparticles containing linear or branched PEI (0.01% w/v) and protamine (0.05% w/v) were produced via HSH. The use of Geleol™ was discontinued since SLNs containing Precirol® in their lipid matrix presented the best results in terms of (A) size and PDI; (B) surface charge (mean±SD, n=3)

Proteins are known to be thermolabile, thus the use of HSH, which involves high temperatures and shear forces (known to be heat sources too), could lead to their denaturation. Whereby, the influence of HSH temperature on hyNP₁P-hyNP₃P quality was studied. New hyNP_xP were produced by protamine adsorption to previously prepared hyNP_x and were used as reference (Figure 4.8; Table 7.8 (Appendix D)). Briefly, 200 μ L of protamine (0.5% w/v) were added to 2mL aliquots of hyNP₁-hyNP₃ containing PEI (0.01% w/v).

Comparison between the results obtained for both techniques (Figure 4.8) revealed that decreased, or identical average sizes, were found for particles produced by HSH, comparatively to the adsorption technique. Additionally, no significant differences were found in terms of mean ZP when comparing both methods, except for hyNP₃P that presented higher values when prepared by adsorption of protamine.

When taken together, the results suggest that HSH is suitable for hyNP_xP production, and that those containing Precirol® are more suitable for intravenous administration.

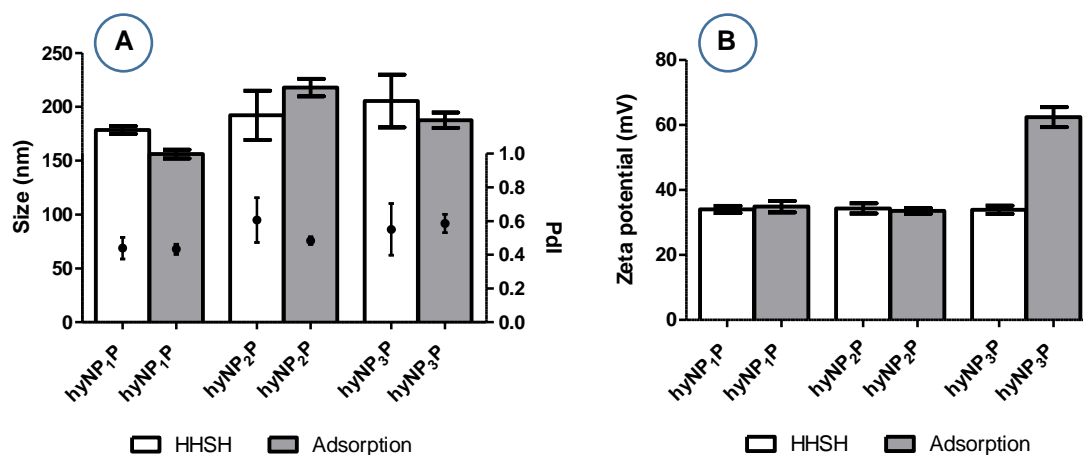


Figure 4.8 Proteins are thermolabile. The influence of temperature on hyNPs containing protamine was assessed by comparing those prepared by HSSH (heat source) and those prepared by protamine adsorption onto previously prepared hyNP (no heat source). Results in terms of (A) Size and PdI; (B) zeta potential. (mean±SD, n=3)

4.1.5 Stability

4.1.5.1 Freeze drying

Storage stability is an important parameter in the design of new formulations, as it involves chemical and physical aspects such as prevention of degradation reactions and size preservation over time³¹. Lyophilization is a widely employed technique to increase chemical and physical SLN stability over extended periods of time. During lyophilization, samples are dehydrated and transformed into a powder, facilitating processing and storage, allowing these samples to be stored and shipped at room temperature^{31,60,61}. However, this process subjects formulations to mechanical stress induced by ice crystallization, which may lead to their destabilization⁶⁰. Different sugars have been employed as cryoprotectants^{31,60,61}. Some of the most commonly used are trehalose (disaccharide), sucrose (disaccharide), glucose (monosaccharide) and sugar-alcohol mannitol⁶⁰.

Two different cryoprotectants, namely trehalose and glucose, were tested. Sugar final concentration was varied and 5, 10% (v/v) of trehalose and 5% (v/v) for glucose was employed. After freeze-dried, samples were placed in the desiccator until further resuspension. The latter was carried out in purified water and through two different approaches – hand mixing or 10 min sonication followed by 3 vortex cycles of 30 seconds each. Despite the different approaches, SLN resuspension remained a difficult task. The first approach proved to be inefficient as the aggregated powder would not resuspend at all. Sonication and vortex of the formulation proved to be more efficient in particle resuspension, although large aggregates were still present in suspension. For these reasons, no measurements were performed.

After sample reconstitution, particles should maintain their physicochemical properties⁶². Despite the increase in particle size and a decrease in zeta potential values – suggestive of

aggregation – reported in the literature for lyophilized samples, authors have been able to demonstrate SLNs adequate resuspension after lyophilization^{31,61,62}. The lyophilization process is complex and requires optimization. Although the obtained results do not agree with those reported in the literature, a more detailed investigation could be conducted in this field. However, SLN suspensions would be preferred due to easier handling (no resuspension needed) and lower costs (vacuum freeze-drying)¹⁴.

4.1.5.2 Storage stability

Colloidal stability is a demanding feature for nanoparticulated systems intended for intravenous administration⁶³, as it indicates its suitability for commercial application⁶⁴. One of the main features, regarding SLN formulations, is their excellent physical stability for, generally, over a year²⁸.

In the present work, the effect of temperature on SLNs' physical stability was investigated. Fresh aliquots were taken from each formulation ($t=0$) and stored for 3 months at 4°C and room temperature (RT), protected from the light. Samples were characterized in terms of size and Pdl each month. Surface charge was only measured at day 1 ($t=0$) and in the third month. The obtained data was compared to the control ($t=0$).

Samples stored at 4°C remained stable during the 3 months (Figure 4.9). No significant differences in terms of size and Pdl were found, except for hyNP₂ where a decrease in particle size occurred within the first month ($p < 0.05$) but remained stable over the remaining time. Zeta potential values, similarly to size and Pdl, did not vary significantly for most samples.

When stored at RT, samples hyNP₂, hyNP₂P and hyNP₃P showed a decrease in particle size within the first month and remained stable over the next months (Figure 4.10). However, no significant size differences, within the evaluated period, were found for hyNP₁, hyNP₃ and hyNP₃P. Interestingly, an increase in surface charge was noted for most of the samples, which could be related to the size decrease observed in the first month. When taken together, these results suggest that hyNP_x and hyNP_xP are stable under RT, for at least 3 months.

Samples stored at 4°C have been reported in the literature to show better stability than those stored at RT^{30,64–66}. However, comparison between Figures 4.9 and 4.10 reveals that, in the present work, sample stability was identical at both temperatures. Siddiqui, A. *et al* (2010)⁶⁷ has also studied the influence of storage conditions on SLNs' quality. In their work, cationic SLNs were prepared from stearyl alcohol and CTAB (cetyl trimethylammonium bromide), with and without phyto-ceramide for the delivery of an oligonucleotide. Size measurements were performed over four weeks for samples stored at refrigeration, room temperature and 37 °C. No significant differences were observed by them for samples without ceramide, stored at RT and under refrigeration. However, when stored at 37 °C, these samples showed significantly increased

sizes. On the other hand, samples comprising ceramide did not show significant increase in particle growth when stored at 37 °C.

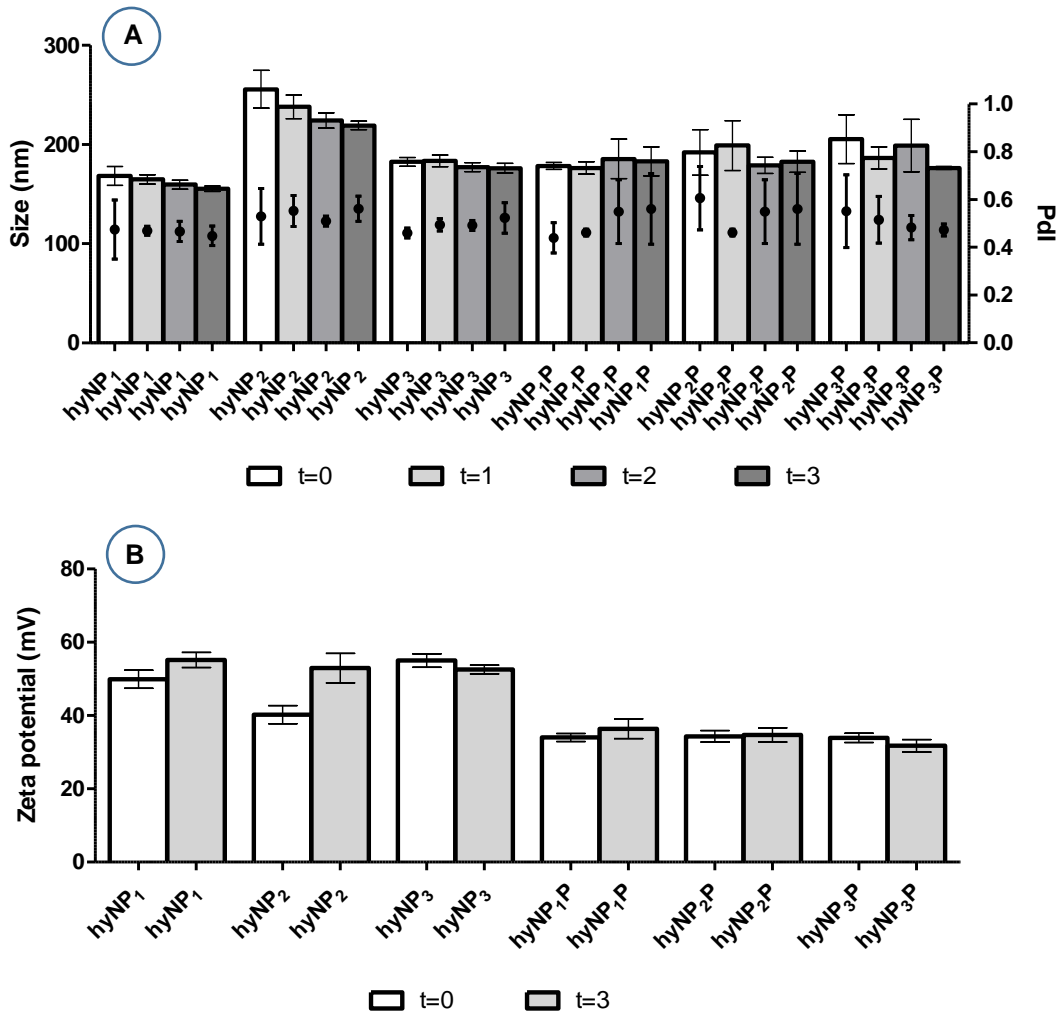


Figure 4.9 The influence of refrigeration temperature (4 °C) on SLNs' (A) size, Pdl and (B) ZP was studied for 3 months. Measurements were performed at day 1 (t=0), 1 month (t=1), 2 months (t=2) and 3 months (t=3) of storage (mean±SD, n=3). It was concluded that SLNs remained stable under refrigeration conditions for 3 months.

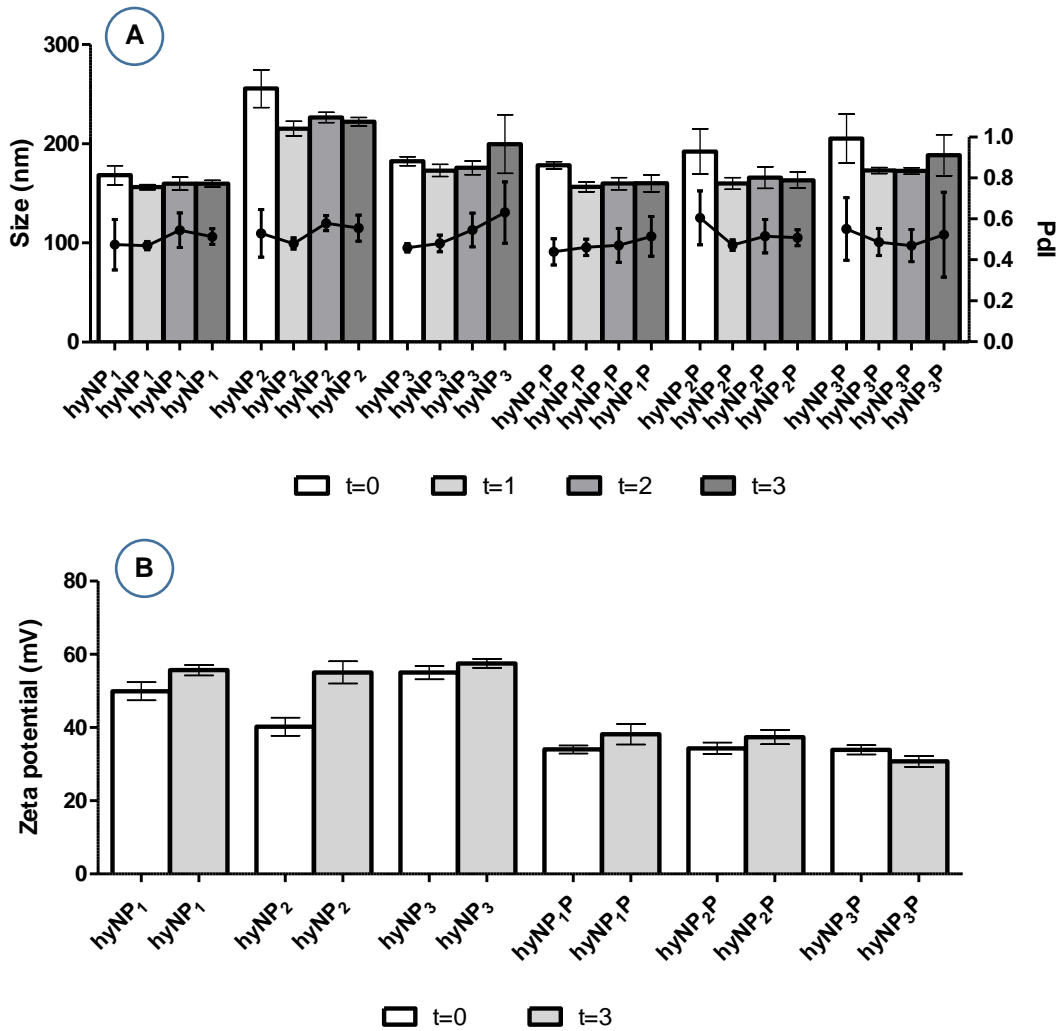


Figure 4.10 The influence of room temperature (RT) in SLN (A) size, Pdl and (B) ZP was studied for 3 months. Measurements were performed at day 1 ($t=0$), 1 month ($t=1$), 2 months ($t=2$) and 3 months ($t=3$) of storage (mean \pm SD, $n=3$). It was concluded that SLNs remained stable under RT for 3 months.

Foreseeing SLN physical stability at body temperature is crucial, as large particles resultant from aggregation processes raise safety concerns, due to the risk of capillary blockage. Hence, aliquots of each formulation were placed in a 37 °C water bath for 2 h (Figure 4.11). Although a significant decrease in ZP values was observed for hyNP₁, hyNP₃, hyNP₂P and hyNP₃P ($p < 0.05$), no significant differences were observed regarding to size and Pdl values, except for hyNP₁, indicating that the majority of the samples are stable under body temperature.

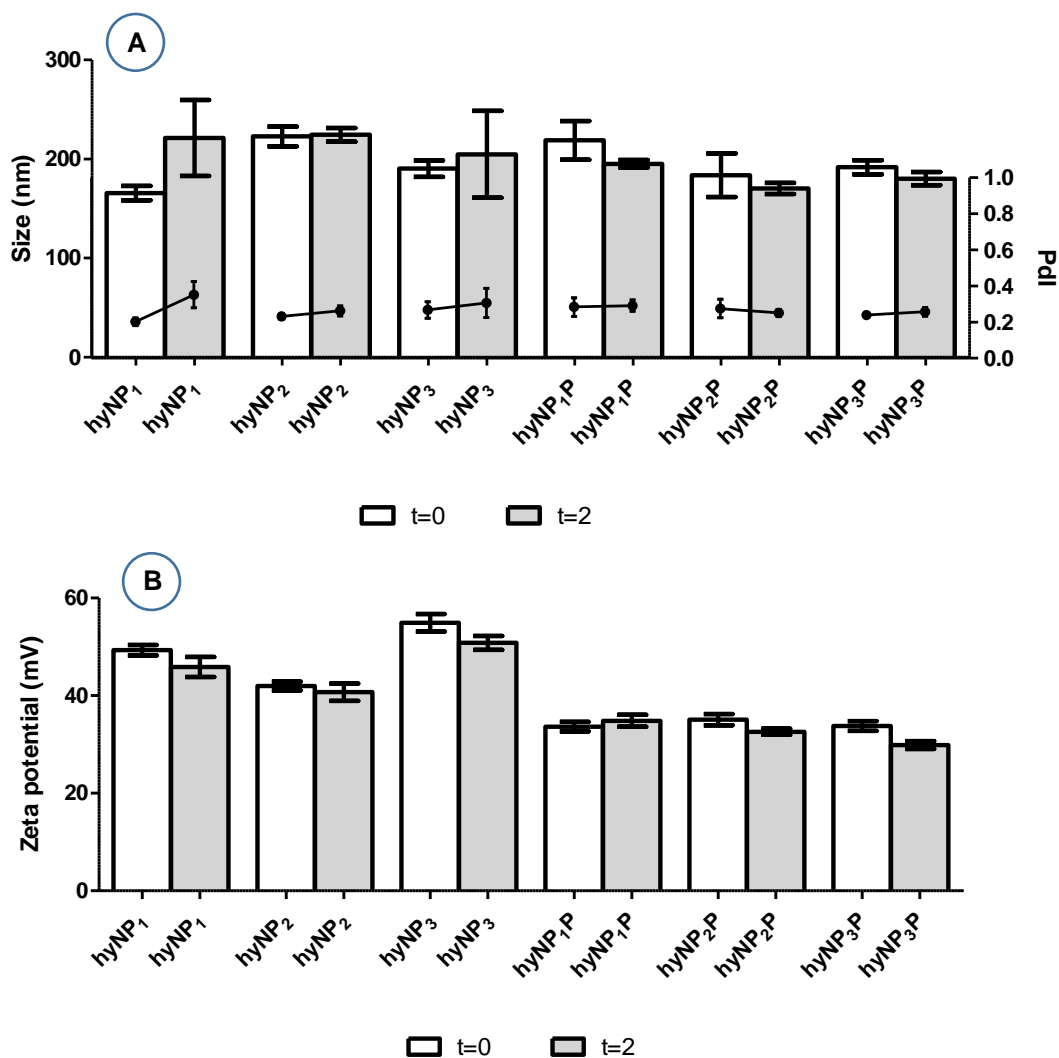


Figure 4.11 The influence of body temperature (37 °C) on SLN (A) size, Pdl and (B) ZP was studied. Measurements were performed at day 1 (t=0), and after sample placement in a 37 °C water bath for 2 h (t=2) (mean±SD, n=3). It was concluded that SLNs remained stable under body temperature for this period of time.

4.1.5.3 Storage medium

Most of reports do not address SLN stability in buffer solutions (at physiological pH and osmolarity) or in cell culture media. This is an important issue, since higher concentration of electrolytes may cause instability and, consequently, SLN precipitation⁶⁸.

Phosphate buffer saline (PBS) and simulated body fluid (SBF) were chosen to test SLN stability under higher electrolyte concentrations. An aliquot of each formulation was diluted 1:4 in buffer solution.

PBS is a water-based salt solution containing sodium chloride and, in some formulations, potassium chloride and potassium phosphate. This buffer solution is used for biological research, because its osmolarity and ion concentrations match those of the human body (<http://www.sigmaaldrich.com/PBS>, consulted in Aug. 13, 2017). Samples placed in contact with

PBS (Figure 4.12; Table 7.9 (Appendix E)) revealed a significant increase in the mean particle size when compared to those kept in the original dispersion medium. As already mentioned along this study, dispersions displaying mean surface charges greater than $|30|$ mV are thought to be more stable, given that at this point repulsion between the dispersed particles is sufficient to avoid their coalescence⁴¹. Therefore, particle coalescence herein observed could be explained by the significant decrease in the mean surface charge ($<+15$ mV), and in some cases charge inversion observed ($p < 0.0001$), resultant from ionic interaction between the buffer and hyNPs.

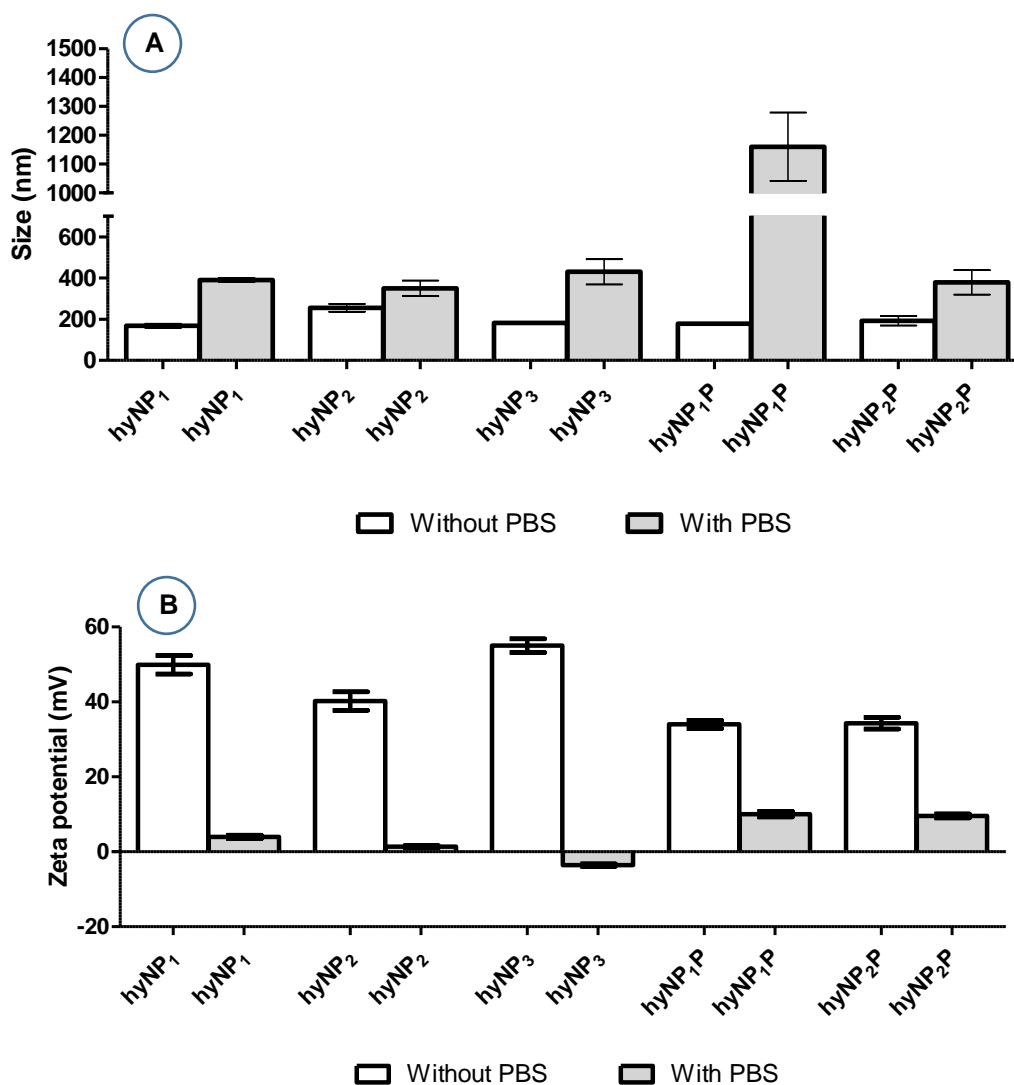


Figure 4.12 Influence of the PBS on SLNs' physicochemical properties. A significant increase in particles average size and a decrease in ZP ($<+30$ mV) was observed, allowing to infer that SLNs were not stable in PBS. Results in terms of (A) Z-ave, size dispersion and (B) surface charge (mean \pm SD, n=3).

he simulated body fluid (SBF) has been used to predict the bioactivity of artificial materials for implants. This solution possesses ion concentrations that are nearly equal to those in the blood plasma. Aiming to predict hyNPs quality in the blood plasma, a SBF solution was prepared according to the instructions of Kokubo, T. & Takadama, H. (2006)⁴². An aliquot of each sample

batch was diluted 1:4 in SBF, and SLNs' quality was assessed over 1 and 24 h. The obtained results presented graphically in Figure 4.13 and in a more detailed manner in Table 7.10 (Appendix E). After 1 h, significant particle growth was only observed for hyNP₁P and hyNP₃. Nevertheless, upon 24 h, coalescence was observed for all samples, except hyNP₂. These results can be explained by significant decrease in the mean surface charges (<+20 mV).

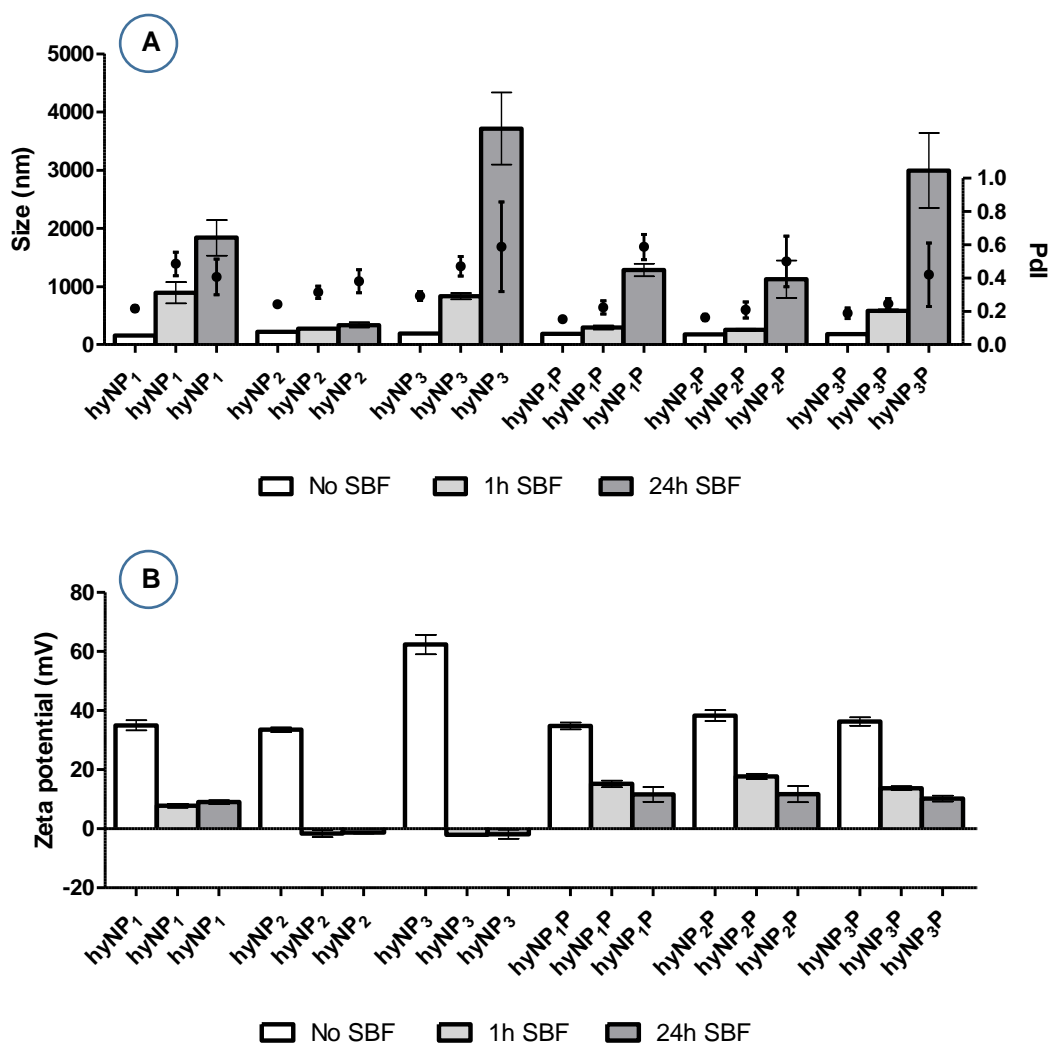


Figure 4.13 Influence of SBF on SLNs' physicochemical properties after 1 and 2 h of exposure. A significant increase in particles average size and a decrease in ZP (<+30 mV) was observed, allowing to infer that SLNs were not stable in PBS. Results in terms of (A) size, PDI and (B) surface charge (mean±SD, n=3).

4.1.5.4 Sterilization

Sterile formulations are required for parenteral administration. The sterilization process should not change the formulations' properties, with respect to their physical and chemical stability. In order to achieve sterility, aseptic production, filtration, γ -irradiation and heating have been employed.

Sterilization by heat is a reliable and commonly used procedure applied for liposomes. However, temperature-induced changes in physical stability are of concern, as the melting of the

lipid particles in the process will cause the formation of an o/w-emulsion. Solid particles will be formed after recrystallization ³¹. In the present study, SLNs were subjected to heat sterilization by autoclaving (121°C/15 min), and its impact on nanoparticle quality was assessed. The obtained results were compared to non-sterilized formulations.

After autoclaving, flocculation was observed for all samples (Table 7.11, Appendix F). Even though high surface charge was displayed by the nanoparticles, particles' mean size was >1 µm and Pdl values were in some cases >0.500 (Figure 4.14), indicating that the obtained results are unreliable for comparison purposes ⁴¹. This outcome is supported by the literature. Destabilization of the colloidal system upon sterilization at 121°C has been reported for nanoparticles stabilized with poloxamer 188 ^{31,49}. Dispersion stabilization by Pluronic® F-68 is possible due to steric repulsion ⁵⁴. Therefore, it was hypothesized that sample flocculation may be caused by a decrease in Pluronic's steric repulsion, since at increased temperatures, dehydration of the ethylene glycol chains can occur, leading to decreased thickness of the protective layer and, ultimately, aggregation of the particles ^{31,49}.

A possible solution to avoid this outcome could be to decrease the autoclave temperature to 110°C and prolong the heat exposition time, as reported in the literature ^{31,49}. However, this can only serve as a guideline, since stability upon autoclaving depends very much on the composition of the SLN ⁴⁹.

Alternatively to these approaches, SLN dispersions could be produced in aseptic conditions identical to those used for parenteral emulsions, in order to attain sterility ⁴⁹.

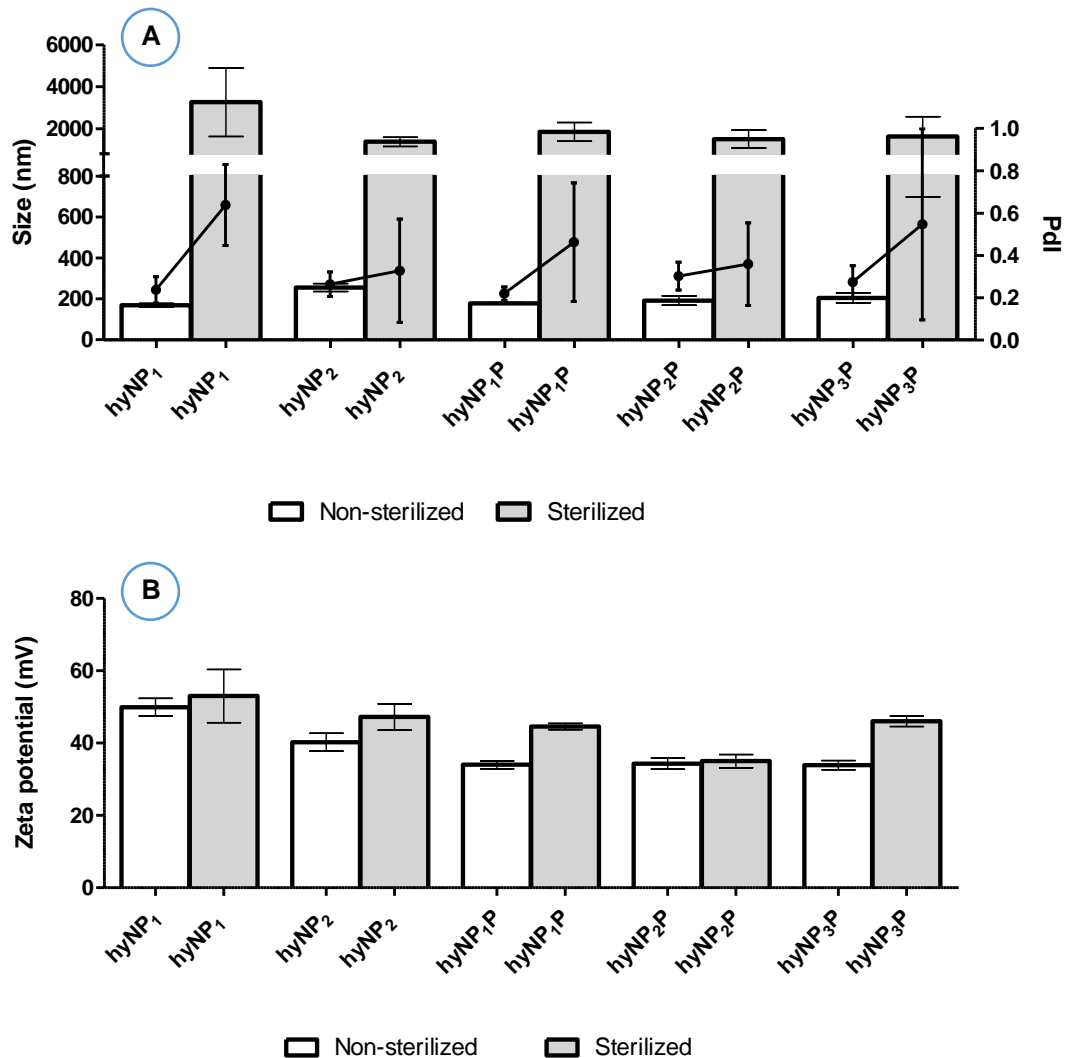


Figure 4.14 Influence of autoclaving on SLN characteristics, regarding (A) particle size, Pdl and (B) ZP. (mean±SD, n=3. Samples did not remain stable during the process of autoclaving since significant increase in particle size was observed.

4.2 SLN morphology

Electron microscopy takes advantage of electrons' smaller wave lengths to attain increased magnification and resolution, comparatively to light microscopy. In the Transmission Electron Microscopy (TEM), electrons are projected through thinly sliced specimen. A two-dimensional image is produced in a phosphorescent screen, where the brightness of a particular area is proportional to the number of electrons that are transmitted through the specimen⁶⁹. Electron microscopy, in contrast to DLS, provides direct information regarding to particle shape³¹. Therefore, nanoparticle morphology was assessed through TEM.

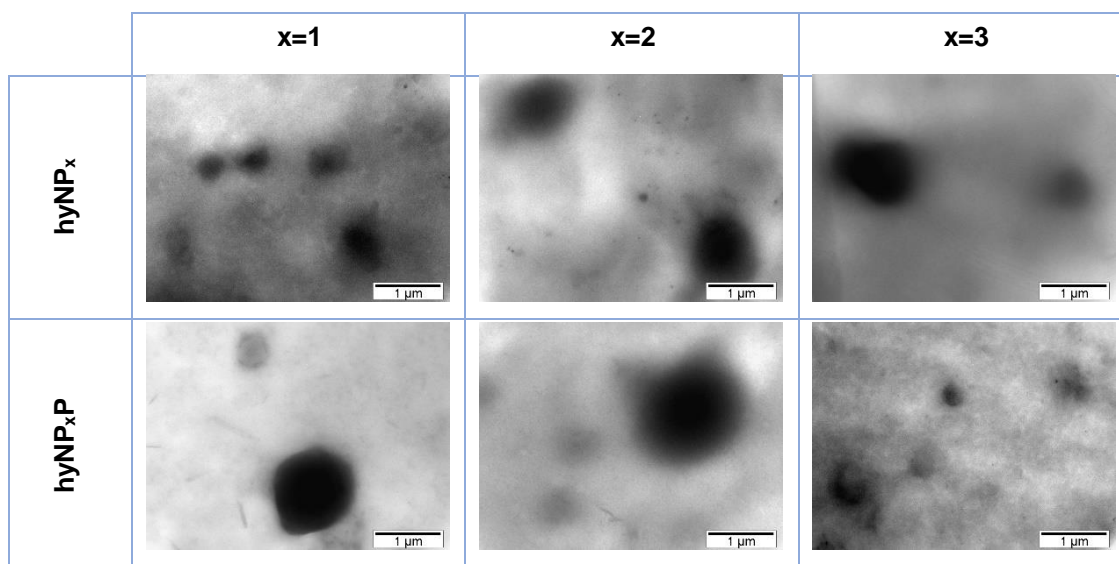
The obtained micrographs (Table 4.7) present a blur, and were not conclusive. However, all particles appear to have a spherical-like structure. As the samples were not previously purified, in order to remove the excessive emulsifying agent in which they were stored, micrographs distortion could be hypothetically explained by its excessive presence. Anisometric platelet

structures have been suggested in the SLN literature ^{31,70} and found to commonly occur during lipid crystallization ³¹.

The poorly defined borders (Table 4.7) made size determination and its comparison to previously obtained data difficult. Increased particle size, comparatively to DLS measurements, was apparent. As vacuum is required for TEM analysis, sample dehydration occurred, which could have led to SLN aggregation, and could explain the increase in particle size.

Another possible explanation for the discrepancy between the collected data from TEM and DLS, regarding particle size, arises from the fact that uncertainties may result when determining SLN size via DLS, as this method assumes a spherical shape of the particles ³¹. Anisometric particles possess smaller diffusion coefficients than spherical particles and slower Brownian motion has been correlated to apparently larger hydrodynamic diameters. According to the Zetasizer manual, reasonable narrow monomodal samples have a Pdl value <0.100 and the collected data revealed that these particles presented Pdl values <0.300 (Table 7.6 (Appendix C) and Table 7.7 (Appendix D)), and therefore is reliable for comparison purposes ⁴¹. Higher polydispersity indexes have been correlated to anisometric particles ⁷⁰, supporting the conclusion that these hyNPs present a spherical-like structure.

Table 4.7 *hyNP_x and hyNP_xP morphology attained by TEM (n=1). All formulations presented a spherical-like structure.*



4.3 *In vitro* cell viability

Non-viral transfection agents have been investigated for gene delivery applications. One of the main requirements of these systems is their non-toxicity ⁶². Solid lipid nanoparticles are composed of physiologically well tolerated compounds. Hence, it is anticipated that they are well tolerated *in vivo* ³¹. Positively charged SLNs are required to condense nucleic acids and enhance

cell transfection⁶². However, cationic molecules, such as PEI, have been related to toxicity events⁷¹. One of the main concerns in the development of new non-viral vectors is their possible toxicity.

In the present work, cationic SLNs' cytotoxicity in HEK293T cell line, following 6 and 24 h exposure, using a concentration of 500 µg/mL of SLNs, was assessed by evaluation of the membrane integrity (Propidium iodide uptake, Figures 4.15 and 4.17) and metabolic activity (Alamar blue, Figure 4.16 and 4.18). The Alamar blue is a colorimetric/fluorometric test, that allows to infer if the cell's metabolic activity has been compromised, as it relies on resazurin reduction by cells⁷². Yet, the effects resultant from cell exposure to SLNs that do not necessarily lead to cell death, should also be considered. Therefore, a complementary assay was necessary. Propidium iodide is a red-fluorescent dye that is not permeant to living cells (https://www.thermofisher.com/Propidium_iodide, consulted in Aug. 13, 2017). For this reason, it was used to assess the cell's membrane integrity.

The obtained results were compared to Pluronic® F-68 (0.1% w/v) and growth medium (negative controls) and SDS (positive control). Kuo, J. S. (2003) reported that Pluronic® F-68 used in a range of 0.01-10% does not exert cytotoxic effects and that its cell viability was comparable to the negative control (100% viability). In fact, when compared to the growth medium, no significant differences, in terms of metabolic activity and membrane integrity, were found between these controls for either times of exposition.

Apart from hyNP₁P and hyNP₃P, no significant cytotoxic effects were observed for cells exposed to the shortest time of exposure. For hyNP₁P and hyNP₃P, at 6 h of exposure, decreased cell membrane integrity was observed ($p < 0.0001$), yet the metabolic activity was not compromised. Though, no conclusions should be made in terms of metabolic activity, since this exposure time could be too short to lead to total inhibition of the metabolic activity. The ISO 10993-5:2009 has stated that a decrease in cell viability by more than 30% is to be considered as a cytotoxic effect. Therefore, it is conclusive that at this tested time point, none of the tested formulations are considered cytotoxic, as in all cases, cell viability was superior to 70%⁷³.

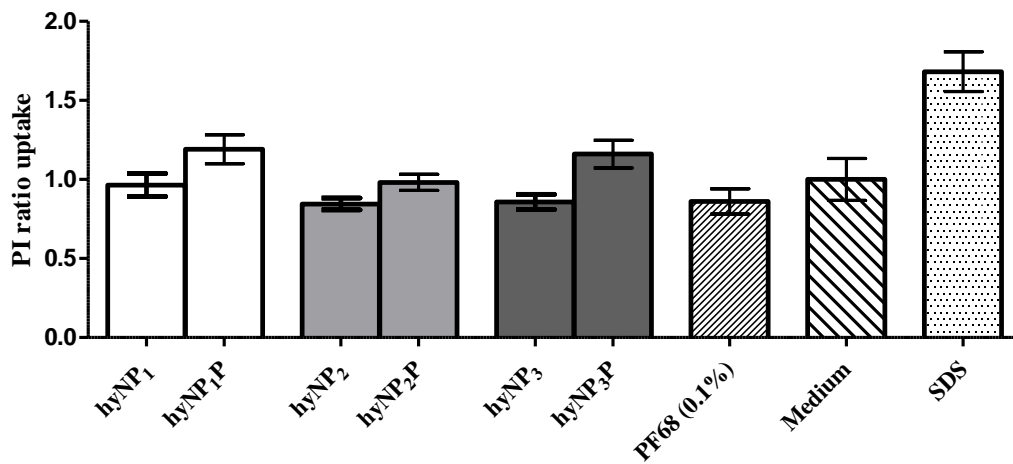


Figure 4.15 The cell's membrane integrity by Propidium iodide uptake assay. HEK293T cells were exposed to SLNs for 6 h (mean±SD, n=8) and their membrane integrity was then assessed. Decreased cell membrane integrity was observed for hyNP₁P and hyNP₃P.

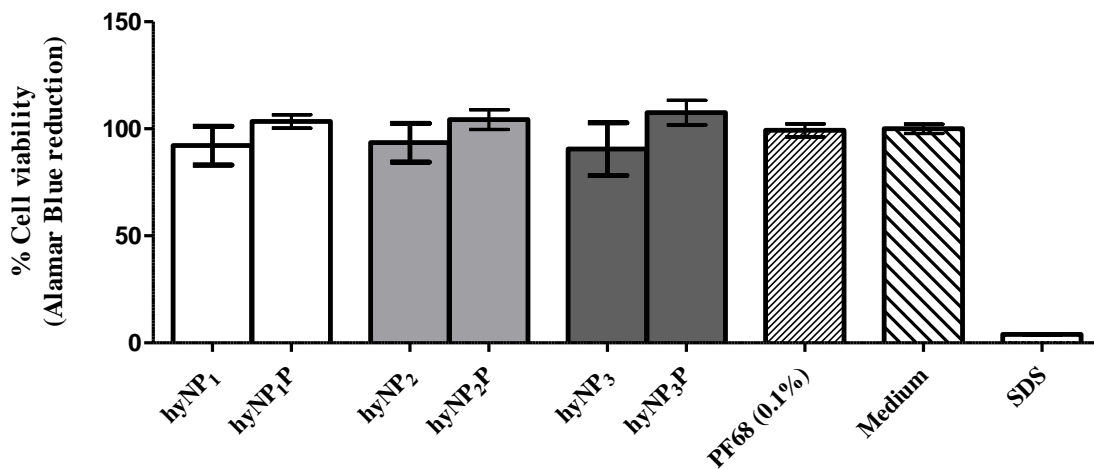


Figure 4.16 The cell's metabolic integrity by Alamar blue assay. HEK293T cells were exposed to SLNs for 6 h (mean±SD, n=8) and their membrane integrity was then assessed. No cytotoxic effects were observed for the metabolic activity for any tested formulation.

Moreover, when the cells were exposed to hyNPs for a period of 24 h, no signs of damage to the cell's membrane or compromised metabolic integrity were found, including for hyNP₁P and hyNP₃P, which previously displayed apparent damage to the membrane (Figures 4.17 and 4.18). Hence, it is possible to conclude that these particles do not exert toxic effects to the cell, regarding to the evaluated parameters, for at least a period of 24 h, since in all cases cell viability was higher than 70% ⁷³.

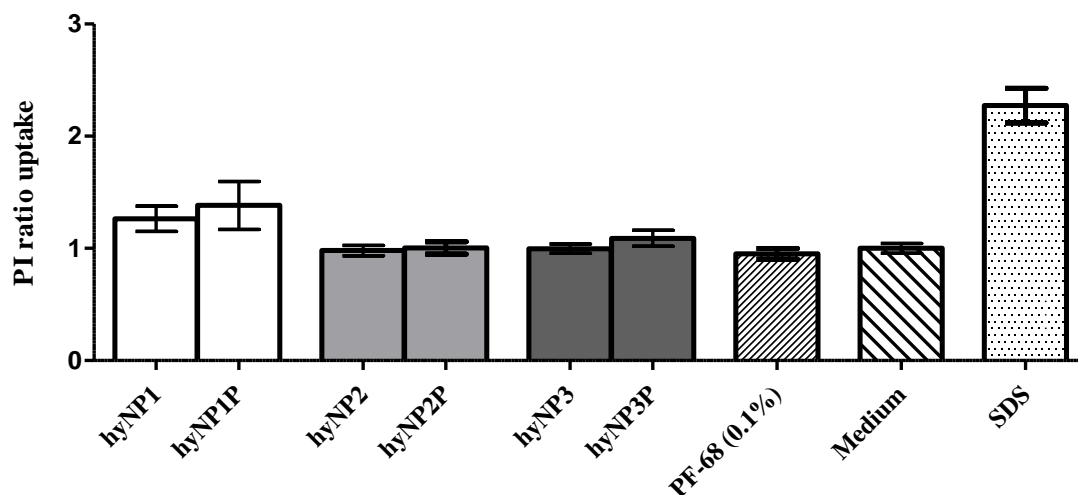


Figure 4.17 The cell's membrane integrity by Propidium iodide uptake assay. HEK293T cells were exposed to SLNs for 24 h (mean±SD, n=8) and their membrane integrity was then assessed. No cytotoxic effects were observed.

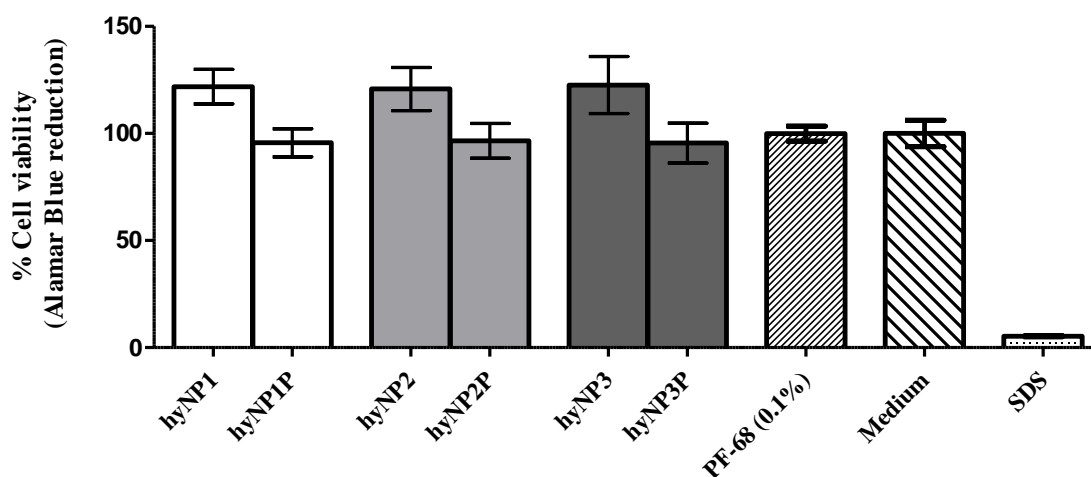


Figure 4.18 The cell's metabolic integrity by Alamar blue assay. HEK293T cells were exposed to SLNs for 24 h (mean±SD, n=8) and their membrane integrity was assessed. No cytotoxic effects were observed.

4.4 pDNA condensation

The interaction between oppositely charged macromolecules, such as cationic polymers and anionic DNA, is an often-used strategy to produce pDNA-NP complexes intended for non-viral gene delivery ³⁷. In the present study, aliquots of each formulation were taken and pDNA

was added at a final $\text{ng}_{(\text{SLN})}/\text{ng}_{(\text{pDNA})}$ ratios of 104:1 and 208:1. Spontaneous pDNA-hySLN complexes were formed after 15 min under mild agitation. The efficiency of plasmid condensation onto nanoparticles, at both ratios, was assessed by gel retardation assay, using agarose 1%. Quantification of the condensation efficacy was made by fluorescence, and polyethyleneimine nanoparticles were used as the control group.

Figure 4.19 refers to the gel retardation assay. Analysis of both gels allowed to conclude that for both ratios tested, NPs were able to condense pDNA adequately, since no bands were observed. These results were corroborated by fluorescence quantification, where it was observed that hyNP_x and hyNP_xP could condense, respectively, 74-86% and 89-92% of the nucleic acid (Figure 4.20). Furthermore, no significant differences in the capacity to bind pDNA were found between the tested ratios. Though, it was found that nanoparticles containing protamine were, in general, able to bind pDNA more efficiently.

Bondi, M. L. *et al* (2007)⁴⁵ also studied the interaction between cationic SLNs and DNA by retardation of the DNA electrophoretic mobility. Herein, and similarly to the performed in the present work, a fixed amount of DNA was mixed with increasing amounts of cationic SLNs, and SLN/DNA ratios were varied from 10:1 to 200:1. The efficacy of DNA complexation was evaluated by the amount of SLNs required to retard the migration of pDNA toward the cathode during the agarose gel electrophoresis. It was observed that the lowest SLN/DNA ratio required to retard pDNA migration was around 100:1⁴⁵.

Additionally, in the present work, when hyNPs were compared to the control group (pDNA-PEI complexes), it was found that for the lowest ratio tested (208:1) a significantly lower condensation efficacy was registered for hyNP_1 and hyNP_2 , which condensed 73% and 79% of the pDNA, respectively. No significant differences were found for the remaining nanoparticles, when compared to the control group.

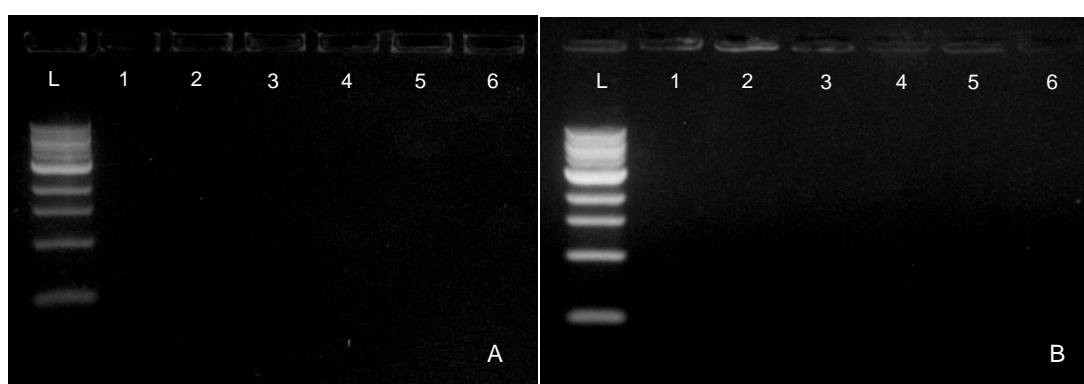


Figure 4.19 Qualitative evaluation of pDNA condensation. Gel retardation assay regarding (A) 104:1 and (B) 208:1 $\text{ng}_{(\text{SLN})}/\text{ng}_{(\text{pDNA})}$. An effective binding of pDNA by the hyNPs was observed for both ratios, since the nucleic acid was retained in the wells. L) Ladder; 1) hyNP_1 ; 2) hyNP_2 ; 3) hyNP_3 ; 4) hyNP_1P ; 5) hyNP_2P ; 6) hyNP_3P .

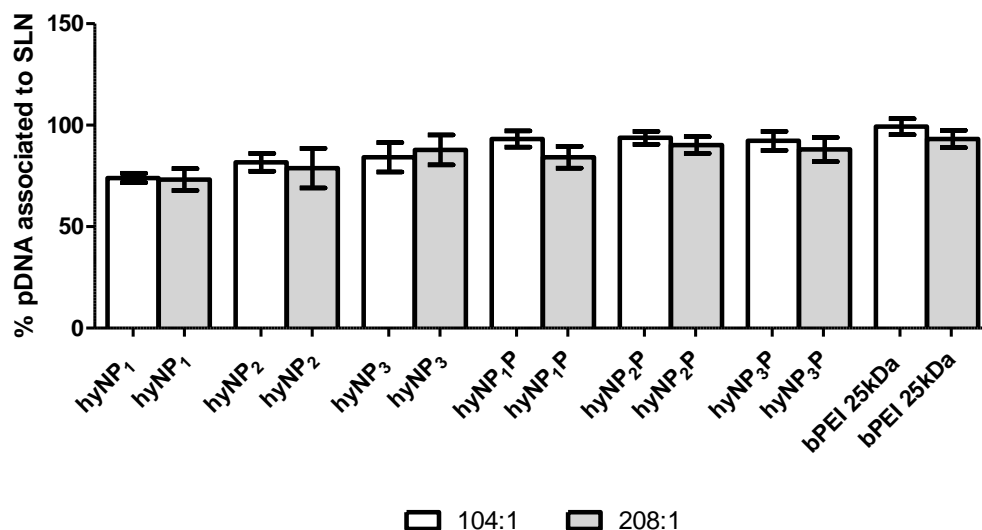


Figure 4.20 Quantification of the efficiency of pDNA condensation regarding the mass ratios SLN/pDNA of 104:1 and 208:1 (mean±SD, n=6), using the gold-standard bPEI (25 kDa) nanoparticles as the control. No significant differences were observed between the prepared hyNPs and the control group.

The physicochemical properties of pDNA-hyNPs were also evaluated. It was observed that pDNA condensation onto the SLNs' surface led to an increase in particles size ($p < 0.05$), however no significant differences were registered for ZP values (Figure 4.21), which could be explained by the high SLN/pDNA ratios used. Polyethyleneimine nanoparticles conjugated with pDNA were used as the control, and it was observed that these particles possessed a lower size and surface charge than those herein developed ($p < 0.05$).

These results were also in agreement with those obtained by Bondi, M. L. *et al* (2007)⁴⁵, that reported an increase in the mean particle size, as the weight ratio SLN/DNA was increased, and hypothesised that a moiety of DNA could form complexes with several particles thanks to the opposite charges between them, leading to the observed increase in the mean particle size.

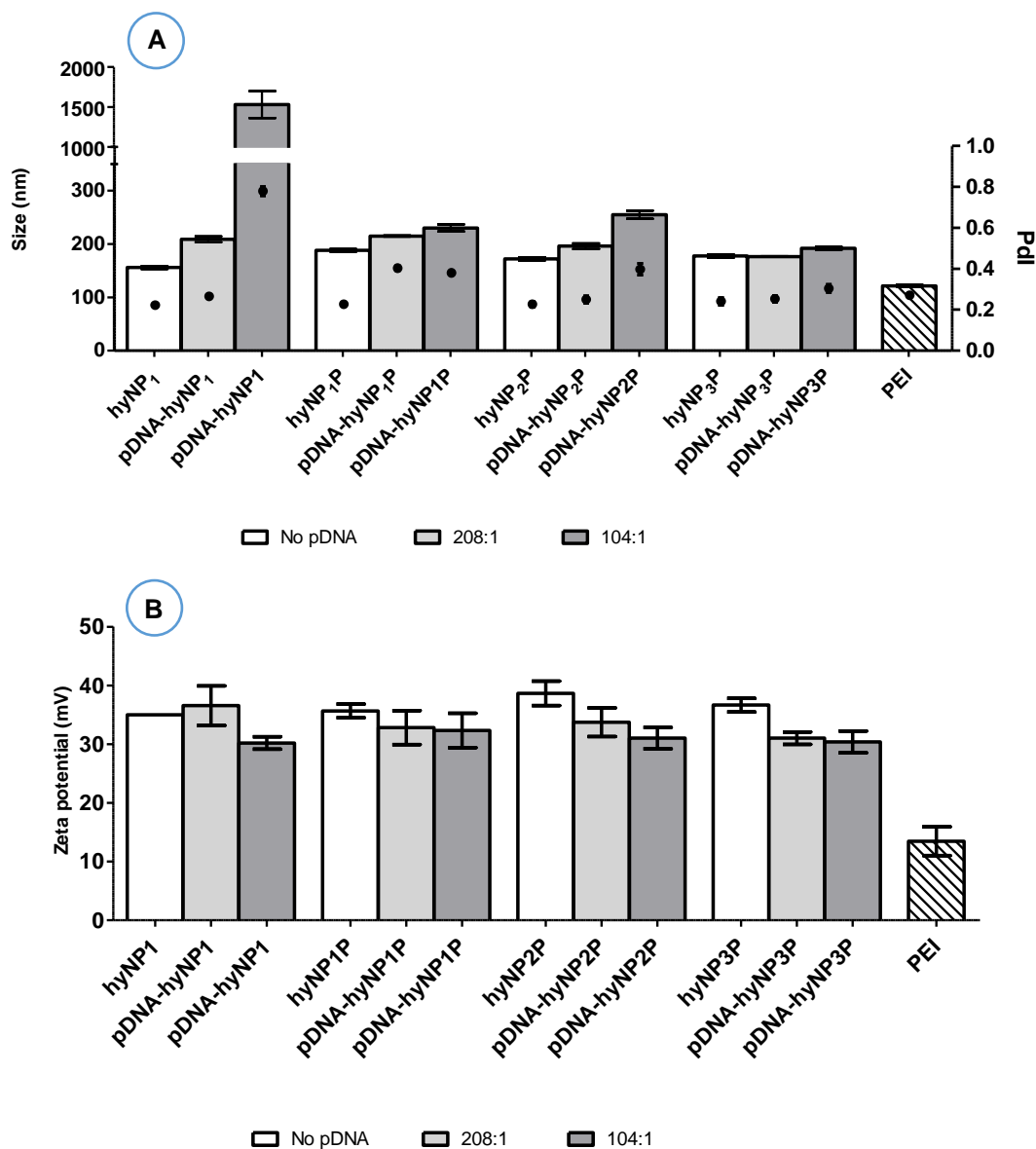


Figure 4.21 pDNA-hyNPs physicochemical properties were determined in terms of (A) size, PDI and (B) zeta potential (mean±SD, n=3) and compared to the gold-standard bPEI 25 kDa nanoparticles. It was observed that an increase in the amount of pDNA led to an increase in particle size, and that the control group possessed lower z-ave and ZP than those herein developed.

4.5 Cell uptake

Several reports have documented that SLNs are promptly internalized by a wide range of cell lines⁶⁸. Optical analysis of SLN uptake by the cell was made using fluorescence. A multi-staining procedure was used to distinguish the nuclei (blue), plasma membrane (red) and Coumarin-6 loaded SLNs (green). Analysis of Figures 4.22 and 4.23 showed that all the tested formulations were able to enter the cell. In addition, it was observed that some hyNPs were positioned near to the nucleus.

Kuo, J. S. (2003) ³⁴ has reported that, in the presence of serum, PEI-DNA complexes stabilized by Pluronic® F-68 presented higher transfection efficacy than PEI-DNA complexes alone, which were very serum-sensitive, and easily inactivated.

An uptake assay using two different concentrations Coumarin-6 loaded hyNPs was also performed (Figure 4.24). The obtained results allowed inferring that SLN uptake was concentration dependent and that protamine, when combined with PEI, did not enhance cell uptake. However, an exception was observed for SLNs containing bPEI 25kDa, for whom protamine enhanced SLN internalization. Furthermore, when put together, both assays demonstrate that SLN uptake by the cell did in fact occur.

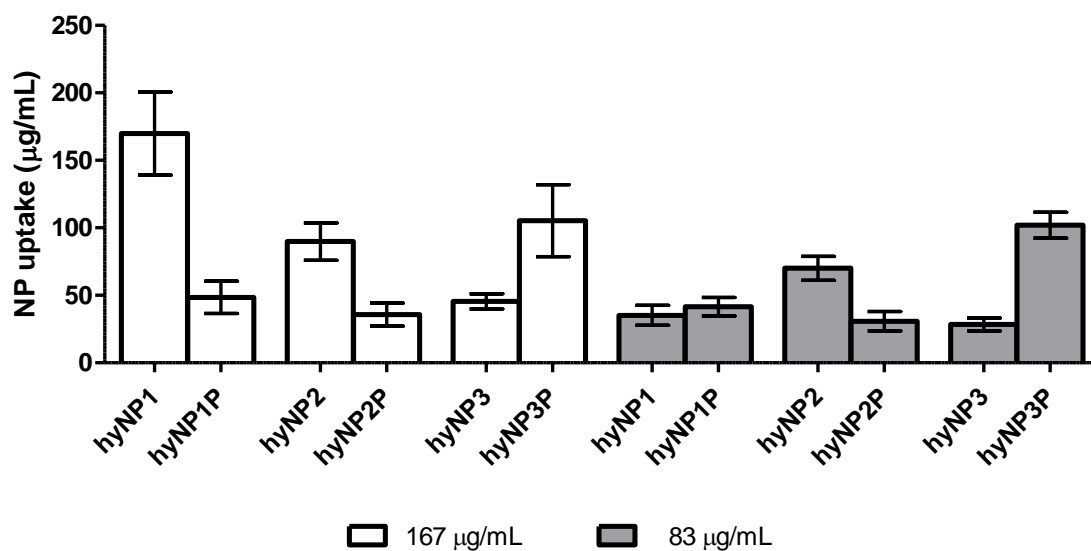


Figure 4.24 Fluorescence quantification of SLN uptake. HEK 293T cells were exposed to hyNPs loaded with Coumarin-6 at a concentration of 167 µg/mL and 83 µg/mL (mean±SD, n=8). The obtained results allowed inferring that the uptake was concentration dependent.

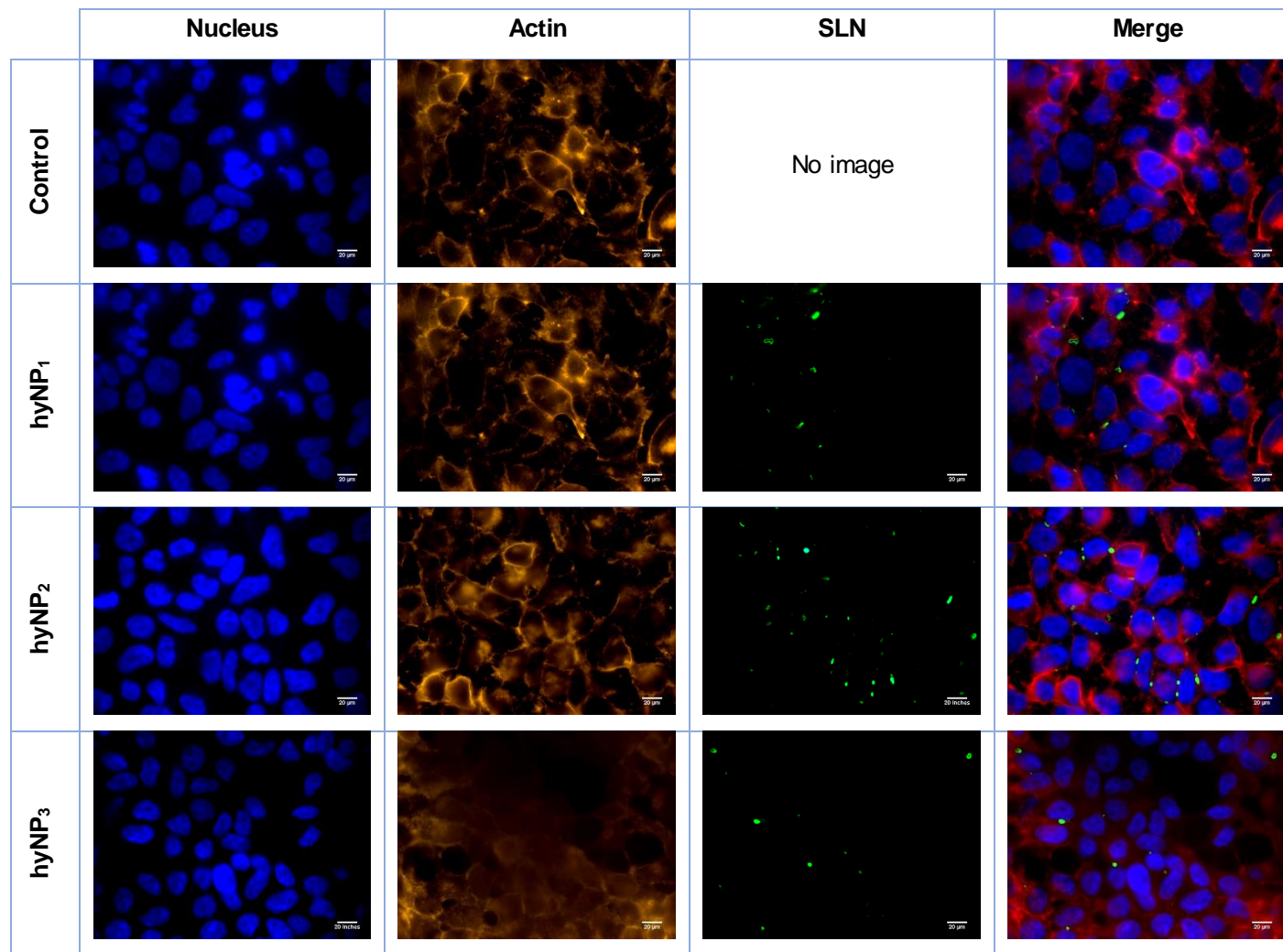


Figure 4.22 *hyNP_x* cellular uptake observed under fluorescence microscopy. Fluorescence microscopy images using 40x amplification. The blue and yellow stain represent the nucleus and plasma membrane, respectively. Coumairn-6 loaded SLN were used and are represented in green. A merge of the images is presented in the last column. *hyNP_x* were internalized and, in some cases, were positioned near the nucleus.

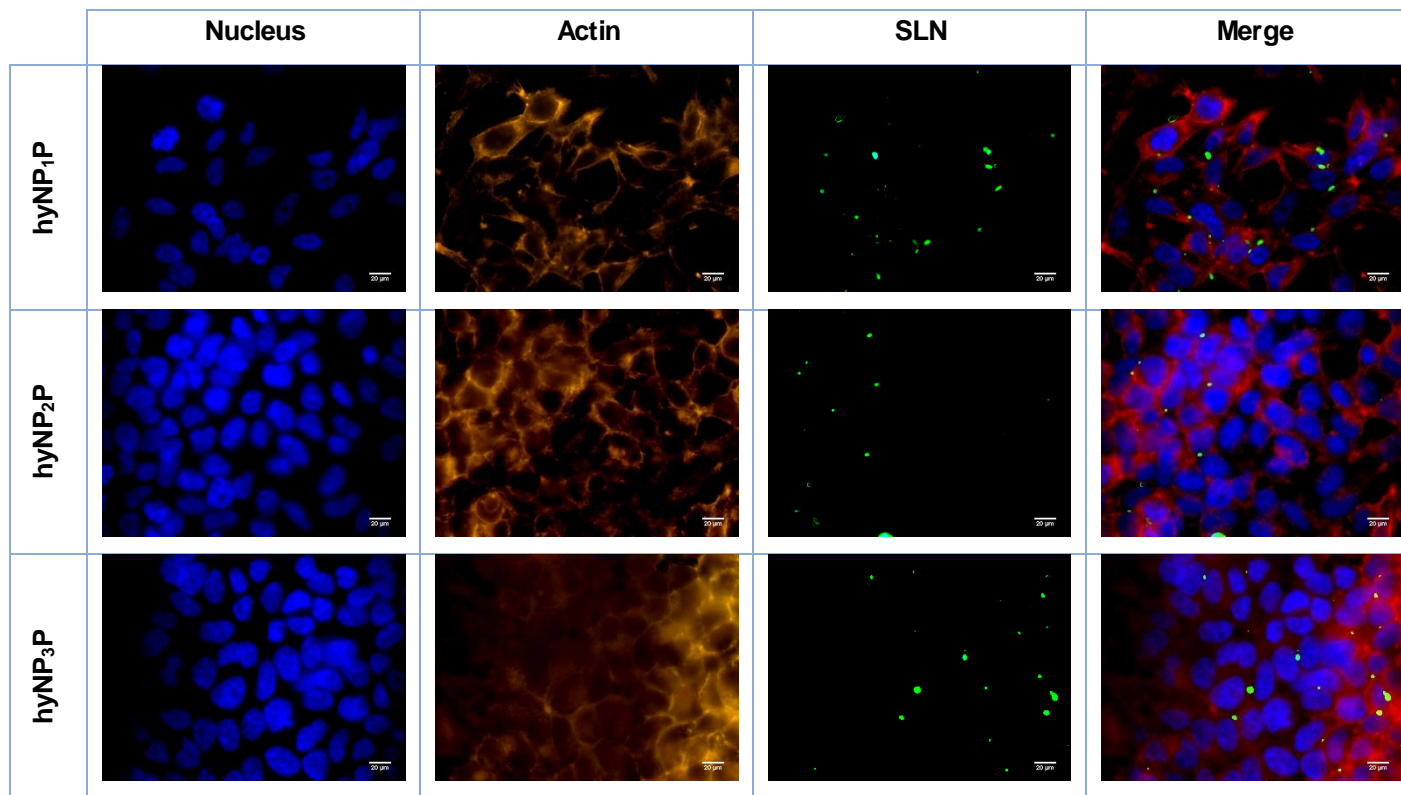


Figure 4.23 *hyNP_xP* cellular uptake observed under fluorescence microscopy. Fluorescence microscopy images using 40x amplification. The blue and yellow stain represent the nucleus and plasma membrane, respectively. Coumairn-6 loaded SLN were used and are represented in green. A merge of the images is presented in the last column. *hyNP_xP* were internalized and, in some cases, were positioned near the nucleus.

4.6 Cell transfection

Cell transfection using a model plasmid expressing fluorescent green protein (pGFP) was also assessed for 208:1 and 104:1 SLN/pDNA ratios. Branched PEI 25kDa has been considered transfections' "gold-standard" ⁵⁸. Hence, pDNA-bPEI_{25kDa} nanoparticles were used as control. Figure 4.25 analysis revealed that pGFP expression was not ratio dependent and that protamine did not enhance nuclear transfection. Moreover, when compared to the control, significant differences ($p < 0.0001$) were observed for all hyNPs tested when 104:1 SLN/pDNA was used. However, when using 208:1 SLN/pDNA, hyNP₁, hyNP₂ and hyNP₂P did not show significant differences regarding to the control group.

Similar results regarding poor transfection efficacy of protamine-SLN complexes, were obtained by Delgado, D. *et al* (2011) ³⁸, whom reported that the incorporation of protamine into SLNs resulted in an unexpected decreased transfection efficacy in HEK 293T cells, in a protamine concentration manner.

As final remark, the found pGFP expression allows to reinforce the affirmations regarding to hyNPs cellular uptake and their placement in the perinuclear region.

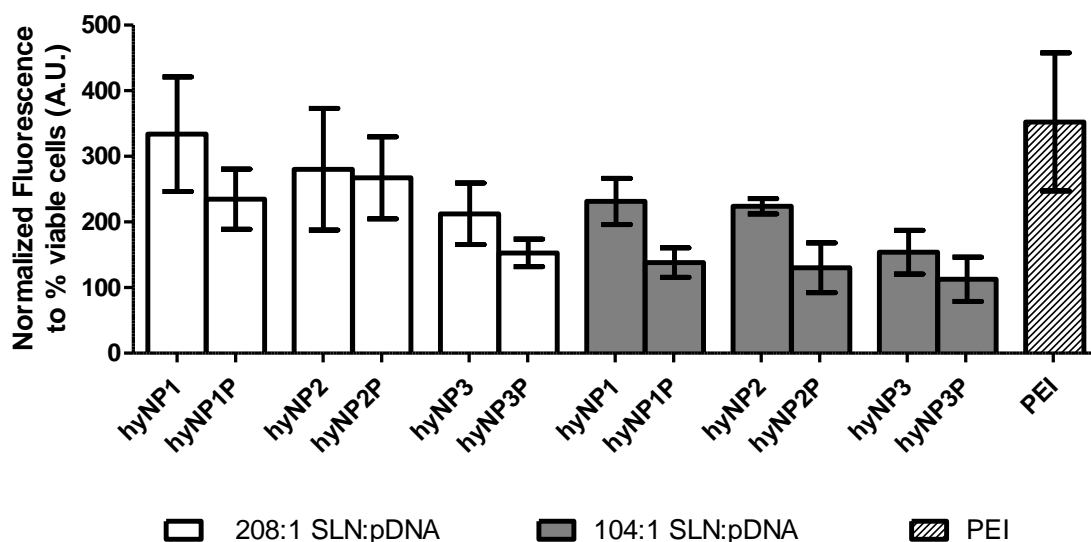


Figure 4.25 Fluorescence quantification of the expression of pGFP (green fluorescence protein), normalized to the percentage of viable HEK 293T cells, at 48 h post-transfection, using 208 and 104 ng SLN/ng pDNA and compared to the "gold-standard" of transfection (mean \pm SD, n=8). hyNPs' transfection efficacy was as efficient as the control's group.

4.7 Haemocompatibility

Solid lipid nanoparticles are composed of biodegradable compounds, with GRAS status, and already in use in pharmaceutical and cosmetic products. Toxicology of nanomaterials intended for medical use has become an important issue nowadays. Although SLNs have shown

higher *in vitro* tolerability than polymeric nanoparticles, and that several encouraging cytotoxicity results have been reported over the last decade, more evidence is still required. Slight variations amongst the research conducted by different groups, such as the tested cell lines, different formulation techniques and purposes of the formulated nanoparticles, make comparison of the reported data difficult⁶⁸. In the present work, SLNs have been intended for intravenous administration. An important indicator on the safety of intravenous intended formulations is the compatibility with red blood cells⁶⁸.

Herein, samples were incubated in a blood/sample ratio of 100:20 (v/v) at 37°C for 2 h, under mild shaking. PBS and Triton X-100 (1% w/v) were used as negative and positive controls, respectively (Figure 4.26). For an easier interpretation, a schematic plate is presented in Table 7.12 (Appendix F). Haemocompatibility criterion was made accordingly to ASTM F756. Therefore, samples presenting a %Haemolysis <2 were classified as non-haemolytic, between 2-5 were considered slightly haemolytic, whereas >5 were considered haemolytic. Analysis of Table 4.8 allowed to conclude that the prepared SLN fall into a wide range of haemolytic classifications, as hyNP₁ and hyNP₁P were classified non-haemolytic, hyNP₂ and hyNP₃ slightly haemolytic and, finally, hyNP₂P and hyNP₃P haemolytic⁷⁴. Thus, the addition of protamine seems to increase the haemolysis.

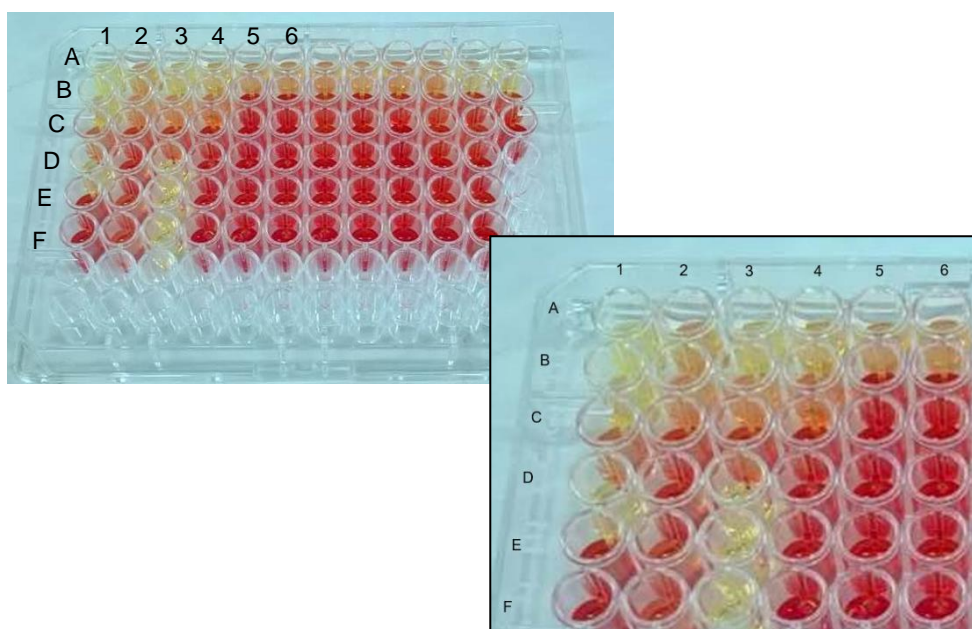


Figure 4.26 Evaluation of the toxic effects exerted on haemoglobin, regarding only the identified rows and columns. Non-haemolytic hyNPs and PBS do not lyse haemoglobin (yellow) while haemolytic samples and the positive control do (red).

Table 4.8 Haemolytic capacity of the tested SLNs, using PBS and Triton X-100 (1%w/v) as the negative and positive controls, respectively. Formulations with a %H <2 were considered non-haemolytic, while formulations with a %H 2-5 or %H >5 were considered slightly haemolytic and haemolytic, respectively.

	hyNP ₁	hyNP ₂	hyNP ₃	hyNP ₁ P	hyNP ₂ P	hyNP ₃ P	Pos. control	Neg. control
%H	1	3	4	1	11	10	81	1
SD	0	0	2	1	0	1	17	0
%CV	4	12	60	82	1	9	21	15

Chapter 5 Conclusion and future work

Gene therapy has gained increased attention over the last decades due to the possibility to treat a disease at its routes. Several vehicles intended to carry and deliver a functional copy of the deficient gene have been developed and non-viral vectors have emerged as an attractive alternative to viral vectors due to the need to create vehicles with higher safety profiles and as effective as the latter.

Thus, the main goal of this project was to develop safe and effective non-viral gene carriers, with surface modulated properties, based on the use of biocompatible excipients.

Hybrid solid lipid nanoparticles (hyNPs), containing polyethyleneimine (PEI) combined, or not, with protamine, were produced by hot high shear homogenization. The obtained nanoparticles showed to be suitable for intravenous administration as they possessed sizes <300 nm and good physical stability for 3 months at the different storage conditions (4°C, room temperature and 37°C). Moreover, these particles showed good plasmid condensation levels and were able to efficiently deliver the gene into the nucleus, though no cellular uptake or nuclear import improvements were found for hybrid nanoparticles containing a combination of PEI and protamine. Additionally, no cytotoxic effects concerning membrane integrity and metabolic activity on HEK 293-T cells were observed after 24 h of exposition. When regarded their haemocompatibility, it was found that SLNs modulated with linear PEI, combined or not with protamine, were non-haemolytic, proving to be an innovative, less cytotoxic and as efficient approach to gene therapy as the “gold-standard” of transfection (PEI nanoparticles). Nevertheless, other endpoint assays, such as genotoxic tests, and cell lines should be tested, since those used may not be enough to assess the all potential toxic effects of these carriers.

As future work, the addition of specific moieties onto the surface of these nanoparticles that allow the targeting of the diseased cells and avoid unwanted cell transfection are a key aspect regarding to systemic administration. Furthermore, extrapolation of the obtained *in vitro* guidelines to *in vivo* models to attain more realistic data regarding to clearance, biodistribution, necessary dose-ranges and overall efficacy of these hyNPs constitutes another key point in the extension of this work.

Chapter 6 References

1. Scott E. McNeil. *Unique Benefits of Nanotechnology to Drug Delivery and Diagnostics*. **697**, (Humana Press, 2011).
2. Commission recommendation of 18 October 2011 on the definition of nanomaterial (2011/696/EU). *Off. J. Eur. Union* **L275**, 38–40 (2011).
3. *Nanotechnologies and Food: Report. House of Lords I*, (2010).
4. Sánchez-Moreno, P. *et al.* Balancing the effect of corona on therapeutic efficacy and macrophage uptake of lipid nanocapsules. *Biomaterials* **61**, 266–278 (2015).
5. Wang, T., Upponi, J. R. & Torchilin, V. P. Design of multifunctional non-viral gene vectors to overcome physiological barriers: Dilemmas and strategies. *Int. J. Pharm.* **427**, 3–20 (2012).
6. Williams, J. Improving DNA Vaccine Performance Through Vector Design. *Curr. Gene Ther.* **14**, 170–189 (2014).
7. Beláková, J. *et al.* DNA vaccines: are they still just a powerful tool for the future? *Arch. Immunol. Ther. Exp. (Warsz)*. **55**, 387–98 (2007).
8. Brown, M. D. ., Schätzlein, A. G. . & Uchegbu, I. F. Gene delivery with synthetic (non viral) carriers. *Int. J. Pharm.* **229**, 1–21 (2001).
9. Tregoning, J. S. & Kinnear, E. Using Plasmids as DNA Vaccines for Infectious Diseases. *Microbiol. Spectr.* **2**, (2014).
10. Wang, D. & Gao, G. State-of-the-art human gene therapy: part II. Gene therapy strategies and clinical applications. *Discov. Med.* **18**, 151–61 (2014).
11. Wang, W. *et al.* Non-viral gene delivery methods. *Curr. Pharm. Biotechnol.* **14**, 46–60 (2013).
12. Hsu, C. Y. M. & Uludağ, H. Nucleic-acid based gene therapeutics: delivery challenges and modular design of nonviral gene carriers and expression cassettes to overcome intracellular barriers for sustained targeted expression. *J. Drug Target.* **20**, 301–328 (2012).
13. Ibraheem, D., Elaissari, A. & Fessi, H. Gene therapy and DNA delivery systems. *Int. J. Pharm.* **459**, 70–83 (2014).
14. Wang, Y. *et al.* Preparation and stability study of norfloxacin-loaded solid lipid nanoparticle suspensions. *Colloids Surfaces B Biointerfaces* **98**, 105–111 (2012).
15. Naldini, L. Gene therapy returns to centre stage. *Nature* **526**, 351–360 (2015).
16. Al-Dosari, M. S. & Gao, X. Nonviral Gene Delivery: Principle, Limitations, and Recent

- Progress. *AAPS J.* **11**, 671–681 (2009).
17. Wong, S. Y., Pelet, J. M. & Putnam, D. Polymer systems for gene delivery-Past, present, and future. *Prog. Polym. Sci.* **32**, 799–837 (2007).
 18. Yi, Y., Noh, M. J. & Lee, K. H. Current Advances in Retroviral Gene Therapy. 218–228 (2011).
 19. Lehrman, S. Virus treatment questioned after gene therapy death. *Nature* **401**, 517–518 (1999).
 20. Yin, H. *et al.* Non-viral vectors for gene-based therapy. *Nat. Rev. Genet.* **15**, 541–555 (2014).
 21. Perez Ruiz de Garibay, A. Endocytosis in gene therapy with non-viral vectors. *Wiener Medizinische Wochenschrift* **166**, 227–235 (2016).
 22. Blanco, E., Shen, H. & Ferrari, M. Principles of nanoparticle design for overcoming biological barriers to drug delivery. *Nat. Biotechnol.* **33**, 941–951 (2015).
 23. Zhang, S. *et al.* Cationic compounds used in lipoplexes and polyplexes for gene delivery. **100**, 165–180 (2004).
 24. Ewe, A. *et al.* Liposome-polyethylenimine complexes (DPPC-PEI lipopolyplexes) for therapeutic siRNA delivery in vivo. *Nanomedicine Nanotechnology, Biol. Med.* **13**, 209–218 (2017).
 25. Lungwitz, U. *et al.* Polyethylenimine-based non-viral gene delivery systems. *Eur. J. Pharm. Biopharm.* **60**, 247–266 (2005).
 26. Pouton, C. W. & Seymour, L. W. Key issues in non-viral gene delivery. *Adv. Drug Deliv. Rev.* **46**, 187–203 (2001).
 27. Zununi Vahed, S. *et al.* Liposome-based drug co-delivery systems in cancer cells. *Mater. Sci. Eng. C* **71**, 1327–1341 (2017).
 28. Wissing, S. A., Kayser, O. & Müller, R. H. Solid lipid nanoparticles for parenteral drug delivery. *Advanced Drug Delivery Reviews* **56**, 1257–1272 (2004).
 29. Vighi, E. *et al.* Nuclear localization of cationic solid lipid nanoparticles containing Protamine as transfection promoter. *Eur. J. Pharm. Biopharm.* **76**, 384–393 (2010).
 30. Geszke-Moritz, M. & Moritz, M. Solid lipid nanoparticles as attractive drug vehicles: Composition, properties and therapeutic strategies. *Mater. Sci. Eng. C* **68**, 982–994 (2016).
 31. Mäder, K. & Mehnert, W. Solid lipid nanoparticles: production, characterization and applications. *Adv. Drug Deliv. Rev.* **47**, 165–96 (2001).

32. Gaspar, D. P. *et al.* Rifabutin-loaded solid lipid nanoparticles for inhaled antitubercular therapy: Physicochemical and in vitro studies. *Int. J. Pharm.* **497**, 199–209 (2016).
33. De Jesus, M. B. & Zuhorn, I. S. Solid lipid nanoparticles as nucleic acid delivery system: Properties and molecular mechanisms. *J. Control. Release* **201**, 1–13 (2015).
34. Kuo, J. S. Effect of Pluronic-block copolymers on the reduction of serum-mediated inhibition of gene transfer of polyethyleneimine-DNA complexes. *Biotechnol. Appl. Biochem.* **37**, 267–271 (2003).
35. Kreuter, J. Application of nanoparticles for the delivery of drugs to the brain. *Int. Congr. Ser.* **1277**, 85–94 (2005).
36. Olbrich, C. *et al.* Cationic solid-lipid nanoparticles can efficiently bind and transfect plasmid DNA. *J. Control. Release* **77**, 345–355 (2001).
37. Cadete, A *et al.* Development and characterization of a new plasmid delivery system based on chitosan – sodium deoxycholate nanoparticles. *Eur. J. Pharm. Sci.* **45**, 451–458 (2012).
38. Delgado, D.*et al.* Understanding the mechanism of protamine in solid lipid nanoparticle-based lipofection: The importance of the entry pathway. *Eur. J. Pharm. Biopharm.* **79**, 495–502 (2011).
39. Ishii, T., Okahata, Y. & Sato, T. Mechanism of cell transfection with plasmid/chitosan complexes. *Biochim. Biophys. Acta - Biomembr.* **1514**, 51–64 (2001).
40. Durán-Lobato, M.*et al.* Comparative study of chitosan- and PEG-coated lipid and PLGA nanoparticles as oral delivery systems for cannabinoids. *J. Nanoparticle Res.* **17**, (2015).
41. *Zetasizer Nano Series User Manual.* (2004).
42. Kokubo, T. & Takadama, H. How useful is SBF in predicting in vivo bone bioactivity? *Biomaterials* **27**, 2907–2915 (2006).
43. Nociari, M. M. *et al.* A novel one-step, highly sensitive fluorometric assay to evaluate cell-mediated cytotoxicity. *J. Immunol. Methods* **213**, 157–167 (1998).
44. QIAGEN Plasmid Purification Handbook. 17–21 (2012).
45. Bondi, M. L. *et al.* Novel cationic solid-lipid nanoparticles as non-viral vectors for gene delivery. *J. Drug Targeting* **15**, 295–301 (2007).
46. Radomska-Soukharev, A. Stability of lipid excipients in solid lipid nanoparticles ☆. *Adv. Drug Deliv. Rev.* **59**, 411–418 (2007).
47. *GRAS Notice 000433: Poloxamer fatty acid esters.* (2012).
48. Lopes, R. *et al.* Lipid nanoparticles containing oryzalin for the treatment of leishmaniasis.

- in *European Journal of Pharmaceutical Sciences* **45**, 442–450 (Elsevier B.V., 2012).
49. Muller, R. H., Mader, K. & Gohla, S. Solid lipid nanoparticles (SLN) for controlled drug delivery - a review of the state of the art. *Eur. J. Pharm. Biopharm.* **50**, 161–177 (2000).
 50. Hao, J. *et al.* Development and optimization of solid lipid nanoparticle formulation for ophthalmic delivery of chloramphenicol using a Box-Behnken design. *Int. J. Nanomedicine* **6**, 683–692 (2011).
 51. Weber, S., Zimmer, A. & Pardeike, J. Solid Lipid Nanoparticles (SLN) and Nanostructured Lipid Carriers (NLC) for pulmonary application: A review of the state of the art. *European Journal of Pharmaceutics and Biopharmaceutics* **86**, 7–22 (2014).
 52. Law, S. *et al.* Gene transfer mediated by sphingosine/ dioleoylphosphatidylethanolamine liposomes in the presence of poloxamer 188. *Drug Deliv.* **13**, 61–7 (2006).
 53. Nelson, D. L., Lehninger, A. L. & Cox, M. M. *Lehninger: Principles of Biochemistry*. **4th Ed**, 344–345 (W. H. Freeman, 2008).
 54. Freitas, C. Stability determination of solid lipid nanoparticles (SLN TM) in aqueous dispersion after addition of electrolyte. *J. Microencapsul.* **16**, 59–71 (1999).
 55. Hong, S.H. *et al.* Aerosol gene delivery using viral vectors and cationic carriers for in vivo lung cancer therapy. *Expert Opin. Drug Deliv.* **12**, 977–991 (2015).
 56. Boussif, O. *et al.* A versatile vector for gene and oligonucleotide transfer into cells in culture and in vivo: polyethylenimine. *Proc. Natl. Acad. Sci.* **92**, 7297–7301 (1995).
 57. Raup, A. *et al.* Compaction and Transmembrane Delivery of pDNA: Differences between I-PEI and Two Types of Amphiphilic Block Copolymers. *Biomacromolecules* **18**, 808–818 (2017).
 58. Ewe, A. *et al.* Optimized polyethylenimine (PEI)-based nanoparticles for siRNA delivery, analyzed in vitro and in an ex vivo tumor tissue slice culture model. *Drug Deliv. Transl. Res.* **7**, 206–216 (2017).
 59. Driscoll, D. F. Lipid injectable emulsions: Pharmacopeial and safety issues. *Pharmaceutical research* **23**, 1959–1969 (2006).
 60. Campos, D. A. *et al.* Technological stability of solid lipid nanoparticles loaded with phenolic compounds: Drying process and stability along storage. *J. Food Eng.* **196**, 1–10 (2017).
 61. del Pozo-Rodríguez, A. *et al.* Short- and long-term stability study of lyophilized solid lipid nanoparticles for gene therapy. *Eur. J. Pharm. Biopharm.* **71**, 181–189 (2009).
 62. Severino, P. *et al.* Development and characterization of a cationic lipid nanocarrier as non-viral vector for gene therapy. *Eur. J. Pharm. Sci.* **66**, 78–82 (2015).

63. Martins, S. *et al.* Physicochemical properties of lipid nanoparticles: Effect of lipid and surfactant composition. *Drug Dev. Ind. Pharm.* **37**, 815–824 (2011).
64. Silva, A. C. *et al.* Long-term stability, biocompatibility and oral delivery potential of risperidone-loaded solid lipid nanoparticles. *Int. J. Pharm.* **436**, 798–805 (2012).
65. Nazemiyeh, E. *et al.* Formulation and physicochemical characterization of lycopene-loaded solid lipid nanoparticles. *Adv. Pharm. Bull.* **6**, 235–241 (2016).
66. Souto, E. B. & Müller, R. H. SLN and NLC for topical delivery of ketoconazole. *J. Microencapsul.* **22**, 501–10 (2005).
67. Siddiqui, A. *et al.* Mixed backbone antisense glucosylceramide synthase oligonucleotide (MBO-asGCS) loaded solid lipid nanoparticles: In vitro characterization and reversal of multidrug resistance in NCI/ADR-RES cells. *Int. J. Pharm.* **400**, 251–259 (2010).
68. Doktorovova, S., Souto, E. B. & Silva, A. M. Nanotoxicology applied to solid lipid nanoparticles and nanostructured lipid carriers - A systematic review of in vitro data. *European Journal of Pharmaceutics and Biopharmaceutics* **87**, 1–18 (2014).
69. Bozzola, J. J. & Russel, L. D. *Electron Microscopy: Principles and techniques for biologists.* (Jones and Bartlett Publishers, Inc., 1998).
70. Jores, K. *et al.* Investigations on the structure of solid lipid nanoparticles (SLN) and oil-loaded solid lipid nanoparticles by photon correlation spectroscopy, field-flow fractionation and transmission electron microscopy. *J. Control. Release* **95**, 217–227 (2004).
71. Hwang, T. L. *et al.* Cationic surfactants in the form of nanoparticles and micelles elicit different human neutrophil responses: A toxicological study. *Colloids Surfaces B Biointerfaces* **114**, 334–341 (2014).
72. Hamid, R. *et al.* Comparison of alamar blue and MTT assays for high through-put screening. *Toxicol. Vitro.* **18**, 703–710 (2004).
73. ISO/EN10993-5. *Int. Stand. ISO 10993-5 Biol. Eval. Med. devices - Part 5 Tests Cytotox. Vitro. methods* **3rd Ed**, 42 (2009).
74. ASTM F 756-00. Standard practice for assessment of hemolytic properties of materials. Philadelphia. *Am. Soc. Test. Mater.* (2000).

Chapter 7 Appendix

Appendix A – Surfactant choice, volume and concentration

Table 7.1 Influence of the surfactants' volume on SLNs physicochemical properties. Average size (Z-ave), Pdl and ZP of the produced SLNs (mean±SD, n=3). The best results were observed for formulations using 10 and 15 mL of surfactant. As no significant differences between these volumes ($p>0.05$) were found, the smallest (10 mL) was chosen for the following steps.

	V_{surfactant} (mL)	Z-ave (nm)	Pdl	ZP (mV)
Tripalmitin	5	187±103	0.487±0.109	-18±1
	10	151±31	0.243±0.172	-17±1
	15	133±35	0.198±0.075	-15±3

Table 7.2 Influence of the Pluronic® F-68 and Pluronic® F-127, and their concentration on SLN physicochemical properties. Values in terms of mean±SD, n=3. Pluronic® F-68 (0.1% w/v) was chosen for the following steps as it allowed to obtain the smallest sizes and lower size dispersion, at the lowest concentration.

			Z-ave (nm)	Pdl	ZP (mV)
Tripalmitin	PF68	2%	194±1	0.396±0.011	+2±1
		1%	134±1	0.254±0.010	-6±1
		0.5%	157±2	0.274±0.001	-10±1
		0.1%	161±2	0.166±0.011	-2±4
	PF127	2%	286±14	0.467±0.062	-5±1
		1%	125±1	0.238±0.006	-3±1
		0.5%	113±1	0.217±0.004	-4±1
		0.1%	492±109	0.831±0.211	-13±1

Appendix B – Lipid choice and concentration



Figure 7.1 *Imwitor® 491 foam-like structure obtained by homogenization with Pluronic® F-68 (0.1% w/v).*

Appendix C – Surface modulation: Cationic polymer

Table 7.3 Surface modulation using different concentrations of PEI 25 kDa. The produced SLNs were evaluated in terms of hydrodynamic surface, size distribution and surface charge (mean±SD, n=3).

	%PEI	Z-ave (nm)	Pdl	ZP (mV)
Precirol®	1	332±14	0.459±0.020	+22±3
	0.5	1590±209	0.276±0.059	+28±2
	0.1	4493±1055	0.262±0.143	+58±2

Table 7.4 Influence of pH in the production of hyNPs, using PEI 25kDa (1% w/v). SLN characteristics were assessed regarding particle size, Pdl and ZP (mean±SD, n=3).

		%PEI	Z-ave (nm)	Pdl	ZP (mV)
pH=7	Precirol®	1	189±3	0.206±0.025	+67±1
	Geleol™	1	330±27	0.275±0.012	+61±2

Table 7.5 Elucidative table respective to sample designation according to their lipid and polyethyleneimine composition. For example, hyNP₁ comprised Precirol® in its lipid matrix and IPEI 10 kDa was used to modulate the surface charge.

	IPEI 10 kDa	bPEI 2 kDa	bPEI 25 kDa
Precirol®	hyNP ₁		
		hyNP ₂	
			hyNP ₃
Geleol™	hyNP ₄		
		hyNP ₅	
			hyNP ₆

Table 7.6 Influence of linear and branched polyethyleneimines on SLN physicochemical properties, at two concentrations (mean±SD, n=3).

	% PEI	Z-ave (nm)	Pdl	ZP (mV)
hyNP₁	0.1	169±4	0.217±0.024	+66±1
	0.01	168±10	0.237±0.062	+50±3
hyNP₂	0.1	188±19	0.287±0.059	+66±2
	0.01	256±19	0.265±0.058	+40±2
hyNP₃	0.1	167±4	0.239±0.013	+62±1
	0.01	182±5	0.230±0.010	+55±2
hyNP₄	0.1	230±5	0.232±0.012	+50±1
	0.01	169±4	0.255±0.009	+53±2
hyNP₅	0.1	266±18	0.301±0.037	+22±1
	0.01	241±9	0.250±0.018	+16±1
hyNP₆	0.1	211±25	0.403±0.068	+67±1
	0.01	208±7	0.305±0.039	+50±2

Appendix D – Surface modulation: Cationic peptide

Table 7.7 HSH produced hybrid solid lipid nanoparticles (hyNP_xP), containing branched or linear PEI (0.01% w/v) and protamine (0.05% w/v) as surface modulators. Samples were named in the same fashion as hyNP_x, and evaluated in terms of size, Pdl and ZP (mean±SD, n=3)

		Z-ave (nm)	Pdl	ZP (mV)
HSH	hyNP ₁ P	178±4	0.220±0.032	+34±1
	hyNP ₂ P	192±23	0.303±0.066	+34±2
	hyNP ₃ P	205±25	0.275±0.076	+34±1
	hyNP ₄ P	411±20	0.205±0.023	+19±1
	hyNP ₅ P	435±53	0.247±0.046	+9±1
	hyNP ₆ P	739±35	0.253±0.039	+12±1

Table 7.8 Hybrid nanoparticles containing protamine were also produced by adsorption of protamine onto the surface of previously prepared hyNP_x. Samples were evaluated in terms of Z-ave, Pdl and ZP (mean±SD, n=3).

		Z-ave (nm)	Pdl	ZP (mV)
Adsorption	hyNP ₁ P	156±4	0.217±0.015	+35±2
	hyNP ₂ P	218±8	0.242±0.011	+34±1
	hyNP ₃ P	188±7	0.293±0.027	+62±3

Appendix E – Stability: Storage medium

Table 7.9 Influence of PBS in SLN stability, regarding size, Pdl and surface charge (mean±SD, n=3).

	Z-ave (nm)	Pdl	ZP (mV)
hyNP ₁	390±10	0.335±0.038	+4±1
hyNP ₂	350±38	0.352±0.069	+1±1
hyNP ₃	430±61	0.411±0.025	-4±1
hyNP ₁ P	1000±259	0.637±0.076	+10±1
hyNP ₂ P	379±59	0.387±0.051	+10±1
hyNP ₃ P	Aggregation		

Table 7.10 Influence of SBF in SLN stability, regarding size, Pdl and surface charge, after 1h and 2h of exposure, (mean±SD, n=3).

		Z-ave (nm)	Pdl	ZP (mV)
1H	hyNP ₁	894±183	0.485±0.070	+8±1
	hyNP ₂	275±6	0.315±0.037	-2±1
	hyNP ₃	830±55	0.471±0.058	-2±1
	hyNP ₁ P	294±32	0.335±0.058	+15±1
	hyNP ₂ P	256±18	0.313±0.073	+18±1
	hyNP ₃ P	582±25	0.367±0.050	+14±1
24H	hyNP ₁	1838±307	0.407±0.107	+9±1
	hyNP ₂	337±43	0.381±0.069	-1±1
	hyNP ₃	3716±618	0.588±0.270	-2±2
	hyNP ₁ P	1281±107	0.880±0.114	+12±3
	hyNP ₂ P	1123±320	0.751±0.228	+12±3
	hyNP ₃ P	3996±2062	0.630±0.285	+10±1

Appendix F – Stability: Sterilization

Table 7.11 Influence of autoclaving on SLN characteristics, regarding particle size, Pdl and ZP (mean±SD, n=3).

	Z-ave (nm)	Pdl	ZP (mV)
hyNP₁	4221±857	0.718±0.071	+53±7
hyNP₂	1375±102	0.328±0.066	+47±4
hyNP₃	Aggregation		
hyNP₁P	2107±401	0.523±0.054	+45±1
hyNP₂P	1504±75	0.360±0.041	+35±2
hyNP₃P	2717±632	0.547±0.143	+46±2

Appendix G – Hemocompatibility

Table 7.12 Schematic representation of the plate used for the hemocompatibility assay.

	1	2	3	4	5	6
A	hyNP ₁	hyNP ₂	hyNP ₃	hyNP ₁ P	hyNP ₂ P	hyNP ₃ P
B	hyNP ₁	hyNP ₂	hyNP ₃	hyNP ₁ P	hyNP ₂ P	hyNP ₃ P
C	hyNP ₁	hyNP ₂	hyNP ₃	hyNP ₁ P	hyNP ₂ P	hyNP ₃ P
D	-	-	Neg. ctrl	Pos. ctrl	Pos. ctrl	Pos. ctrl
E	-	-	Neg. ctrl	Pos. ctrl	Pos. ctrl	Pos. ctrl
F	-	-	Neg. ctrl	Pos. ctrl	Pos. ctrl	Pos. ctrl